



HAL
open science

Characterization of heat and mechanical damage in the mortar by nonlinear acoustic waves

Ismail Yousfi

► **To cite this version:**

Ismail Yousfi. Characterization of heat and mechanical damage in the mortar by nonlinear acoustic waves. Civil Engineering. Ecole Centrale de Lille; Université de Sherbrooke (Québec, Canada), 2015. English. NNT : 2015ECLI0009 . tel-01277134

HAL Id: tel-01277134

<https://theses.hal.science/tel-01277134>

Submitted on 22 Feb 2016

HAL is a multi-disciplinary open access archive for the deposit and dissemination of scientific research documents, whether they are published or not. The documents may come from teaching and research institutions in France or abroad, or from public or private research centers.

L'archive ouverte pluridisciplinaire **HAL**, est destinée au dépôt et à la diffusion de documents scientifiques de niveau recherche, publiés ou non, émanant des établissements d'enseignement et de recherche français ou étrangers, des laboratoires publics ou privés.

N° d'ordre : 259

ECOLE CENTRALE DE LILLE

THESE

Présentée en vue d'obtenir le grade de

DOCTEUR

En

Spécialité : Génie Civil

Par

Ismail YOUSFI

DOCTORAT DELIVRE PAR L'ECOLE CENTRALE DE LILLE

**DOCTORAT DELIVRE SIMULTANEMENT PAR L'ECOLE CENTRALE DE LILLE ET
(UNIVERSITE DE SHERBROOKE) DANS LE CADRE D'UNE COTUTELLE INTERNATIONALE
DE THESE**

Titre de la thèse :

**Caractérisation de l'endommagement thermique et mécanique dans le mortier par les
ondes acoustiques non linéaires**

**Characterization of heat and mechanical damage in the mortar by the nonlinear
acoustic waves**

Soutenue le **29 Mai 2015** devant le jury d'examen

Pr Anand PUPPALA	University of Texas at Arlington	(USA) Président du Jury
Pr Patrice RIVARD	Université de Sherbrooke	(Canada) Rapporteur
Pr Jean-Paul BALAYSSAC	Université Paul Sabatier	(France) Rapporteur
Pr Denis DAMIDOT	Ecole des Mines de Douai	(France) Examineur
Pr Richard GAGNE	Université de Sherbrooke	(Canada) Co-directeur de Thèse
Pr Zoubeir LAFHAJ	Ecole Centrale de Lille	(France) Directeur de Thèse

Thèse préparée dans le Laboratoire de Mécanique de Lille, UMR, CNRS 8107

Ecole Doctorale SPI 072 (Lille I, Lille III, Artois, ULCO, UVHC, EC Lille)

PRES Université Lille Nord-de-France

Acknowledgements

The research project reported in this thesis was a part of a cooperation between l'Ecole Centrale de Lille (France) and l'Université de Sherbrooke (Canada) . I would like to express my sincere gratitude to my supervisors Professor Zoubeir LAFHAJ and Professor Richard GAGNE , who gave me the chance to work within this collaboration on this interesting project.

I extend my warmest thanks to Mr. Zoubeir LAFHAJ, professor at Ecole Centrale de Lille, and to Mr. Richard GAGNE, professor at Université de Sherbrooke, for their great contributions to the successful completion of this work. Their valuable guidance, inspiring discussions, great patience and confidence helped to complete the project in good conditions.

I would like to record my debt of gratitude to Mr. Patrice RIVARD, Professor of Civil Engineering at the Université de Sherbrooke, for offering me the opportunity to work in his laboratory (Groupe de Recherche en Auscultation et en Instrumentation de Sherbrooke) .

I would also like to express my gratitude to Mr. Serge KODJO for his help and inspiring discussions. The discussions I had with him were always very interesting and very fruitful.

I would like to thank Professors, Anand PUPPALA, Patrice RIVARD, Jean-Paul BALAYSSAC, Denis DAMIDOT for giving me the honor to accept being part of my thesis jury.

I would like to thank the whole team and the staff of the Ecole Centrale de Lille and Université de Sherbrooke for their cooperation and support.

My very heartfelt thanks go to my friends in France and Canada who shared a lot of laughter, debates, ideas, above all, proved their support and understanding.

Last, I owe much to my parents, brothers and sisters for their long-distance encouragement and support.

Abstract

The objective of this work is the characterization of heat and mechanical damage in the mortar by the nonlinear acoustic waves. The correlation between non-linear/linear acoustic parameters and damage in mortar is studied based on experiments and modelling.

Experimental measurements of non-linear acoustic parameters as a function of temperature and crack size were performed on mortar.

The velocities showed a decrease when increasing the degradation and the non-linear parameters showed an increase when increasing the damage.

For the heat damage, cylindrical specimens were prepared and were characterized by studying the porosity and saturation. Then, the temperature controls the degradation. Indeed, the linear acoustic (UPV) and non-linear acoustic (Higher harmonic generation) were applied to characterize the damage. The linear acoustic tests have shown that the longitudinal, transverse velocities and modulus of Young of the mortar decreases in function of the temperature. The non-linear acoustic tests have shown that beta increases in function of the temperature.

For the mechanical damage and the self-healing, an annular specimens were prepared and cracked by controlling the size of each crack. Then the self-healing phenomenon was characterized by the permeability and the acoustic tests. Indeed, the permeability tests have shown that the airflow and the crack size decreases quickly in the first month then slowly for the rest of the self-healing process. On the other hand, the non-linear acoustic tests shown that the alpha and beta decreases according to the self healing process which means that the nonlinear parameters are good indicators to characterize the self-healing. Moreover, the analysis of the experimental results indicates that the frequency resonant technique is more efficient to characterize the defects in the mortar than the higher harmonic generation.

From the experimental tests and to get a general result independent for our case study, the nonlinear parameters were related to a damage index. A polynomial correlations of a 2nd degree was established between the nonlinear parameters and the index damage.

A numerical model based on the finite element volume was proposed to establish a correlation between the crack size and the airflow. The numerical results were compared with the results of the permeability tests and shown a good agreement.

The findings of this work should be most appropriate as a foundation for the study of the self healing by the nonlinear acoustic waves.

Keywords: nonlinear acoustic, self-healing, mortar, heat damage, mechanical damage, linear acoustic, porosity, resonant frequency, higher harmonic generation.

Résumé

L'objectif de ce travail est la caractérisation de l'endommagement thermique et mécanique dans le mortier par les ondes acoustiques non linéaires. La corrélation entre les paramètres acoustiques linéaires et non-linéaires étudiée est basée sur les essais expérimentaux et la modélisation.

Des mesures expérimentales des paramètres acoustiques non linéaires en fonction de la taille de la fissure et la température ont été effectuées sur mortier.

Les vitesses ont montré une diminution et les paramètres non-linéaires ont montré une augmentation en augmentant le degré de fissuration.

Pour l'endommagement thermique, des éprouvettes cylindriques ont été préparées et ont été caractérisées par l'étude de la porosité et la saturation. Ensuite, la température contrôle la dégradation.

En effet, l'acoustique linéaire (UPV) et l'acoustique non linéaire (génération d'harmoniques) ont été appliqués afin de quantifier l'endommagement. Les essais acoustiques linéaires ont prouvé que les vitesses transversales, longitudinales et le module d'Young du mortier diminue en fonction de la température. Les essais acoustiques non linéaires ont montré l'augmentation du bêta fonction de la température.

Pour l'endommagement mécaniques et l'auto-cicatrisation, des anneaux de mortier ont été préparés et fissurés en contrôlant la taille de chaque fissure. Ensuite, le phénomène d'auto-cicatrisation est suivi par la perméabilité et les essais acoustiques. Les essais de perméabilité ont montré que le débit d'air et la taille de la fissure diminue rapidement au cours du premier mois, puis lentement durant le reste du processus d'auto-cicatrisation. D'autre part, les tests acoustiques non linéaires ont montré que « alpha » et « bêta » diminuent durant le processus de l'auto-cicatrisation qui signifie que les paramètres non linéaires sont un bon indicateur pour caractériser ce phénomène.

En outre, l'analyse des résultats expérimentaux indique que la technique de résonance de fréquence est plus efficace pour caractériser les défauts dans le mortier de la génération d'harmoniques plus élevés.

A partir des essais expérimentaux et dans le but d'obtenir un résultat plus général indépendant de notre cas d'étude, les paramètres non linéaires ont été liés à un index d'endommagement. Une corrélation polynomiale de 2ème degré a été établie entre les paramètres non linéaires et l'index d'endommagement.

Un modèle numérique basé sur la méthode des volumes finis a été proposé afin d'établir une corrélation entre la taille de la fissure et le flux d'air. Les résultats numériques ont été comparés avec les résultats des tests de perméabilité et montré un bon accord.

Les résultats de ce travail représentent un bon départ pour étudier le phénomène de l'auto-cicatrisation par les ondes acoustiques non linéaires.

Mots clés: acoustique non linéaire, auto-cicatrisation, mortier, endommagement thermique, endommagement mécanique, acoustique linéaire, porosité, fréquence de résonance, génération d'harmoniques.

Summary

General Introduction	17
Chapter 1: Performance approach and durability of cement-based materials	20
Introduction	21
1. Course of the performance-approach	22
2. Indicators of the durability	23
3. Classes and limit values for indicators of durability	26
Conclusion	28
Chapter 2: Healing and self-healing of cement based materials: Definition, process	
and advantages	29
Introduction	30
1. Definition of healing	30
2. Phenomena involved in the healing process	32
3. Study of healing: different approaches	34
4. Parameters affecting the healing process	36
5. The kinetics of healing of inactive cracks	42
6. The healing effect on the mechanical behavior	43
7. The benefits of self-healing	44
7.1. Gain of mechanical properties after being subjected to freeze-thaw	44
7.2. Gain of mechanical properties after damage by bending	45
7.3. Gain of mechanical properties after damage in traction	46
7.4. Gain of mechanical properties after damage in compression	48
Conclusion	49
Chapter 3: The different techniques of the Non Destructive Testing (NDT)	50
Introduction	51
1. Magnetic Control	51
2. X-ray tomography	52
3. Infrared thermography	53
4. Ultrasonic and Acoustic emission	54
5. Criterias for choosing a NDT method	56
Conclusion	58
Chapter 4: Comparison between the linear and the nonlinear acoustic & the different	

techniques used in the nonlinear acoustic waves	59
Introduction	60
1. Linear acoustic	60
2. The difference of the response between the linear and nonlinear acoustic wave	61
3. The different techniques using in the nonlinear acoustic waves	63
3.1. Mixed Frequency Response.....	63
3.2. Higher Harmonic Generation	66
3.3. Shift of Resonance Frequency	69
4. Evaluation of damage in cement based materials by non linear acoustic	71
4.1. Mechanical damage.....	72
4.2. Thermal damage	76
Conclusion	77
Chapter 5: Definition of the project.....	78
1. Context of the study.....	79
2. Problematic	80
3. Objectives.....	81
Chapter 6: Heat damage: Protocol, results and discussion.....	83
Introduction	84
1. Experimental procedure	81
1.1. Mortar sample preparation and generation of heat treatment	84
1.2. Porosity and density	86
2. Linear acoustic	87
2.1. Experimental device.....	87
2.2. Effect of saturation.....	89
2.3. Effect of heat damage.....	92
3. Nonlinear acoustic	93
3.1. Experimental device.....	93
3.2. Effect of saturation.....	95
3.3. Effect of heat damage.....	97
Conclusion	98
Chapter 7: Self-Healing: Protocol, results and discussion	99
Introduction	100
1. Specimens preparation	100

2. Airflow and permeability tests	104
3. Results: Self-healing effect	107
3.1. The evolution of the airflow	108
3.2. The evolution of the crack size	110
4. Linear acoustic waves	111
4.1. Effect of self healing on longitudinal velocity.....	115
5. Nonlinear acoustic waves.....	118
5.1. Choice of resonance frequency.....	118
5.2. Evolution of non-linear parameter “Alpha” for 12 KHZ	122
5.3. Effect of airflow on Alpha.....	124
6. Correlation between non-linear parameter and airflow	127
6.1. Correlation: Alpha 12 KHz and airflow	127
6.2. Correlation: Beta 12 KHz and airflow	129
6.3. Correlation Alpha 15 KHz and airflow	131
6.4. Correlation Beta 15 KHz and airflow	132
7. Correlation between non-linear parameter and damage index	134
7.1. Correlation Alpha 12 KHz and damage index.....	135
7.2. Correlation Beta 12 KHz and damage index	136
7.3. Correlation Alpha 15 KHz and damage index.....	137
7.4. Correlation Beta 15 KHz and damage index	138
Conclusion	140
Chapter 8: Numerical modelling	141
Introduction	142
1. Problem.....	142
2. Equations and model.....	143
3. Results.....	147
3.1. Convergence of the solution	147
3.2. Pressure	148
3.3. Vertical velocity.....	148
3.4. Horizontal velocity.....	150
4. Comparison between numerical and experimental airflows	153
Conclusion	155
General Conclusion	156

References..... 158

Figures

Fig. 1: Confederation Bridge (1997)	21
Fig. 2: Bridge Rion-Antirion, 2004. (Photo: J. Hartley)	22
Fig. 3 : Porosity water.....	24
Fig. 4: Measuring coefficient of chloride diffusion.....	24
Fig. 5: Accelerated carbonation test	25
Fig. 6: Micro cracks before (a) and after (b) the self-healing (Yang et al., 2009).....	31
Fig. 7: Phenomena causing the decreasing in the flow of water in cement materials.....	33
Fig. 8: Evolution of the relative flow vs. time for crack openings $w = 0.05$ mm, 0.1 mm and 0.15 (Reinhardt & Jooss, 2003)	37
Fig. 9: Evolution of the opening of cracks of concrete vs. time (Argouges & Gagne,2009).....	38
Fig. 10: Time required for full healing cracks according to their opening two hydraulic gradients (Nanayakkara, 2003).....	39
Fig. 11: Mechanical behavior of specimens at reloading after storage in air or water for 20 weeks (Granger et al., 2007)	46
Fig. 12: Mechanical behavior of specimens at reloading, after different durations of storage in water (after a Granger et al. (2007))	46
Fig. 13: Principe of the magnetic control. (Bray & McBride, 1992).....	51
Fig. 14: Test of the magnetic control.....	52
Fig. 15: Test of the X-ray.....	53
Fig. 16: Test Procedure of X-ray.....	53
Fig. 17:Principe of Infrared thermography	54
Fig. 18: Defect seen by Infrared tomography.....	54
Fig. 19: Test of transmission and reflection of a wave	55
Fig. 20: The different percentages of the utilization of each NDT techniques (Shull, 2002)	58
Fig. 21: Longitudinal wave	60
Fig. 22: Shear wave	61
Fig. 23: The linear acoustic response.....	63
Fig. 24: The nonlinear acoustic response.....	63
Fig. 25: Sample with flaw: a - closed by vibration compression, b –open under dilation (Sutin, 2005).....	64
Fig. 26: Amplitude modulation of probe signal: (a) vibration, (b) ultrasonic signal (Sutin, 2005). 64	64
Fig. 27: Illustration of the nonlinear acoustic vibro-modulation effect	65
Fig. 28: Response in the case of linear acoustic	65
Fig. 29: Response in the case of nonlinear acoustic	65
Fig. 30: Distortion in the waveform during propagation by the nonlinear elasticity and higher harmonic generation power of fundamental.....	67
Fig. 31: 2 nd harmonic generation in the quadratic nonlinear system.....	67
Fig. 32: Nonlinear relationship between stress and strain.....	68
Fig. 33: A result of NRUS : healthy material.....	70
Fig. 34: A result of NRUS: damage material	71

Fig. 35: Relative changes of the linear and nonlinear characteristics derived from SIMONRAS analysis of an RC beam as function of damage due to consecutive loading steps	73
Fig. 36: Acoustic emission parameter and nonlinear acoustic parameter vs. the applied load (w/c = 50%) (Shaha and Ribakov (2010))	74
Fig. 37: Superposition of results from different specimens. (a) The variation of α for different specimens leads to the definition of a curve that describes the different stages of damage evolution. (b) and (c) point out that linear indicators show a linear evolution of damage (Antonaci et al (2010))	75
Fig. 38: Total results of the hysteretic nonlinearity parameter according to the	76
Fig. 39: Relative variation of the nonlinear parameter and velocity of pressure waves as a function of the damage temperature (Meo et al. (2014)).....	77
Fig. 40: Samples of mortar.....	85
Fig. 41: Time evolution of temperature during heat treatment.....	85
Fig. 42: Loss of mass	86
Fig. 43: Porosity vs. W/C	86
Fig. 44: Density vs. Porosity	87
Fig. 45: Experimental device of linear acoustic	88
Fig. 46: Determination the time of flight	88
Fig. 47: The variation of the velocity for dry and saturated cases according to porosity	89
Fig. 48: Modulus of Young vs. Porosity.....	90
Fig. 49: Modulus of Young vs. Temperature	92
Fig. 50: Experimental device of the nonlinear acoustic waves	94
Fig. 51: Principle of the High Harmonic Generation technique.....	94
Fig. 52: Example of determination of nonlinear parameter beta	95
Fig. 53: Evolution of the Non-Linear Parameter β with porosity for dry and saturated specimens	96
Fig. 54: Evolution of the Non-Linear Parameter β with Temperature (linear trend).....	97
Fig. 55 : Evolution of the Non-Linear Parameter β with Temperature (exponential trend).....	97
Fig. 56 : An example of a specimen	101
Fig. 57: A mold to make a specimen	101
Fig. 58: Experimental process	102
Fig. 59: Specimen with the expansive core.....	103
Fig. 60: Crack created by the expansive core.....	104
Fig. 61: A cell of air permeability	105
Fig. 62: Initial crack taken by a video microscope (in the order of 100 μm).....	106
Fig. 63: Initial crack size Vs. Airflow	107
Fig. 64: The evolution of the airflow before and after self-healing in humid chamber for all the cracks.....	108
Fig. 65: The variation of the airflow for different cracks Vs. Time	108
Fig. 66: The evolution of the size of crack before and after self-healing in humid chamber.....	110
Fig. 67: The variation of the crack size for different cracks Vs. Time	111
Fig. 68: The crack is placed between the two transducers	112
Fig. 69:Example of velocity measurement	112
Fig. 70: Zoom for the previous example of velocity measurement.....	113

Fig. 71: The variation of the velocity vs. time for the sample N° 1.....	115
Fig. 72: The variation of the velocity vs. time for the sample N° 2.....	116
Fig. 73: The variation of the velocity vs. time for the sample N° 3.....	116
Fig. 74: The variation of the velocity vs. time for the sample N° 4.....	117
Fig. 75: The variation of the velocity vs. time for the sample N° 5.....	117
Fig. 76:The variation of the velocity vs. time for the sample N° 6	118
Fig. 77:definition of the domain of the resolution	119
Fig. 78:Triangular Mesh	119
Fig. 79:Frequency of resonance 12 KHz	120
Fig. 80:Frequency of resonance 15 KHz	120
Fig. 81: Shift resonance of a sound sample.....	121
Fig. 82: Shift resonance before and after self-healing for a cracked sample.....	121
Fig. 83: The variation of the alpha vs. time for the sample N° 1	122
Fig. 84: The variation of the alpha vs. time for the sample N° 2	122
Fig. 85: The variation of the alpha vs. time for the sample N° 3	123
Fig. 86: The variation of the alpha vs. time for the sample N° 4	123
Fig. 87: The variation of the alpha vs. time for the sample N° 6	124
Fig. 88: The variation of the alpha vs. airflow for the sample N° 1	125
Fig. 89: The variation of the alpha vs. airflow for the sample N° 2	125
Fig. 90: The variation of the alpha vs. airflow for the sample N° 3	126
Fig. 91: The variation of the alpha vs. airflow for the sample N° 4	126
Fig. 92: The variation of the alpha 12 vs. airflow with an exponential approximation	128
Fig. 93: The variation of the alpha 12 vs. airflow with a polynomial approximation	128
Fig. 94: The variation of the beta 12 vs. airflow	130
Fig. 95: The variation of the beta 12 vs. airflow	130
Fig. 96: The variation of the alpha 15 vs. airflow	131
Fig. 97: The variation of the alpha 15 vs. airflow	132
Fig. 98: The variation of the beta 15 vs. airflow with a linear approximation	133
Fig. 99: The variation of the beta 15 vs. airflow with a polynomial approximation.....	133
Fig. 100: Mean radius of the annular specimen.....	134
Fig. 101: Alpha 12 Vs. Damage Index.....	135
Fig. 102: Beta 12 Vs. Damage Index.....	136
Fig. 103: Alpha 15 Vs. Damage Index.....	137
Fig. 104: Beta 15 Vs. Damage Index.....	138
Fig. 105: Schema of the crack.....	142
Fig. 106: Domain of the resolution	143
Fig. 107: Boundary conditions	143
Fig. 108: Meshing of domain of resolution	145
Fig. 109: The convergence of the solution in time	147
Fig. 110: The convergence of the solution in time (Logarithmic scale)	147
Fig. 111: Variation of the pressure in the crack	148
Fig. 112: Convergence of the V-velocity in the crack (10 nodes)	149

Fig. 113: Convergence of the V-velocity in the crack (40 nodes)	149
Fig. 114: Convergence of the V-velocity in the crack (10 nodes)	150
Fig. 115: Convergence of the U-velocity in the crack (10 nodes)	151
Fig. 116: Convergence of the U-velocity in the crack (40 nodes)	151
Fig. 117: Convergence of the V-velocity in the crack (10 nodes)	152
Fig. 118: Curve 3D of velocities (U and V) and velocity field in the crack before the flow establishment.....	152
Fig. 119: The establishment of the flow in the crack in time	153
Fig. 120: Variation of the Airflow with crack size (experimental and numerical).....	154

Tables

<i>Tab 1: Summary of classes and limit values (indicative) for indicators of durability.....</i>	
<i> General (G) or Substitution (S): porosity, electrical resistivity, coefficient of.....</i>	
<i> diffusion and permeability (Baroghel-Bouny v.,2004).</i>	<i>27</i>
<i>Tab 2: Most important studying of the healing for different values of opening cracks</i>	<i>37</i>
<i>Tab 3: Summary of techniques of NDT: Costs, advantages & drawbacks.....</i>	
<i> (Kouzoubachian C. ,2006).....</i>	<i>57</i>
<i>Tab 4: Correlation between porosity and linear acoustic parameters</i>	<i>91</i>
<i>Tab 5: Number of cracks on each sample</i>	<i>114</i>

General Introduction

In the areas of advanced industrial (nuclear, aerospace etc...), assessing the damage of the materials is the key to control the durability and reliability of materials in service. In this perspective, it is necessary not only to quantify the damage but also to identify the different responsible mechanisms. It is therefore essential to characterize the material and identify the most sensitive indicators of the damage presence to prevent their ruin and use them optimally. In order to resolve this problem, the acoustic methods seem to be interesting because of their non-destructive aspect and their sensitivity to damage. Thus, the ultrasonic linear acoustic methods have often shown their ability to characterize the damage through changes in velocity and attenuation of ultrasonic waves. However, several experiments have shown that linear acoustic methods are not sensitive enough to detect and localize the damage. Often, the first damage mechanisms are the precursors of final fracture, thus they are therefore very important to be identified. Faced with such difficulty, the nonlinear acoustic methods offer an important alternative that can detect and potentially characterize the weak or damage early, even localized or diffuse. Thus in recent years, nonlinear acoustics is becoming more like very promising new way in non-destructive evaluation and control of structural materials. Indeed, even if nonlinearities can be pertinent in heterogeneous materials such as rocks and cement-based materials, they increase significantly in presence of damage. Many potential applications exist in nonlinear acoustics for the characterization of both macroscopic localized cracks and diffuse damage assessment due to the presence of micro-cracks. In the latter case, because of their high sensitivity, nonlinear acoustic methods are particularly effective especially in the detection and characterization of early damage. The most known techniques in nonlinear acoustic are nonlinear elastic wave spectroscopy (NEWS) methods. These techniques (Shift resonance, higher harmonics generation...) are powerful, and present new tools in interrogation of damage in materials. Due to material nonlinearity, a wave can distort, creating accompanying harmonics, multiplication of waves of different frequencies, and, under resonance conditions, changes in resonance frequencies as a function of drive amplitude.

In other hand, for many concrete structures in the course of their lifetime, the assessment of durability is a key parameter needed in order to know whether safety is ensured or not. The presence of cracks, due to mechanical stresses or time dependent effects (shrinkage, creep...) is one of the major factors which can influence durability and serviceability of concrete structures in terms of resistance, permeability and transfer properties.

Self-healing of cracks is phenomenon acting positively in durability problems of cement-based materials. This process can take place only in presence of water (dissolved CO_2 is not always needed), and consists of chemical reactions of compounds exposed at the cracked surfaces. These reactions produce crystals, and the accretion of these from the opposite surfaces of a crack can re-establish the continuity of the material eventually. The essential requirement, with water, is the presence of compounds capable of further reaction. Thus, cement, hydrated or not, is the essential reactive element. There are two major assumptions regarding the reactions of healing: the hydration of unhydrated clinker available in the microstructure of hardened concrete (important for concrete with low water/cement ratio), or the precipitation of calcium carbonate CaCO_3 . Some studies carried out until now highlight the self-healing phenomenon by means of water permeability tests. A diminution of the flow rate through cracked concrete is the main technique used to characterize self-healing of cracks.

The thesis is composed to 5 chapters as described below:

First chapter is contributed to a short bibliographical review about the performance approach and durability of cement based materials.

The second chapter introduces the self-healing phenomena: definition, the different techniques used to follow the self-healing process and it main advantages.

The third chapter focuses in the non-linear acoustic waves. First, the linear technique is exposed then the non-linear acoustic. Second, the main difference between both techniques is discussed. Finally, two non-linear techniques are presented: Higher Harmonic Generation and Shift resonance.

The fourth chapter is dedicated to the description of the objectives of this study with details in plus the experimental protocol adopted during this thesis.

The fifth chapter presents and evaluates the results of acoustic testing for the mortar sample before and after the heat damage. The longitudinal, shear velocities and modulus of

Young obtained by the linear acoustic wave are compared to the non-linear parameter beta measured by the higher harmonic generation. These results were discussed with the already published and correlated to the porosity, water cement ratio and temperature...

The sixth chapter is contributed to the self-healing. The evolution of the air flows and cracks size measured by the permeability tests and the non-linear acoustic parameters alpha and beta are analysed which helps to characterize the self-healing process.

The last chapter is a numerical study designed to model the permeability test done in the sixth chapter. The variation of the airflow with crack size obtained numerically is compared to the experimental results.

Chapter 1: Performance approach and durability of cement-based materials

Introduction

Currently, in various countries, considerable research is devoted to development of new approaches to durability, to increase the lifetime of reinforced concrete structures at the lowest cost. These new approaches are based on selecting durability indicators, the definition of adequate performance-criteria on these indicators and evaluation of the life of the structure subject to predictive models.

The objective of this approach is to design concrete resistant to internal hazards (Alkali-reaction, reinforcement corrosion...) and external (sulphated environments, ocean ...) for a given lifetime.

From a practical standpoint, the predictive approach can be applied, first phase design of structures and secondly for the monitoring of existing structures (degraded or not).

The performance approach requires the use of models more or less sophisticated. It offers the engineer and the designer a complete methodology for the assessment and prediction of the durability of structures, with greater freedom and technical / economic benefits (Fig.1, Fig.2)

Examples:

1)



Fig. 1: Confederation Bridge (1997)

- Lifetime: 100 years
- Risks:
 - Reinforcement
 - Corrosion (chlorides)
 - Abrasion of concrete by ice
 - Freeze / thaw

2)



Fig. 2: Bridge Rion-Antirion, 2004. (Photo: J. Hartley)

- Lifetime: 120 years
- Risk: reinforcement corrosion (chlorides)

1. Course of the performance-approach

The performance-approach (Baroghel-Bouny v., 2005) proceeds in general as follows:

- Defining the category of structure by determining its economic importance and strategic and particularly in selecting the requisite life;

- Definition of environmental conditions including, for example the type of aggressiveness, variations in humidity, ...
- Defining risk of degradation; reinforcement corrosion, alkali reaction, ...
- Choice of durability indicators and characteristics of the material as a function of characteristics of structure, environment and construction details;
- Selection of specifications for durability indicators based on the importance of structure, type of environment, life and required structural arrangements;
- Choosing a predictive model of life where durability indicators appear as input data.

2. Indicators of the durability

The application of performance-approach in the design phase requires, first time, a census of durability indicators. These indicators are chosen in function of their importance by the durability characteristics of structure and its environment and choice of structural arrangements (coating...). They are simple but relevant parameters to quantify the phenomena and to develop predictive tools.

✓ *General indicators of durability*

Durability indicators general, listed below, are the first order parameters to assessing and predicting durability. They are essential to prevent the corrosion and alkali reaction. The number of these parameters is very small and they are complementary and are not routinely required to each case study.

These indicators are:

- Porosity accessible to water (NT BUILD 443, 1995) (Fig.3)
- Diffusion coefficient (effective or actual) of chloride ions (NT BUILD 443, 1998; NT BUILD 492, 1999) (Fig.4)
- Permeability to liquid water and gas (AFPC-AFREM ,1998; NF EN 12390-8,2001)

- Content of portlandite ($\text{Ca}(\text{OH})_2$) (Baroghel-Bouny v.,2004)
- Carbonation test (Fig.5)

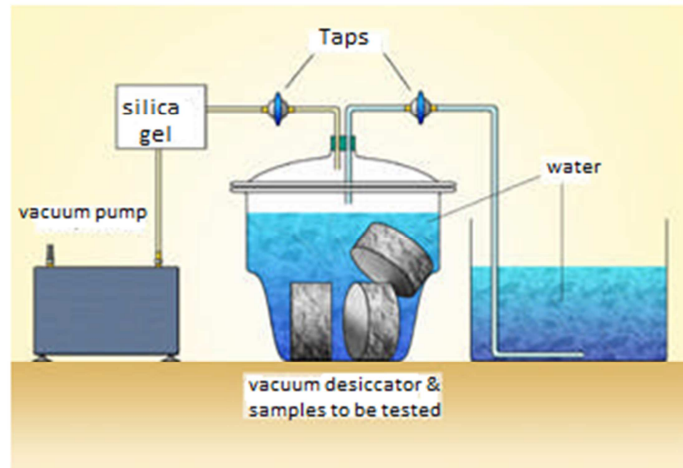


Fig. 3 : Porosity water

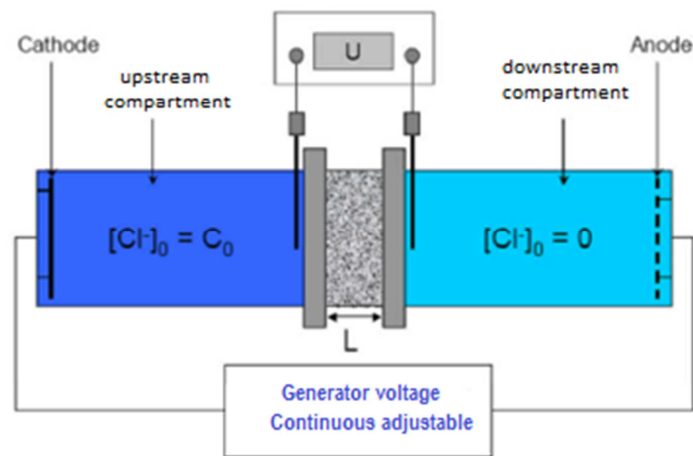


Fig. 4: Measuring coefficient of chloride diffusion

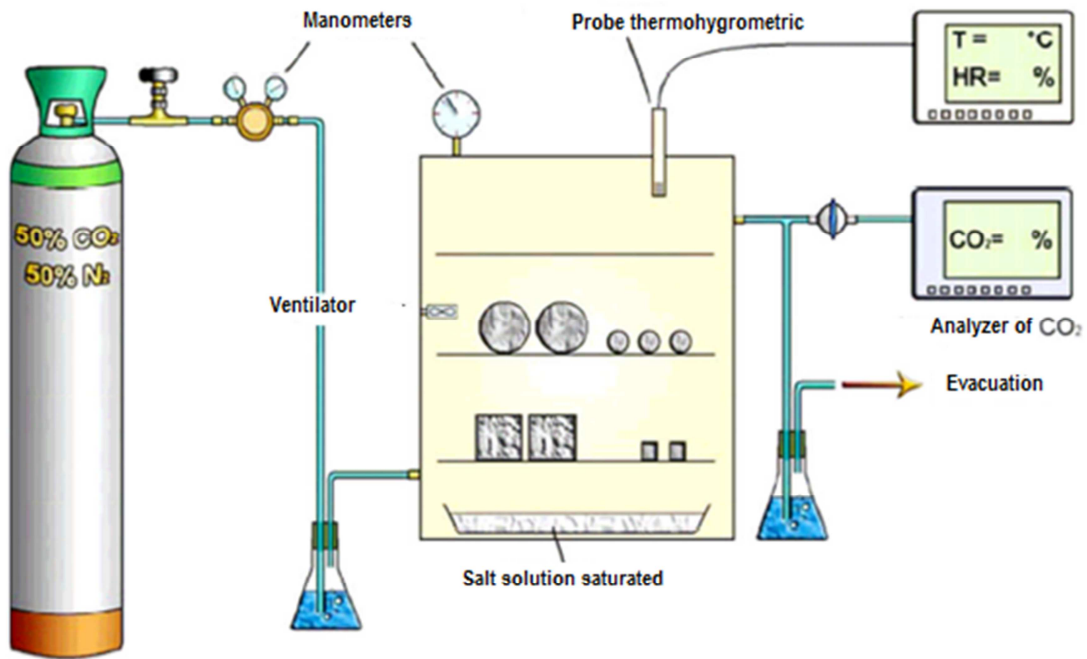


Fig. 5: Accelerated carbonation test

✓ *Indicators of the substitution*

The general indicators can be substituted by agreement of the contracting authority, by parameters that are easier to identify more specific problems or more adapted to the models used. These parameters are as follows:

- * Porosity accessible to mercury (Baroghel-Bouny V.2004)
- * Electrical resistivity (Baroghel-Bouny V.,2004)
- * Quantity of electricity (Baroghel-Bouny V.,2004)
- * Diffusion coefficient of CO₂ or O₂ (Baroghel-Bouny V.,2004)
- * Capillary absorption coefficient (AFPC-AFREM,1998)

✓ *Additional parameters:*

The additional parameters previously defined indicators are required when the predictive model uses as input data or to assist in the interpretation of durability. The choice of these parameters is often subjected to prior to the probation of the owner.

Among these indicators:

- Characteristics of the porous structure,
- Degree of hydration of cement,
- Nature's hydrates,
- Content of C-S-H,
- Rate of water saturation,
- Isotherms of adsorption-desorption of water vapor .
- Diffusion coefficient of water vapor,
- Heat of hydration,
- Tensile Strength.

3. Classes and limit values for indicators of durability

Durability indicators (General and Substitution) used primarily for definition of classes depending on the potential durability of the level "very low" to rated "very high".

These classes will be used for a qualitative or quantitative Durability "potential" in terms of the material. The limits associated with indicators (Tab.1) are relative to measurements made in laboratories, according methods described in the standards guides (design of concrete for a given lifetime of works) applied on specimens or molded concrete cores stored in laboratories.

Performance evaluation of a given concrete can be achieved by comparing values of durability indicators that have been obtained for the formula to be considered corresponding classes offered (Table 1). This table is a simple tool that can be used by the designer to select the concrete on the basis of predefined criteria, and / or to optimize the formulation or to control the quality of the material.

Tab 1: Summary of classes and limit values (indicative) for indicators of durability General (G) or Substitution (S): porosity, electrical resistivity, coefficient of diffusion and permeability (Baroghel-Bouny V.,2004).

		Classes and limit values				
Potential durability		Very high	Hight	Medium	Low	Very low
G	Porosity accessible to water (%)	> 16	14 to 16	12 to 14	9 to 12	6 to 9
S	Porosity measured by mercury intrusion (%)	> 16	13 to 16	9 to 13	6 to 9	3 to 6
S	Electrical resistivity (Ohm.m)	< 50	50 to 100	100 to 250	250 to 1000	> 1000
G	Effective diffusion coefficient of chlorides (10^{-12} m^2)	> 8	2 to 8	1 to 2	0.1 to 1	< 0.1
G	Effective diffusion coefficient chlorides(10^{-12} m^2)	> 50	10 to 50	5 to 10	1 to 5	< 1
G	Effective permeability to gases (10^{-18} m^2)	> 1000	300 to 1000	100 to 300	10 to 100	< 10
G	Liquid water permeability (10^{-18} m^2)	> 10	1 to 10	0,1 to 1	0,01 to 0,1	< 0,01

High durability potential

Medium durability potential

Low durability potential

Very low durability potential very

Conclusion

The performance approach is now an indispensable tool. It allows you to specify the design phase, especially for large projects, performance-very relevant criteria and objectives for sustainability. The identification of sustainability indicators requires the completion of studies relatively long because of the importance of the duration of the tests recommended. These indicators must be taken into account before constructing. The application of this approach will provide performance-formulas regional references taking into account the sustainability indicators. These are determined by the characteristics of local materials, the rate of aggressive medium and the required lifetime.

*Chapter 2: Healing and self-healing of
cement based materials: Definition,
process and advantages*

Introduction

The aging of infrastructure generates significant investment because of the so large number of structures damaged and very high costs of repair. Indeed, there is an explosion in the budget to repair these structures in order to ensure the reclamation and maintenance of its quality. The life of a cement-based structure is very often linked to the ability of the cement-based materials to prevent the penetration of aggressive agents in the porous network. The ability of strength cement based materials was the intrusion of these agents is characterized by physical quantities: the permeability, porosity...

Cracking is a key parameter for durability of cement structures. But the coupling between cracking and the durability is complex, because the cracks can be evolutive. Their location and geometry (crack opening) may vary as a result of internal stresses (alkali-aggregate reaction, freeze-thaw) or external (mechanical loads, thermal cycling). The self-healing mechanisms may also contribute to changing the geometrical properties of cracks (length, breadth and openness) and consequently the transport mechanisms in the cracking plane.

Approaches to take account of cracking on the kinetics of degradation of cement structures and the prediction of its life span are still relatively poorly developed. This lack of reliable and efficient tools stems in particular from poor understanding of the mechanisms and kinetics of self-healing cracks in the cement matrices.

1. Definition of healing

The term healing is often associated with medical field to designate "the spontaneous repair of body tissue affected by a lesion." This term has been extended to the field of cement based materials designer for healing / repair of cracks on the structures presented. The phenomena involved in this process can be of different natures. Some consequences are inherent properties of the material: water in the presence of chemical or physical reactions take place within cracks and reseal can (partially or wholly) the latter. Cracks can also be healed / fixed per injection of different sealers.

Various terms are used in the literature depending on the type of healing studied. These terms

are very similar and the reader can sometimes mix between different concepts. Indeed, different authors sometimes use a same word to designate and separate phenomena, a same phenomenon is sometimes designated by different words. It is then interesting to take stock of the vocabulary used in the literature in order to have clear ideas on the terms to be used according to the studied phenomenon. This helps to avoid a misinterpretation of the data of the literature.

A distinction is first made between the autogenous healing and healing / repair provoked by human. These two categories are then redivided into two. Autogenous healing includes the natural healing and self-healing (Fig.6).

Despite these differences, autogenous healing is associated with the capacity of cement based materials, once produced, has partially or wholly reseal cracks, in the presence of water thanks to chemical and physical phenomena within the crack.

Neville (2002) defines the phenomenon as autogenous healing to restore the continuity of the two lips of a crack without external intervention to the material.

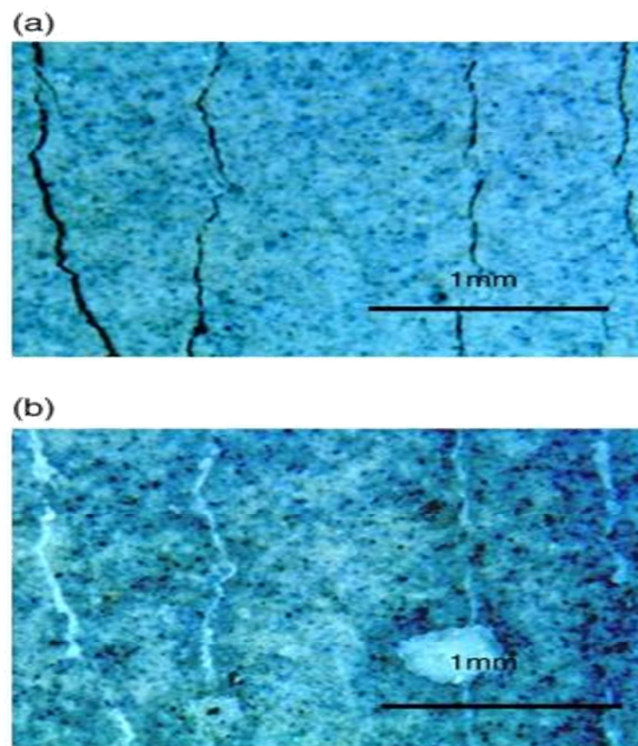


Fig. 6: Micro cracks before (a) and after (b) the self-healing (Yang et al., 2009)

2. Phenomena involved in the healing process

For many years, information about the phenomenon of healing was limited. The first description of healing back to the French Academy of Sciences in 1836 (Clear, 1985; Hearn, 1998). Subsequently, many researchers have studied the phenomenon of healing and have confirmed its existence in the presence of water in a crack, the latter is able to close in part or in whole.

However, as mentioned by Neville (2002) and Hearn (1998), the literature has not always been unanimous in regard to phenomena at the origin of healing of cracks. Several phenomena involved in the healing process are mentioned in the literature. Some studies conclude that a single phenomenon is a cause of healing, while others think it is couples of different effects physico-chemical phenomena. The main phenomena that could potentially be at the origin of healing were already largely identified in 30 years (Turner, 1937) and are deferred in almost all introductions articles on this topic. The following phenomena can then take place (Fig.7):

- The formation of calcium carbonate (CaCO_3) and, more specifically of calcite in the crack (Clear, 1985; Edvardsen, 1999, Homma et al., 2009; Lauer & Slate, 1956; Li & Yang, 2007; Loving , 1936; Nanayakkara, 2003);
- Continuous hydration of cement (anhydrous cement) in the flow path (lips of the crack to crack the case of concretes) (Li & Li, 2011; Schlangen et al., 2006; Zhong Yao & , 2007);
- Blocking the flow of water due to the presence of impurities in it or particles of concrete that have "Spare parts" of the lips of the crack and blocking the passage of water.

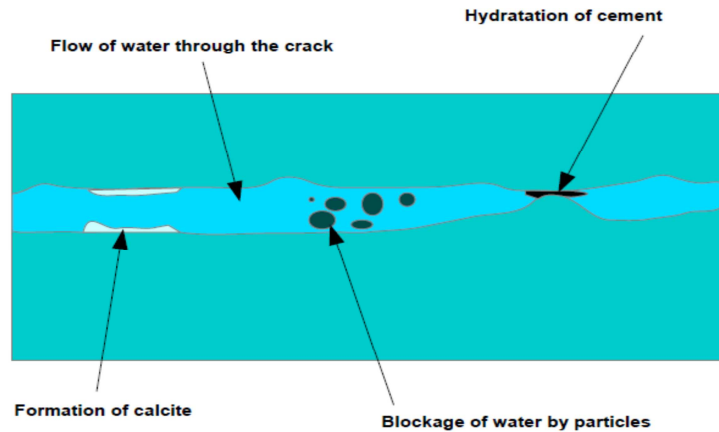


Fig. 7: Phenomena causing the decreasing in the flow of water in cement materials

Hearn (1998) draws the reader's attention to phenomena that could be construed as causes of healing but, in reality, are not. She calls this a false healing since it is then reversible phenomena. An example is the lack of saturation of the specimen in testing permeability to water. In this case, the presence of air in the concrete matrix or swelling of the cement paste when water penetrates into the concrete, can cause a decrease in permeability over time. This can then be the consequence of poor saturation and not necessarily due to healing. In tests of permeability, a measure of the flow as input and output, or the evolution of the weight of the specimen can check the good condition of saturation of the test specimen and thus avoid a misinterpretation of results.

When there is formation of calcite, white marks are often visible at the cracks. In 1936, the carbonation reaction (formation of CaCO_3) seems to cause full healing of cracks presented in numerous aqueducts (Loving, 1936). These cracks could go up to the surface openings of 1.5 mm and had been observed 5 years earlier, in 1931, shortly after the construction of aqueducts. Lauer and Slate (1956) confirm the importance of this reaction in the healing mechanism with the help of chemical and petrographic analyzes and has the help of microscopic observations of compounds forms (size, arrangement, distribution, crystal orientation). Subsequently, the formation of calcium carbonate on the lips of the crack is the

phenomenon that attracts the most attention because it is often regarded as the predominant phenomenon in self- healing (Hearn, 1998; Li & Yang, 2007; Neville, 2002). Edvardsen (1999) estimates that just consider this reaction as the cause of healing, other phenomena that have no or very little influence.

As mentioned previously, some studies conclude that hydration is the only explanation for the healing of concrete, while excluding the healing by the formation of CaCO_3 . In the beginning of research on self- healing, continuous hydration has often been regarded as the main phenomenon involved (Igarashi et al., 2009). Nevertheless, an analysis of the results of these studies allows us to see that they focus on concretes tested at a young age, that is to say cracks in the early days and "subject" of a healing. Thus the phenomenon of continuous hydration is essentially a phenomenon that has its importance for concretes at very young age and would therefore have much less importance for concretes walls (Hearn, 1998; Neville, 2002).

3. Study of healing: different approaches

In the literature, techniques and different approaches are used to discuss and study the healing. Given that this phenomenon has a particular interest in the cracked structures that would present a problems of sustainability and loss of bearing capacity of their damage. Most studies on self- healing include the creation of cracks. These last are generally induced tensile tests (Edvardsen, 1999, Homma et al., 2009; Hosoda et al., 2009; Lauer & Slate, 1956; Nanayakkara, 2003; Jooss & Reinhardt, 2003; Ying -Zi et al., 2005), and bending tests (Granger et al., 2007; Schlangen, et al., 2006) or sometimes even through compression tests (Yao & Zhong, 2007), although this is much less frequent. For other studies, cracking results from freeze-thaw cycles (Jacobsen et al., 1996, Jacobsen et al., 1995, Jacobsen & Sellevold, 1996; Sukhotskaya et al., 1983).

Following a cracking, the specimens are sometimes put in moist curing (often an immersion in water) and then refills to evaluate the mechanical advantages that could make healing products forms. Such studies compare the difference in terms of strength, stiffness, dynamic modulus of elasticity, damage, etc., before and after healing. These studies were then used primarily permeability tests and sometimes a test penetration of chloride ions. In the case of permeability tests, the decrease in the coefficient of permeability over time indicates the potential for healing. From the tests of permeability, it is sometimes possible to determine the

evolution of the crack opening equivalent in time, that is to say, to estimate the volume of the crack filled with healing products. The studies described above (mechanical approach or sustainability) are often accompanied by microscopic observations of different characterization techniques of materials, and chemical analysis to identify the nature and geometrical characteristics of the compounds form during the process healing.

The main techniques used in literature to study self-healing are:

- Continuous tests of permeability to water, with a continuous flow under a pressure gradient, during which healing takes place (Clear, 1985; Edvardsen, 1999; Hosoda, et al., 2009; Li & Yang, 2007; Nanayakkara, 2003) ;
- Immersion of specimens in water and testing water permeability (Homma et al., 2009; Hosoda, et al., 2009, Yang et al., 2009) or measuring air permeability (Argouges & Gagné , 2009; Ismail ,2006);
- Testing of penetration of chloride ions (Li & Yang, 2007);
- Mechanical tests (Granger, et al., 2007; Homma et al., 2009; Jacobsen, et al., 1996, Jacobsen & Sellevold, 1996; Lauer & Slate, 1956; Li & Li, 2011; Sukhotskaya, et al., 1983, Yang et al., 2009; Zhong & Yao, 2007);
- Chemical analysis of water (Clear, 1985; Edvardsen, 1999);
- Analysis by X-ray diffraction (Clear, 1985; Edvardsen, 1999, Ismail 2006; Jacobsen, et al., 1995; VC Li & Yang, 2007) and analyzed by Raman spectroscopy (Homma et al., 2009);
- Optical microscopy (Clear, 1985; Edvardsen, 1999; Hosoda, et al., 2009; Lauer & Slate, 1956) or digital microscopy (Homma et al., 2009);
- Chemical and petrographic analysis of compounds forms on the lips of the cracks (Lauer & Slate, 1956);
- Scanning electron microscopy (SEM) conventional or variable pressure (Ahn & Kishi, 2010; Edvardsen, 1999; Homma et al., 2009; Kishi et al., 2007; Li & Yang, 2007);
- Visual observation of the white precipitate at the cracks (Argouges & Gagne, 2009; Clear, 1985);
- Analysis of acoustic emission (Granger et al., 2007) whose technique "Ultrasonic Pulse Velocity, UPV" (Jacobsen & Sellevold, 1996; Zhong Yao, 2007);

- Analysis of the frequencies of resonances (Li & Yang, 2007);
- Technique of time reversal mirrors (Granger et al., 2008).

This first section aimed to define what is healing, more particularly autogenous healing. The main phenomena involved in this process have been described and the different approaches taken in the literature to study the phenomenon have been enumerated. It is now interesting to understand under what conditions it occurs and is favoured. A good understanding of the physicochemical processes (and parameters influencing them) which caused healing is necessary to know when this phenomenon occurs in the structures. A good understanding of the phenomenon may also permit the development of cement based materials with better healing ability. The following section aims to describe the main parameters that influence the ability to heal cracks.

4. Parameters affecting the healing process

- **Influence of crack opening and its length**

The healing potential of a crack is strongly linked to its opening. Several studies have studied the influence of crack opening on the ability of healing (Argouges & Gagne, 2009; Clear, 1985; Edvardsen, 1999; Hosoda, et al., 2009, Ismail 2006; Nanayakkara, 2003; Yang et al., 2009, Yi et al., 2011). These studies focus on the openings of cracks less than 0.4 mm (surface). Table 1 shows the crack openings studied in the various references listed above.

Tab 2: Most important studying of the healing for different values of opening cracks

Year	Authors	Opening of cracks
2003	Reinhardt & Jooss	0.05, 0.1 and 0.15 mm
2009	Argouges & Gagné	0.05, 0.1 and 0.22 mm
1985	Clear	0.1, 0.15, 0.2 and 0.3 mm
1995	Ramm & Biscopig,	0.2, 0.3 and 0.4 mm
2009	Hosoda, et al.	0.1, 0.2 and 0.4 mm
1999	Edvardsen	0.1, 0.2 and 0.3 mm
2003	Nanayakkara	0.1, 0.15, 0.2 and 0.25 mm
2009	Yang, et al.	0 to 0.3 mm
2006	Ismail	0.078, 0.092 and 0.117 mm
2011	Yi, et al.	0.03, 0.05 and 0.1 mm

By studying the ability of healing with the permeability tests, several studies (Argouges & Gagne, 2009; Clear , 1985; Reinhardt & Jooss, 2003) conclude that the healing is faster for the small initial opening crack than the big one.. Fig.8 illustrates this result.

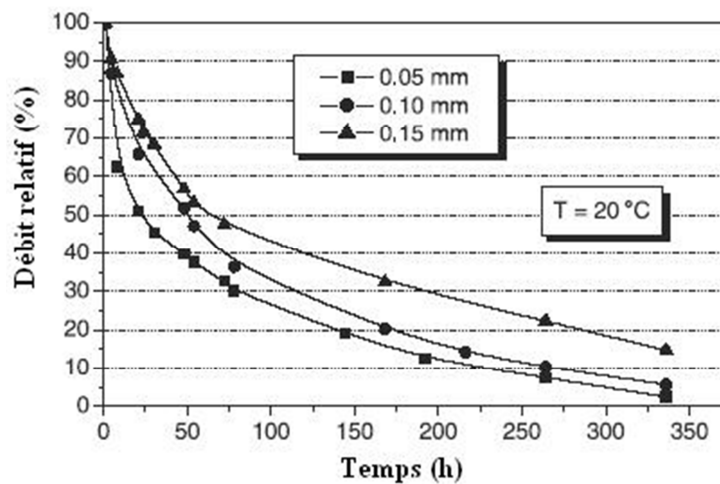


Fig. 8: Evolution of the relative flow vs. time for crack openings $w = 0.05$ mm, 0.1 mm and 0.15 (Reinhardt & Jooss, 2003)

This figure, which represents the evolution of the relative flow (% of initial flow) over time for crack openings of 0.05, 0.1 and 0.15 mm (Reinhardt & Jooss, 2003), shows that the relative flow rate decreases more quickly to the crack opening of 0.05 mm than for 0.1 and 0.15 mm. Argouges and Gagne (2009) obtained the same type of result: the

crack is more refined when the flow decreases with time, especially in the first month of storage.

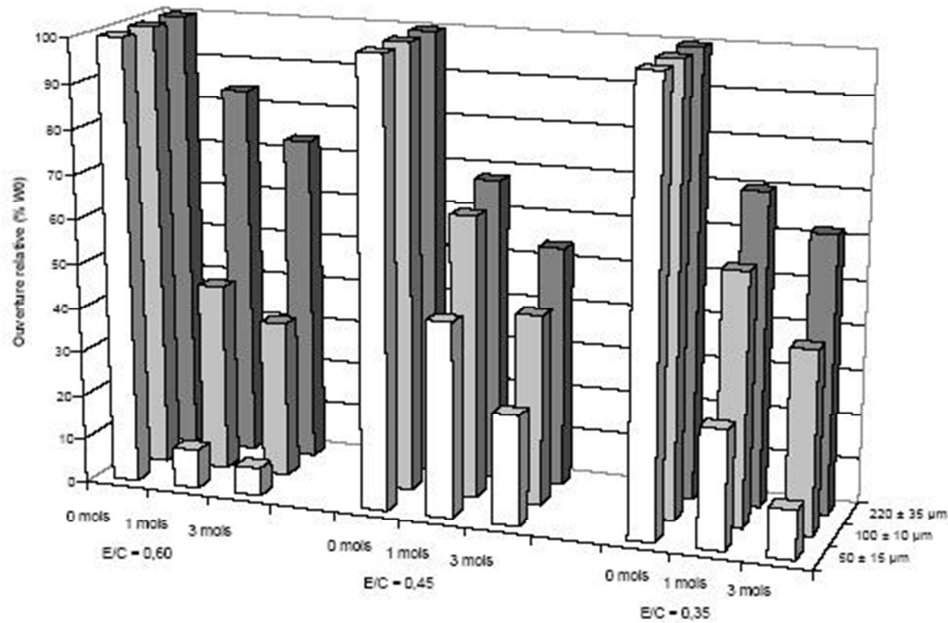


Fig. 9: Evolution of the opening of cracks of concrete vs. time (Argouges & Gagne,2009)

It is interesting to note that Fig.8 and Fig.9 represent the evolution of relative values. These values give information about the importance of the effects of healing, but not really on the mechanisms involved in the healing process. We must remain cautious in interpreting the results. Saying that a thinner crack heals faster does not necessarily mean that the healing process is different depending on the crack opening and crack a finer would have more potential to form products of healing. Indeed, after Argouges and Gagne (2009), the rate of product formation of healing forms on the lips of the cracks conserved one month has a relative humidity of 100% does not significantly change depending on the opening of crack. A same thickness of healing products has more impact in terms of gain durability, if the opening of initial crack is smaller, because the proportion of products filled with crack healing is more important.

Although several studies show that the effect of healing is faster in thinner crack, the literature is not entirely unanimous. Nanayakkara (2003) showed, by studying cracks with openings on the surface of the specimen between 0.1 and 0.25 mm and by deducting the

corresponding equivalent crack openings (deduced from the law of Poiseuille flow through a crack), there is a crack opening for which the optimal time needed to completely heal the crack is minimal (Fig.10). It would be longer to heal the crack to an opening smaller and larger than the optimum aperture. Nanayakkara (2003) explains this phenomenon by the fact that for a crack opening too low, the water flow is low and is thus longer react to calcium ions (Ca_2^+) from the cement paste to form of calcite (CaCO_3).

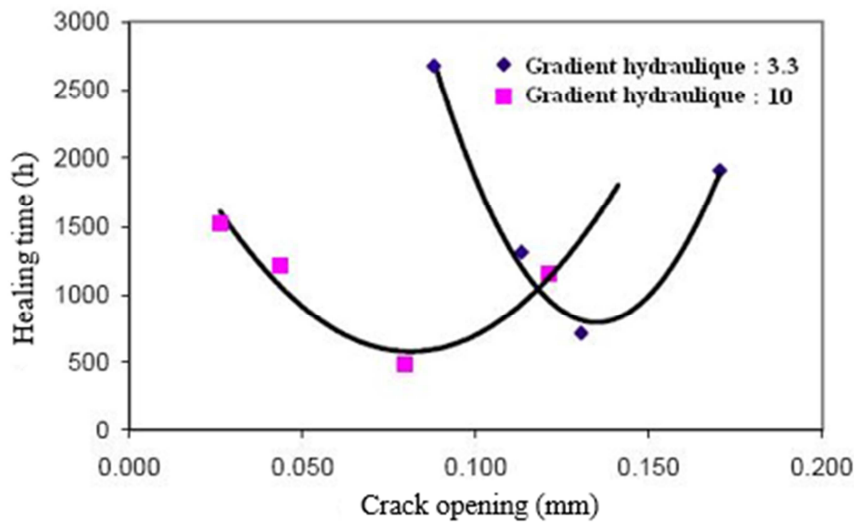


Fig. 10: Time required for full healing cracks according to their opening two hydraulic gradients (Nanayakkara, 2003)

On the other hand, when the crack opening is larger than the optimum aperture, the water flow in this case may be too high and, although a larger amount of CaCO_3 can potentially be formed, some of these new compounds are probably washing. Ismail (2006) indicates that for a crack opening of $78 \mu\text{m}$, healing is slower than for a crack open more than $117 \mu\text{m}$ after 1 month of storage in a humid chamber. This result then joined in part the idea of Nanayakkara (2003): the finer the crack does not always heal faster. Ismail (2006) combines this result has a lower capacity of penetration of water in the crack finer and more precisely the lack of intake of carbon dioxide (CO_2) dissolved while limiting the formation of calcite in the first months of storage in humid conditions. This explanation also supports the hypothesis Nanayakkara (2003). Due to lack of supply of CO_2 , it takes longer to react Ca_2^+ ions to form calcite.

In the preceding paragraphs, the influence of the crack opening on the sustainability was

discussed. Other studies have instead focused on the question of the influence of crack opening on the recovery properties of mechanical properties and damage by following the phenomenon of healing. Then, different testing techniques have been used. Yang (2009) studied the recovery properties of the resonance frequency of healed specimens as a function of crack opening. The test parameters of this study are different than in the previously cited studies. While, they focused mainly on ordinary concretes or mortars, Yang (2009) studied a fiber mortar containing PVA fibers. This material has the peculiarity of having a very ductile behavior in tension and a multi-micro cracking (very fine cracks up to reach break) while having a percentage of fiber length 6 mm less than 2% by volume. Moreover, rather than being canned in water continuously, this time specimens cracks are subjected to cycles of wetting-drying. The resonance frequencies obtained on specimens healed are compared to those obtained on a same specimen without healed cracks. The results indicate that for a crack width (w) less than 50 μm , a total recovery properties of the resonance frequency is possible. It therefore becomes identical to that of the specimen before cracking. Their recovery becomes less and less important when w evolves between 50 and 150 μm . These results are strongly linked to those obtained on the influence of crack opening on the durability of concrete gain brings the healing. Indeed, Yang (2009) validates the above conclusions by permeability tests that show a marked decrease of the permeability for $w = 50 \mu\text{m}$. For $w = 150 \mu\text{m}$, there is no difference in permeability between specimens that underwent 10 cycles of wetting drying and those who have not healed.

Schlangen et al. (2006), for their part, observed the influence of crack opening on the recovery of mechanical strength due to the healing. The parameters studied are the characteristics of cracks (Ex: length, roughness, etc..) Associated with different crack openings before healing. These cracks are created at young age by three-point bending until it reaches a certain openness. Subsequently, the crack lips are held together. Compressive stress is to keep the lips initiates cracks in contact during the healing process. The compressive loading was done in order to reproduce loading cases that may occur on the concrete at early age in dams for example. For this type of loading (bending), the crack size is more higher

than in the previously tests. Despite a certain dispersion of results, it seems there is no significant influence of the crack opening on the recovery properties of resistance to bending. Some authors studied the influence of hydraulic gradient on the critical crack opening can heal completely (Edvardsen, 1999; Nanayakkara, 2003).

❖ Influence of humidity

Healing can take place only in the presence of water since it is mainly the result of chemical reactions between water and certain compounds of concrete exposed close to the crack. Water is essential. However, it may be stationary or to flow through the crack. The ideal for there to be healing of cracks is a relative humidity of 100%, which is the case in most studies on this phenomenon. When the rate of moisture decreases, the self-healing is much less pronounced (Neville, 2002). This result can be explained by the fact that if we do not have 100% humidity there is a lot less CO_2 dissolved in water available for the reaction of calcite formation (Lauer & Slate, 1956; Neville, 2002). In addition, after Lauer and Slate (1956), $\text{Ca}(\text{OH})_2$ can react with dissolved CO_2 in water can migrate more easily if the water is in sufficient quantity. These authors also studied the difference in self-healing (in reality the recovery of tensile strength caused by healing) depending on whether the specimen was undergoing a wet cure (immersion in water: 100% humidity) or if it was left in an environment with a relative humidity of 95%. Their conclusion is that water saturation is essential for optimal healing with mechanical gain. For a relative humidity of 95%, the specimens found at best 25% of the strength of specimens immersed in water (100% humidity). In this study, the kinetics of healing (in terms of renewed strength here) also seems different rates depending on the humidity. For an immersion in water, the evolution of renewed strength in the first 90 days is parabolic in nature, whereas for a relative humidity (RH) of 95%, this evolution is slower and seems rather linear suggesting that the healing reaction takes place over a longer period of time.

5. The kinetics of healing of inactive cracks

The kinetics of healing appears faster in the early stages and then slows thereafter (Argouges & Gagne, 2009; Clear, 1985; Edvardsen, 1999; Hosoda, et al., 2009, Ismail 2006; Lauer & Slate, 1956; Nanayakkara, 2003; Biscopig & Ramm, 1995; Jooss & Reinhardt, 2003). When specimens (concrete or mortar) cracks are stored in water, the healing appears to occur predominantly in the first three months (Argouges & Gagne, 2009, Ismail 2006; Lauer & Slate, 1956). Kinetics is faster in the first month then slowed between the 1st and 3rd month after the creation of the crack (Argouges & Gagne, 2009). In case the healing is done under flow, that is to say that pressure is applied on the specimen to initiate a flow of water through the cracks or, three months of this period is reduced to a few tens or hundreds of hours, depending on the level exerts pressure (Edvardsen, 1999; Nanayakkara, 2003; Reinhardt & Jooss, 2003). This shows that although the kinetics of healing is dependent by the test conditions (crack openings, temperature, pressure, humidity, etc.).

The kinetics of self-healing is followed through several types of tests. This can be highlighted by evaluating the decreasing in the coefficient of permeability over time, by studying the recovery properties of certain mechanical properties or by observing the amount of product forms of healing. Lauer and Slate (1956) measure the evolution in time of the mechanical properties of a specimen crack heals. In their study, the increased resistance over time is of parabolic (faster at the beginning and then slows down). Yang et al. (2009) found a variation in the kinetics of healing by studying the recovery properties of the resonance frequency for specimens that have healed under wetting-drying cycles. Homma et al. (2009), whether by studying mortars with polythene fiber, steel or a mix of both (hybrid fibers), found that the thickness of the product (formed by healing) is more important in the early days and then slows by on. This result has been validated subsequently by tests of permeability.

This healing kinetics may be explained by the phenomena involved in the healing process. In the case of concretes at very young age, the healing would be associated primarily to a continuous hydration of anhydrous cement (Neville, 2002; Schlangen, et al., 2006; Zhong & Yao, 2007) and the kinetics of healing could then be explained by the nature of the hydration process of the early days of concrete. After 28 days, most researchers agree that the formation of calcium carbonate is the main cause of self-healing of mature concretes (Yang et al., 2009). However, once the nucleation of calcite, it is possible to distinguish two phases of growth

(Edvardsen, 1999). The first is controlled on the surface, while the second results from a phenomenon of diffusion of Ca_2^+ ions through the concrete and the calcite layer already formed.

The first phase of growth occurs while there is a sufficient amount of Ca_2^+ ions on the surface. Growth of calcite then occurs rapidly. Once these Ca_2^+ ions are no longer available directly on the surface of the crack, they diffuse through the concrete thanks to this concentration gradient between the surface and the crack inside the concrete. During this growth phase, the time required for ions to diffuse through the concrete and already formed the layer of calcite is often longer than the time necessary for these same ions to be absorbed by the layers through which it passes. Therefore, in this phase, the growth rate depends on the diffusion rate and thus the microstructure of concrete. These phenomena may therefore explain the growth kinetics decreasing healing observed in the literature.

6. The healing effect on the mechanical behavior

It has been shown previously that healing causes a decrease in permeability and that this phenomenon has an interest in sustainability. Another aspect of healing is to see if this phenomenon may provide an advantage in terms of mechanics, restoring the strength or gain of rigidity. Several studies have examined to understand the effect of healing on the mechanical behavior of concretes. Mechanical tests (tensile, bending and compression) and non-destructive testing (acoustic techniques) were performed to evaluate the mechanical behavior of the damaged specimens and the evolution of the healed cracks. The acoustic emission tests have enabled to characterize the micro-cracks in a cracked specimens before and after healing (Granger et al., 2007). These approaches give a better understanding about the cracking of a healed crack. This damage starts with a shattered healing products. Subsequently the pre-existing crack continues to spread (Granger et al., 2006). Li and Yang (2007) also noticed that, if an uniaxial tension is applied to a healed specimens, cracking takes place generally in the healed cracks. This is explained by the low resistance of healing products compared to products of hydration (Li & Yang, 2007). The observation of surface

cracks of lips healed and unhealed shows that the non-healing concrete presents a dense structure compared to that of crystal forms during healing (Granger et al., 2007; Granger et al., 2008; Jacobsen, et al., 1995). These come in the form of clusters less dense and therefore have different mechanical properties of the material before cracking. This would explain that when reloading a healed specimen, the damage take has first place in the healed zones.

Later in this section, we summarize the main results obtained in terms of mechanical effects has caused by healing, depending on the type of initial damage and mechanical properties tested.

7. The benefits of self-healing

7.1. Gain of mechanical properties after being subjected to freeze-thaw

Jacobsen and Sellevold (1996) have noted a small increase in compression resistance of 4 to 5% on specimens of ordinary concrete healed after three months of storage in water due to damage by freeze thawing. During these cycles, the specimens had lost 22 to 29% of their initial compressive strength. In another study in which the identical specimens were preserved in three months in saturated lime water after having undergone various cycles of freezing-thawing, the specimens underwent 31 cycles with a recovery properties were present in 10% of the compressive strength whereas specimens that have undergone more cycles (61 and 95 cycles) did not show gain resistance (Jacobsen et al., 1996). Parallel to these tests, analysis of acoustic tests conducted on identical specimens showed that the resonance frequency (dynamic modulus of elasticity) have found, after healing, 85 to 98% of their initial value. Healing would have absorbed much of the damage to freeze thaw, but this phenomenon don't recover the compression strength. Observation of cracks showed that they were only partially filled by the healing products, which can explain the small increase in compression strength after healing (Jacobsen et al., 1995). The positive effect of healing, after a freeze-thaw damage, has also been highlighted by Sukhotskaya et al. (1983). They have found that, proceeding with a regular periods of immersions water at certain times during the freeze-thaw

cycles, can limit the damage to these cycles, thus increasing the frost resistance.

Jacobsen et al. (1995), Sukhotskaya et al. (1983) also noted a gain of dynamic elasticity modulus. The immersion of the specimens in the water periodically decrease the loss of compressive resistance to freeze-thaw: the compressive strength after 300 continuous cycles (without immersion in water) has decreased by 18%, while this reduction is only 7% when there is an immersion after 500 cycles.

7.2. Gain of mechanical properties after damage by bending

Granger et al. (2007) have carried out a bending tests on the 3 points on a matrix of a high-performance concrete. It was cracked (10 μm) and then recharged after storage in water ranging from 1 to 20 weeks. They observed that healing allows a global recovery in rigidity of damaged concrete and a slight recovery in bearing capacity. When the specimen is preserved in the air, the mechanical properties of the samples tested are not improved compared with those obtained in the case of a reload directly after cracking, unlike the case of storage in water (Fig.11). Their recovery of partial mechanical properties of specimens stored some time in water is especially important as the immersion time is long, this being associated with a greater advanced the healing process (Fig.12). The rigidity of the healed specimens after immersion in water of about 10 weeks is approaching to the initial rigidity of the healthy specimen. Nevertheless, the bearing capacity and resistance (bending) of the non-cracked concrete are not completely reached due to the healing.

Schlangen et al. (2006) also study the mechanical recovery properties of cracked concretes at early age by a 3-point bending test, until it reaches an opening crack of 50 μm . The healing conditions are different in this study because the specimen is subjected to a compressive force (0, 0.5, 1 or 2 MPa) to maintain the two crack lips closed. It is then immersed in water and then retests 3 points bending. Schlangen et al. (2006) found that recovery properties of the flexural strength and the stiffness is possible when the crack is made at very young age and that the lips of the crack are then kept closed due to the compression.

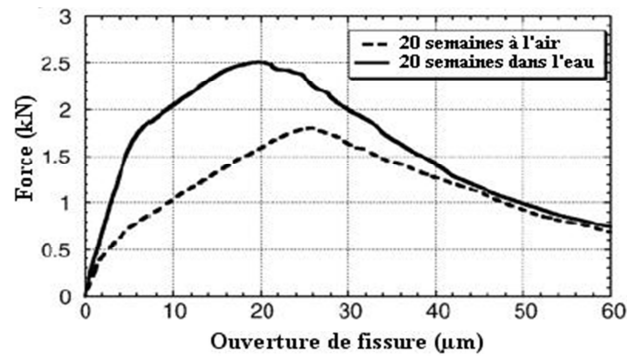


Fig. 11: Mechanical behavior of specimens at reloading after storage in air or water for 20 weeks (Granger et al., 2007)

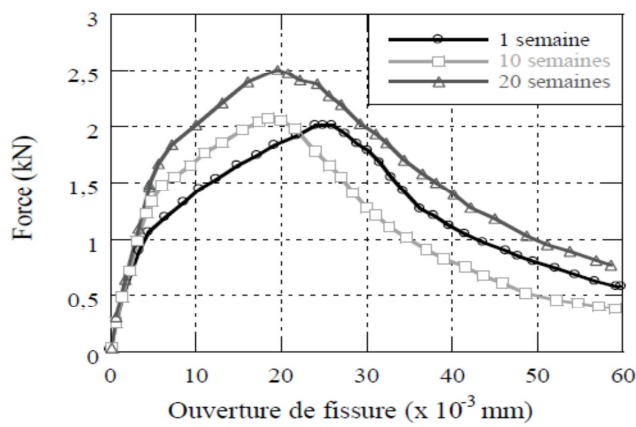


Fig. 12: Mechanical behavior of specimens at reloading, after different durations of storage in water (after a Granger et al. (2007))

7.3. Gain of mechanical properties after damage in traction

Lauer and Slate (1956) studied the tensile strength of a cement paste of w / c ratio of 0.4. After the specimens have been immersed in water for 90 days, the first tensile test shows that

25.1% of the tensile strength has been found after healing. When the specimen had been cracked, they are tested at 7 days and then again after 90 days in water, 14.2% of resistance was reached. Thus, there is a resurgence of strength tension when the specimens are cracked at a young age and the proportion of that gain appears to occur in the first 90 days. Lauer and Slate (1956) have seen the size, arrangement, shape, orientation of compounds forms of healing within the crack and the proportion of the surface crack covered by the compounds. The resurgence of resistance could be explained by the interpenetration of healing products in the surface of the cement paste, by Van der Waal forces between the crystals, the paste and aggregates, as well as the link between crystal forms (Lauer & Slate, 1956). By observing the thin sections under the microscope, they also noted that the increase in resistance is directly related to the percentage of the crack where both lips are in contact (instead of full healing) and the area of the crack filled with these compounds.

Li and Yang (2007) have also studied the recovery properties in uniaxial tension test of a cracked specimens. The cement composite has the particularity to enable a very fine crack and a very ductile behavior in tension. This material contains less than 2% of PVA fibers of length 8 mm, no large aggregates and ductility has a 200 to 500 times greater than that of a concrete reinforcing by a conventional fiber. After healing, the specimens are reloaded and their tensile strength is compared to: the behavior obtained during the first loading and the behavior of unhealed specimens. Li and Yang (2007) observed a recovery properties of the initial dynamic elasticity modulus for most specimens tested when the specimen has undergone 10 cycles of wetting-drying (periods of 24 h drying at 21°C ambient air and 50% RH). Moreover, after these 10 cycles of wetting-drying, the specimens reloaded show a rigidity. These results are consistent with the results of resonance frequency, which are directly related to the stiffness of the material.

Li and Li (2011) continued the studies of the same material as that studied by Li and Yang (2007). The specimens are always triggered by traction. Nevertheless, this time the specimens preloaded at 0.5, 1 or 1.5% tensile strain are immersed in saline (NaCl) for 30, 60 or 90 days to observe the healing process in a marine environment or exposed to salt. The specimens are

then retested in tension. These specimens, immersed in this solution, show a decrease in resistance to first cracking and ultimate strength of 7 to 13% compared to the specimen preload. Nevertheless, immersion in the NaCl solution does not affect the ductility of the material nor the multicracking. Thus the healed specimens show a reversal of rigidity and tensile ductility compared to the unhealed specimens. Healing products can reseal the microcracks, but also reshape links between fibers and matrix (Li and Li, 2011).

7.4. Gain of mechanical properties after damage in compression

The studies examining the effect of healing on specimens loaded in compression are much less numerous. Nevertheless, Zhong and Yao (2007) were damaged a cylinder by compression of an ordinary concrete and high-performance concrete at a young age. They found, after UPV test (Ultrasonic Pulse Velocity), some repair of the damage due to the healing phenomenon. They also found that the recovery of compressive strength due to healing is dependent on the degree of damage to specimens:

- More damaging the concrete at an early age more the renewed strength is important.
- The effect of healing decrease with the increase of damage.

Zhong and Yao (2007) explain this by the fact that healing is associated with the hydration of anhydrous cement grains in concrete. Thus, if the damage is not large enough, the amount of anhydrous cement available for hydration remains low. Nevertheless, if the damage exceeds a certain threshold, the anhydrous cement is available, but the damage is too great for healing products can form bridges between the lips of the cracks. In this case, the impact of healing on the recovery properties of compressive strength becomes weaker.

Conclusion

This literature review has to take stock of current knowledge in the field of healing. There are a lot of information about gains in terms of sustainability and on the mechanics that can bring healing cracks. Researchers trying to understand and identify different phenomena have caused scarring. An effort is also made to target parameters that influence this process. Many experimental techniques have been used in various research projects in order to visualize and report, quantitatively or qualitatively, the phenomenon of healing stage of product formation was that of healing their damage during reloading. As a measure that seems a new study, the phenomenon is becoming increasingly well understood and it is possible to have an idea about the conditions that favor or not the process. Knowledge of chemical reactions at the origin of the phenomenon allows the development of concretes with a greater capacity for healing.

*Chapter 3: The different techniques of the
Non Destructive Testing (NDT)*

Introduction

Methods of nondestructive evaluation of structures are derived from the need for engineers to ensure the safety of goods and people. This type of evaluation has long been used in high-tech industries, but much more recent in civil engineering.

The techniques of nondestructive testing of materials and structures are tools of investigation and diagnosis. They allow contractors and builders to have an inventory of structures and pathologies.

1. Magnetic Control

This method (Fig.13, Fig.14) is based on magnetic forces and does highlight defect on the surface of magnetic materials (Bray & McBride, 1992). By magnetizing the part to be tested, lines of force are disturbed at the location of each discontinuity in the properties magnetic (crack or inclusion non-magnetic). Small particles of iron suspension of iron filings (developer), spread over the surface, where the focus lines of force emerge.

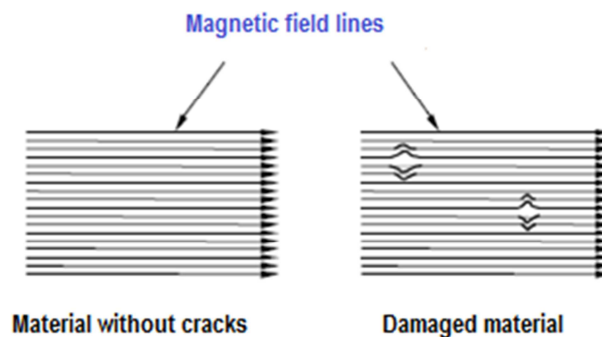


Fig. 13: Principe of the magnetic control. (Bray & McBride, 1992)

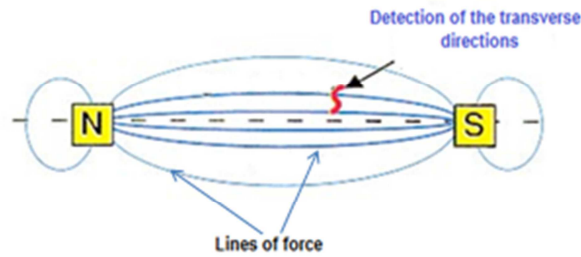


Fig. 14: Test of the magnetic control

The lines of force (and therefore the flow) are substantially parallel to the north-south axis. This method makes it possible to detect discontinuities transverse (or perpendicular) to this axis.

2. X-ray tomography

This technique (Fig.15, Fig16) is directly derived from the medical world (Bray & McBride,1992; Fournier & Brousset, 2006) . The devices used are quite comparable to the "scanning" medical. The major advantage of this technique is that it achieves 3-D images of a defect.

In addition, the images are delivered in digital form, which simplifies their processing. Furthermore, new devices called "micro-tomography" are able to obtain a resolution of a few tens of microns.

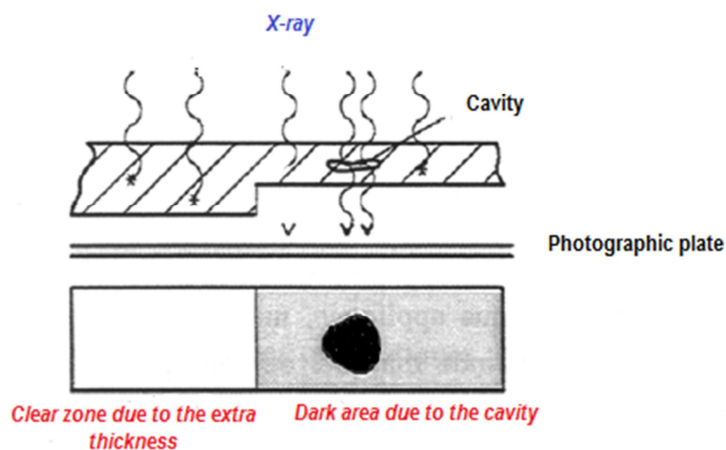


Fig. 15: Test of the X-ray

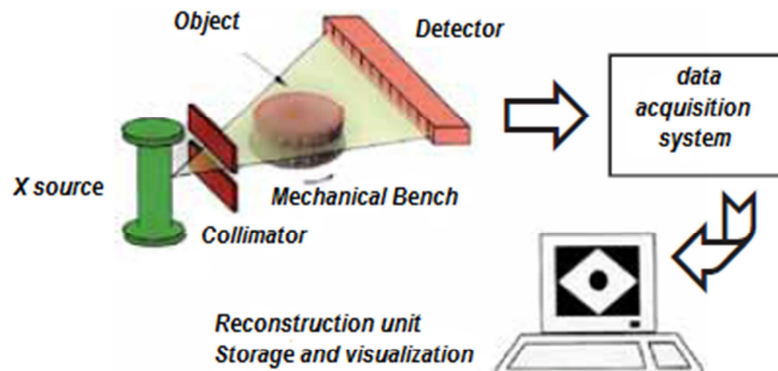


Fig. 16: Test Procedure of X-ray

3. Infrared thermography

Thermal NDT (Fig.17, Fig.18) methods (Ettemeyer, 2004; Huber & Berger, 2006) are based on detection of a disturbance of the thermal field that appears when, in the structure to be inspected, it induces a permanent or transient heating. The distortion can be induced by the presence of a defect in one of the interfaces. Methods based on the temporary transfer of heat supply as much information, they are:

- Rapidly heating the surface to be inspected,
- Record changes in temperature on surface with an infrared camera.

The fault behaves as a thermal barrier and the cooling is slower than over a healthy area.

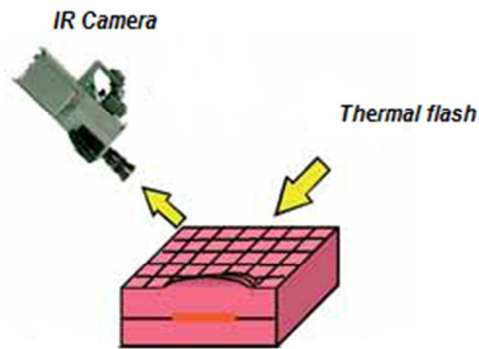


Fig. 17: Principe of Infrared thermography

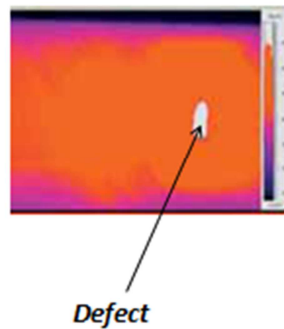


Fig. 18: Defect seen by Infrared tomography

The limitations of this technique are mainly from the thermal diffusion that depends on the nature of the materials and thickness.

Infrared thermography is a method of controlling overall relatively easy to implement and which, in some favorable cases, to establish a relationship between thermal diffusivity and the membership level.

4. Ultrasonic and Acoustic emission

Ultrasounds (Kouzoubachian, 2006) (Fig.19) are mechanical vibrations of electrical origin, which propagate in a solid or liquid media. The principle is to emit an ultrasonic wave that propagates through the test piece and is reflected in the manner of an echo on the obstacles it encounters (faults, cavities). These waves are emitted by one or several "translators" manipulated by an operator or an automated system.

The use of a "coupling", usually an aqueous gel between the probe and the sample to allow a good transmission of the waves between them, is often necessary.

The echoes are analysed on a screen by the controller or processed in a measuring system for automatic installations. These methods are sensitive to detect the discontinuities in the defected materials by transmission and reflection.

Acoustic emission also uses the wave propagation in materials: when the material changes, warps, cracks under the action of an external stress (mechanical, thermal, chemical, etc..), he creates spontaneous waves "elastic".

The discontinuous release of energy in the form of trains of mechanical waves occurs for each change of state of matter. These trains of waves propagate in the material according to its acoustic properties and geometry and reach the sensors installed on the equipment to examine.

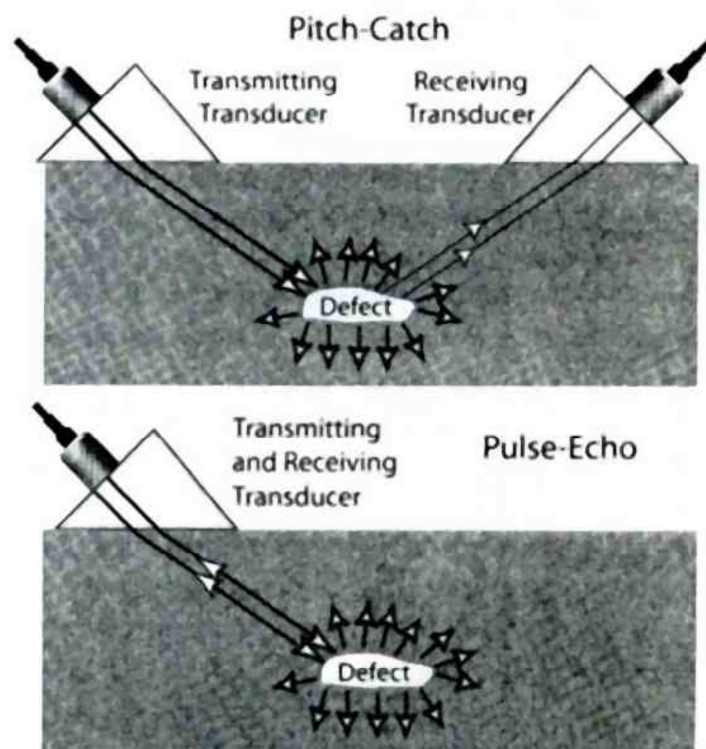


Fig. 19: Test of transmission and reflection of a wave

The signals collected and processed by a measuring system used to locate the area of degradation (a mapping) and to evaluate its intensity as a function of the stress imposed. Measurement quality depends in part on the choice and positioning of sensors. In the next chapter, this method will be explained with more details.

5. Criterias for choosing a NDT method

We just very briefly present the main NDT techniques applicable to the bonding and application domain.

Each case is unique; it is difficult to choose a simple control technique. If certain considerations or factors are neglected during the implementation of the means of control, it can quickly lead to failures such as the outstanding reliability of the method or results. It is imperative to take into account not only the physical and technical parameters but also the importance of human factor and procedures manual and possibly the financing of feasibility or preliminary work of developing the process. Nevertheless two main selection criteria emerge:

- ❖ NDT must be technically suitable for the test object:
 - ✓ Good detection, interpretation of results without ambiguity
 - ✓ Mechanical compatibility
 - ✓ Security
- ❖ NDT must be economically adapted to the goal
 - ✓ Equipment cost - outstanding reliability,
 - ✓ Periodic control

This last criterion is often crucial in the choice. As the table below (Tab.3) demonstrates, the cost of certain techniques is not negligible.

With technological advances of recent years, particularly computer processing, these control techniques are increasingly used in industry. These means of control have become automated, reliable and simple use.

The fact remains that the qualification of operators who will implement these controls remains paramount.

Tab 3: Summary of techniques of NDT: Costs, advantages & drawbacks (Kouzoubachian ,2006)

Techniques	Equipment costs (K€)	Advantages	Drawbacks
Acoustic	20 to 300	<ul style="list-style-type: none"> - Good sensitivity - Location and sizing of defects - Well suited to automated 	<ul style="list-style-type: none"> - Coupling the sample with sensors
Thermography	40 to 200	<ul style="list-style-type: none"> - Cartography 	<ul style="list-style-type: none"> - Thermal diffusivity according to the material - Limited to the interfaces near the surface - Characterization of defects
X-ray	250 to 400	<ul style="list-style-type: none"> - Industrial Method 	<ul style="list-style-type: none"> - Expensive equipment - Safety related to radiation - Image interpretation
Optical methods	200	<ul style="list-style-type: none"> - Good resolution 	<ul style="list-style-type: none"> - Environmentally sensitive - Sample must be subject to stress

The last table shows the many advantages of the acoustic method and especially its cost is less expensive compared to other techniques.

In addition, statistics (Fig.20) show that the acoustic techniques are increasingly used to make non-destructive testing.

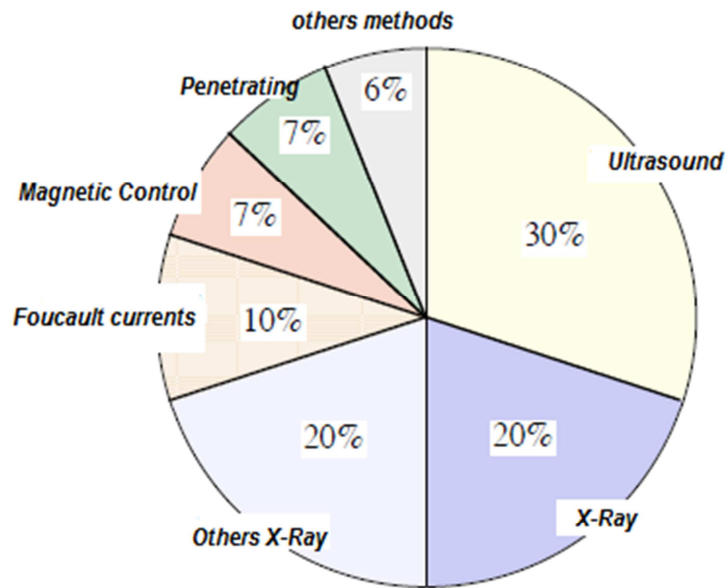


Fig. 20: The different percentages of the utilization of each NDT techniques (Shull, 2002)

Conclusion

The term non-destructive testing grouped all techniques and processes capable of providing information on the health of a structure without introducing alterations detrimental to their future use. In this sense, non-destructive testing (NDT) appears as a major component of quality control products. Each technique presented in this chapter allows certain advantages and disadvantages in terms of instructions and cost. The technique of the acoustic wave is the most used and most pertinent so it will be adopted to continue the work.

Chapter 4: Comparison between the linear and the nonlinear acoustic & the different techniques used in the nonlinear acoustic waves

Introduction

The evaluation of structural changes of materials and constructions and monitoring their ultimate strength and endurance in operation is required for many industrial structural integrity problems. Especially the evaluation of accumulated damage or degradation in the material properties at the early stage of fracture is important in refinery plants, nuclear power plants, or aircraft parts in order to ensure their structural safety. One of the most useful non-destructive ways of evaluating material degradation is the ultrasonic method since the characteristics of ultrasonic wave propagation are directly related to the properties of the material.

1. Linear acoustic

Ultrasonic linear waves can be of different types according to the mode of vibration of the material. There are:

- Body waves: longitudinal wave (compression or primary waves), transverse wave (shear waves or secondary waves).
- The guided waves: Rayleigh wave, Love wave, Lamb wave...

This section describes the body waves.

Body waves are mechanical vibrations that propagate inside the material. Depending on the mode of propagation, we define two types of waves

- ✚ **Longitudinal waves:** Their transition in a medium results in a succession of expansions and compressions (Fig.21). The direction of the deformation generated is parallel to the direction of propagation of the wave. Their velocity is denoted V_L or V_p .

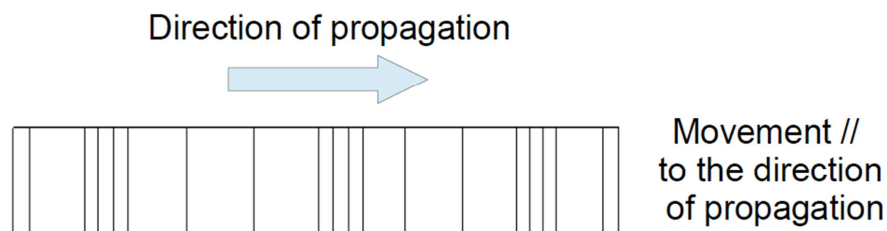


Fig. 21: Longitudinal wave

✚ **Shear waves:** The movement of particles accompanying their passage is perpendicular to the direction of propagation (Fig.22). Shear waves can propagate only in solids. But the fluids (gas or liquid) do not constitute a support material for this type of vibrations, with the exception of highly viscous liquids where shear waves arrive to spread despite high attenuation. They are slower than longitudinal waves. For the shear wave propagation velocity is denoted V_T or V_s

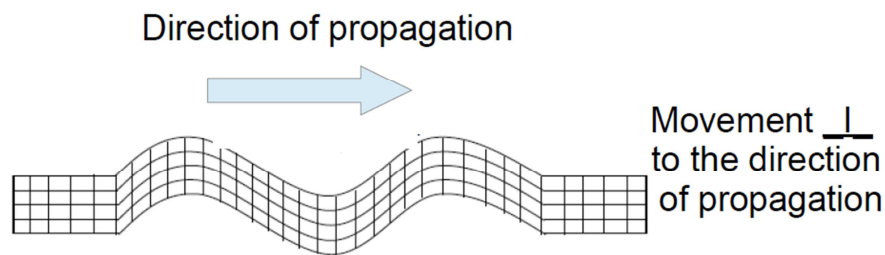


Fig. 22: Shear wave

2. The difference of the response between the linear and nonlinear acoustic wave

Traditional ultrasonic NDE is based on linear theory and normally relies on measuring some particular parameter (sound velocity, attenuation, transmission and reflection coefficients) of the propagating signal to determine the elastic properties of a material or to detect defects (Birks, 1991). The presence of defects changes the phase and/or amplitude of the output signal, but the frequency of the input and output signals is the same. However, the conventional ultrasonic technique is sensitive to gross defects or opens cracks, where there is an effective barrier to transmission, whereas it is less sensitive to evenly distributed microcracks or degradation. An alternative technique to overcome this limitation is nonlinear ultrasonic. The principal difference between linear and non-linear acoustic (Fig.23, Fig.24) is that in the latter the existence and characteristics of defects are often related to an acoustic signal whose frequency differs from that of the input signal. This is related to the radiation and propagation of finite amplitude (especially high power) ultrasound and its interaction with discontinuities, such as cracks, interfaces and

voids. Since material failure or degradation is usually preceded by some kind of non-linear mechanical behavior before significant plastic deformation or material damage occurs, considerable attention has recently been focused on the application of nonlinear ultrasonic (Jhang, 2000; Jeong, 2003). Linear acoustics deals with propagation of vibrations through medium. Deviations from the equilibrium state of a medium that are caused by these vibrations are assumed to be small; that is, the propagating wave is assumed to have small amplitude or a low intensity. The propagation of finite-amplitude (or high-intensity) ultrasonic waves is accompanied by a number of effects, whose magnitudes depend on the vibration amplitude. Investigation of the propagation of finite-amplitude elastic waves in gases, liquids, and solids has been of continuing interest. The presence of nonlinear terms in the wave equation causes intense acoustic waves to generate new waves at frequencies which are multiples of the initial sound-wave frequency. The nonlinear third-order elastic constants of solids were first measured in the early 1960's and harmonic generation of bulk waves was soon reported by a number of authors (Parker, 1964; Carr, 1964). This resurgence of interest led to more convenient formulations of nonlinear acoustic propagation by (Thurston & Brugger, 1964) and by (Wallace, 1970).

Thereafter, it was found in a solid exposed to a strong ultrasonic field that there occur such nonlinear effects as sub-harmonic generation, shift of resonance frequency, or mixed frequency response as well, besides the higher harmonic generation.

All these phenomena can exert a strong effect on the structure and interaction of solids, making intense ultrasound applicable in material characterization. Moreover, these effects are enormous in damaged material but nearly un-measurable in undamaged materials, hence the interest in applying nonlinear ultrasonic. Those are expected to be much more sensitive to micro-damage than the conventional linear characteristics of ultrasonic wave, where the ability of several nondestructive and destructive methods is summarized in the detectable defect size.

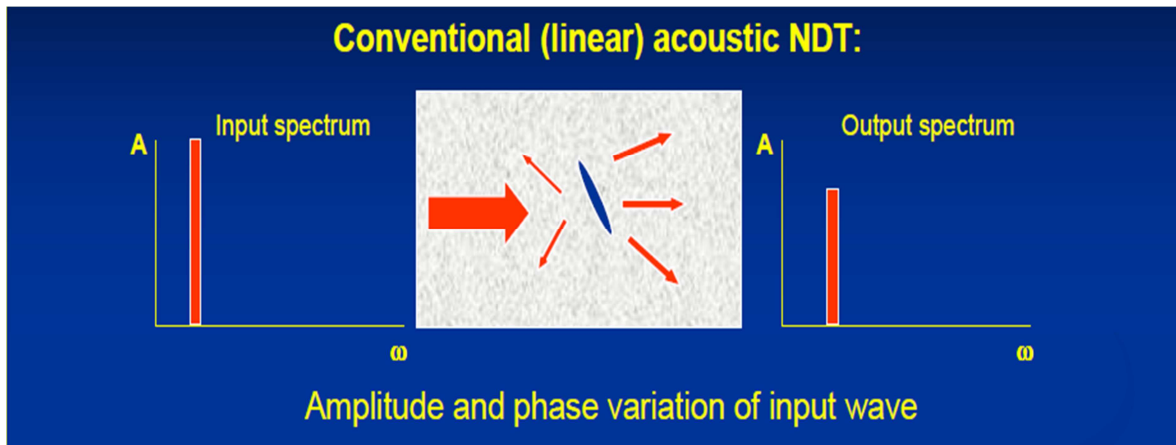


Fig. 23: The linear acoustic response

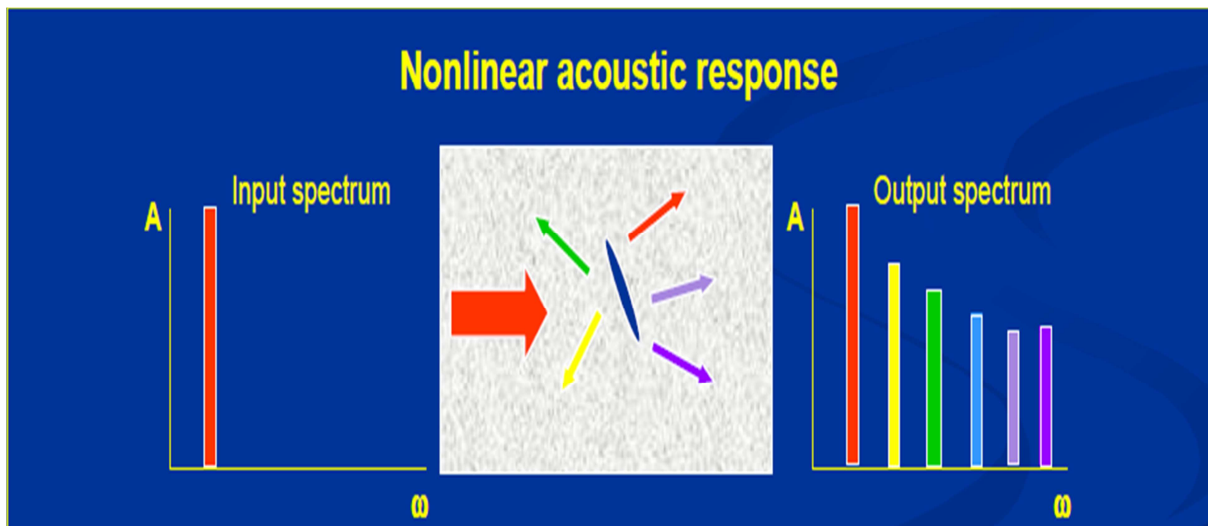


Fig. 24: The nonlinear acoustic response

3. The different techniques using in the nonlinear acoustic waves

3.1. Mixed Frequency Response

One of the simplest ways to evaluate nonlinear acoustic properties of a material is to measure the modulation of an ultrasonic wave by low-frequency vibration (Van Den Abeele, 2000; Van Den Abeele, 2001; Korotkov, 1994).

This method is known as nonlinear wave modulation spectroscopy (NWMS). The physical nature (Fig.25, Fig.26) of this modulation can be explained simplistically as follows (Sutin, 2005):

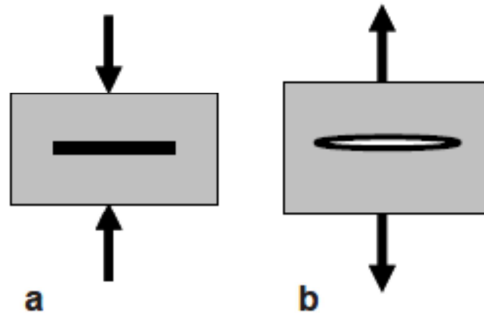


Fig. 25: Sample with flaw: a - closed by vibration compression, b –open under dilation (Sutin, 2005)

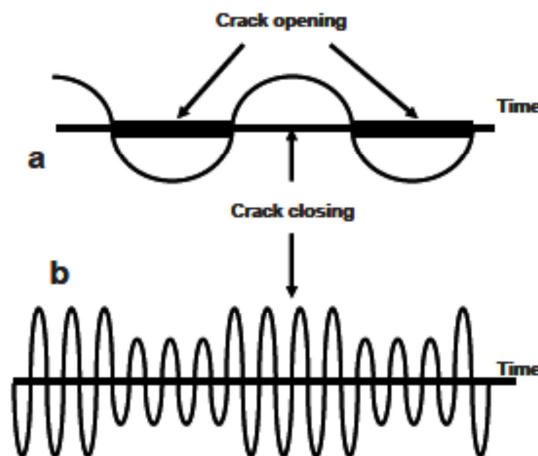


Fig. 26: Amplitude modulation of probe signal: (a) vibration, (b) ultrasonic signal (Sutin, 2005)

Non-resonance methods are used to study nonlinear effects on elastic waves propagating through the medium. According to the previous experimental work (Jun, 2010; Payan, 2010), intermodulation phenomena can be observed in the structural response of damaged material when an excitation as shown in Fig.27 is used. In particular, the excitation is made by the superposition of two sine waves with fundamental frequencies f_1 and f_2 respectively.

The spectrum response of the sample is characterized by two effects: the presence of harmonics of both fundamental excitations frequency (nf ; $n=1,3,5\dots$; for example: $3f_1$, $5f_1\dots nf_1$ and $3f_2$,

$5f_2 \dots nf_2$), and the generation of sidebands around f_2 ($f_2 \pm nf_1$; $n=2,4,\dots$; for example: $f_2 - 2f_1$, $f_2 + 2f_1 \dots f_2 - nf_1, f_2 + nf_1$) as shown in Fig. 28.

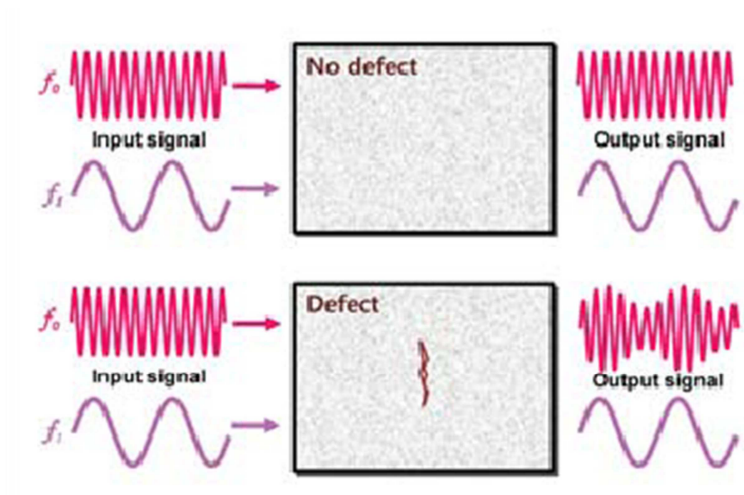


Fig. 27: Illustration of the nonlinear acoustic vibro-modulation effect

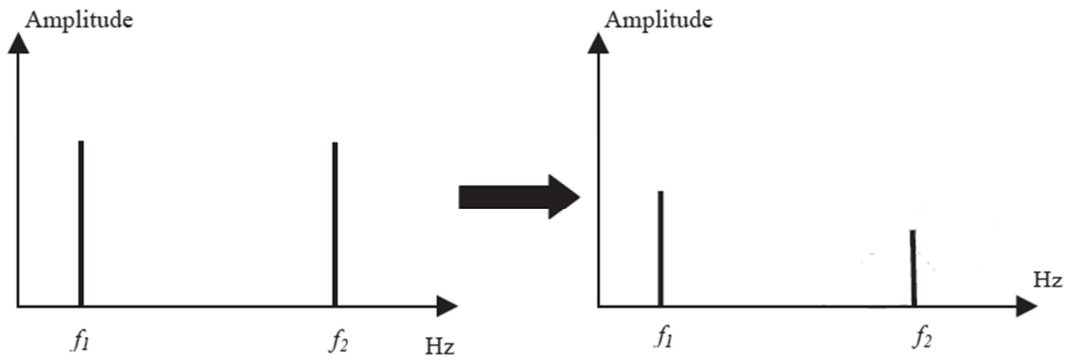


Fig. 28: Response in the case of linear acoustic

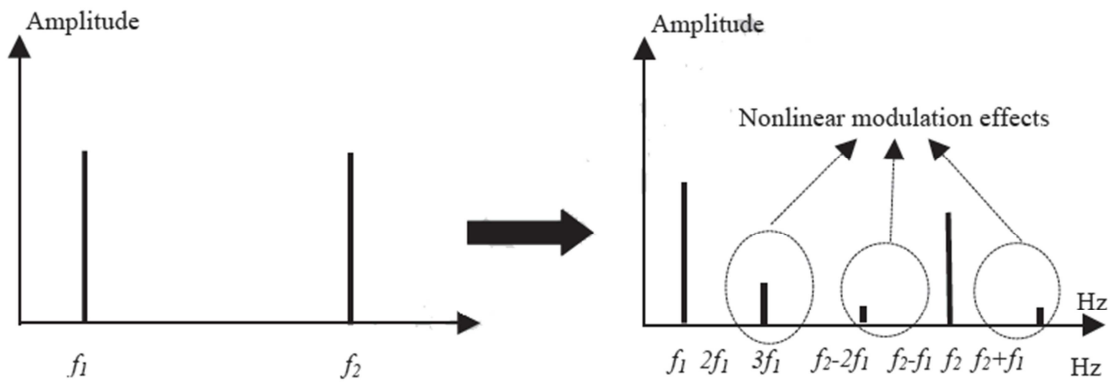


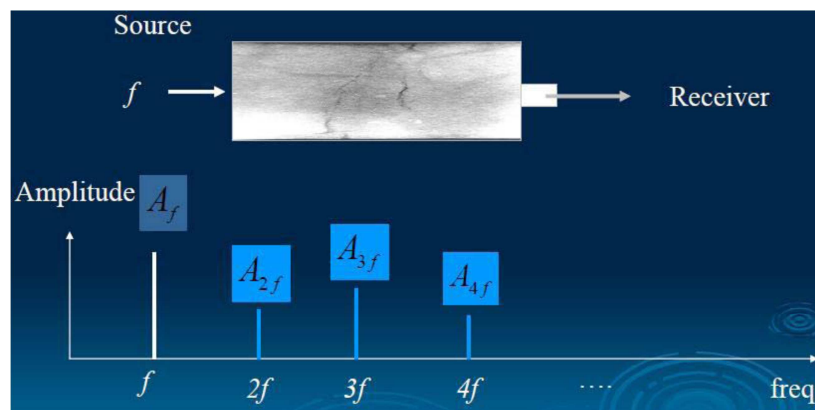
Fig. 29: Response in the case of nonlinear acoustic

Alternatively, the vibro-modulation technique (Zagrai, 2004) utilizes two excitation signals: an ultrasonic probing signal and a low frequency vibration as shown in Fig. 29. An exciting vibration at f_2 creates appreciable stress in the material affecting interfaces at all scales of damage. An ultrasound probe wave f_1 traveling through these interfaces is modulated due to vibration induced changes in the interface condition and, as a result, additional spectral components appear at the frequencies $f_1 \pm n.f_2$. The presence and the level of modulation can be used for damage assessment (Straka, 2008; Yost, 1998; Donskoy, 2001).

3.2. Higher Harmonic Generation

Higher harmonic generation (Guillaume et al., 2008; Tae & Keyung, 2009; Ankit & Francesco, 2010) is the most classical phenomenon that the waveform of incident wave is distorted by the nonlinear elastic response of medium to the incident wave, and so that higher harmonic waves are generated in the transmitted wave as shown in Fig. 30.

This phenomenon can be understood simply by considering the nonlinear system (Zaitsev, 2010). Let's consider a 2nd order nonlinear system as shown in Fig. 31, and a sine wave is given as input. Then the output of this system will have 2nd order higher harmonic wave component.



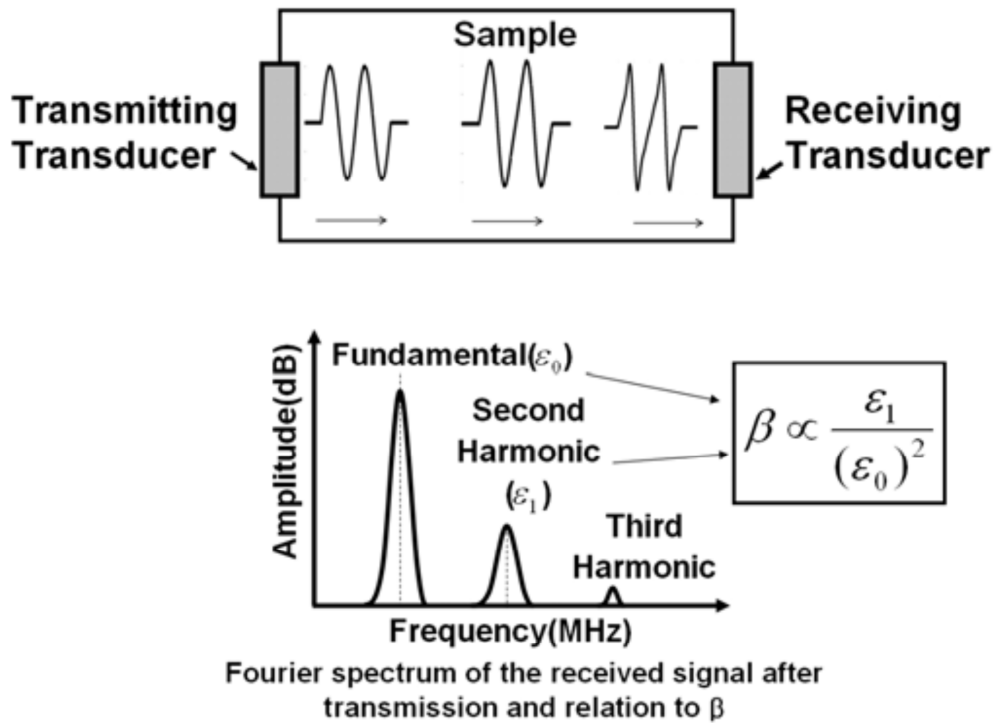


Fig. 30: Distortion in the waveform during propagation by the nonlinear elasticity and higher harmonic generation power of fundamental

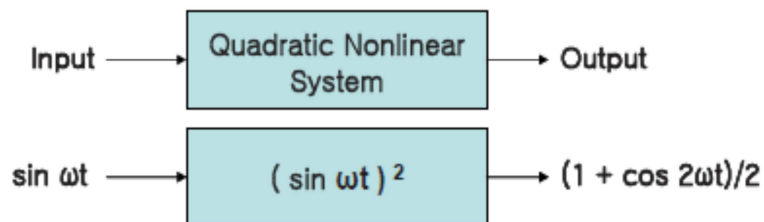


Fig. 31: 2nd harmonic generation in the quadratic nonlinear system

When we consider 3rd or higher order nonlinearity, then the system output will have 3rd or higher harmonics also. However, usually the nonlinear effect of 3rd or higher orders is much smaller than 2nd order, therefore we used to consider up to 2nd order nonlinearity.

Physically the phenomenon of higher harmonic generation is related with the nonlinearity in the elastic behavior of material, as shown in Fig. 32. That is, the relationship between stress σ and strain ϵ is nonlinear, which is called the nonlinear version of Hooke's law as shown in Eq. 1 for the simple one-dimensional case (Jhang, 2000; Jeong et al., 2003; Na et al., 1996) :

$$\frac{\partial \sigma}{\partial \epsilon} = E(1 - \beta \epsilon + \dots) \quad \text{Eq. 1}$$

Where, E is Young's modulus and β is 2nd order nonlinear elastic coefficient which called the nonlinear parameter.

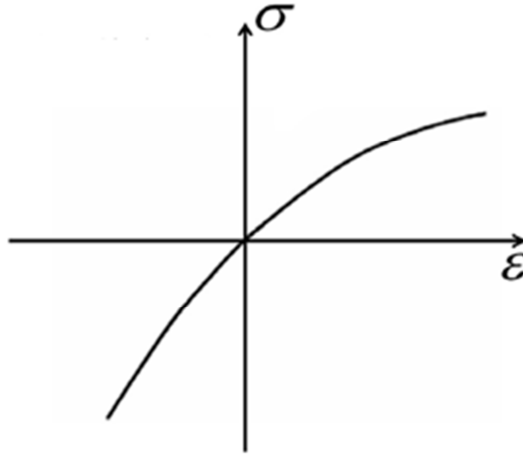


Fig. 32: Nonlinear relationship between stress and strain

In order to explain the generation of higher order harmonic waves, let's now consider the case where a single frequency ultrasonic wave (longitudinal) incident upon one end of a thin circular rod propagates through the rod with degradation and is detected on the other end.

If it is now assumed that the attenuation can be neglected, then the equation of motion for longitudinal and planar waves in the thin circular rods can be represented as follows:

$$\frac{1}{\rho} \frac{\partial \sigma}{\partial x} = \frac{\partial^2 u}{\partial t^2} \quad \text{Eq. 2}$$

Where, ρ is the density of the medium, x is the propagation distance, σ is the stress and u is the displacement. Using Eq. 1 and 2 and the relationship between strain and displacement, we can obtain the nonlinear wave equation for displacement $u(x,t)$ as follows:

$$c^2 \left(1 - \beta \frac{\partial u}{\partial x} \right) \frac{\partial^2 u}{\partial x^2} = \frac{\partial^2 u}{\partial t^2} \quad \text{Eq. 3}$$

We can find the expression of the nonlinear coefficient given by the authors (Shah & Ribakov, 2009) :

$$\beta = \frac{8}{d k^2} \frac{A_2}{A_1^2} \quad \text{Eq. 4}$$

Where:

- A_1, A_2 : the fundamental and the second harmonics in the Fig.30.
- d : the distance of the propagation
- K : the wave number

The magnitude of harmonic waves depends on medium material properties. Thus, it would be possible to evaluate the degradation of elastic property by monitoring how much magnitude of higher harmonic wave is generated in the transmitted wave (Hikata et al.,1963; Johnson, 2001; Meo et al, 2008) .

3.3. Shift of Resonance Frequency

Resonant ultrasound spectroscopy (RUS) (Visscher et al., 1991; Antonaci, 2010) is a linear ultrasonic or acoustical technique which can be applied to extract all the elastic constants of a sample based on the values of its resonance frequencies, its geometry and its density. This method is very accurate when applied to samples having a well-defined geometry and homogeneous elastic constants. However, RUS is an inherent linear technique, and it is not be sensitive to the early stages of damage development inside a sample. Contrarily, nonlinear version of RUS, which is called Nonlinear RUS (NRUS) (Van Den Abeele et al., 2000; Jun, 2010) analyzes the dependence of the resonance frequency on the strain amplitude while exciting the sample at relatively low amplitudes. By observing the relative frequency shift, it is possible to have a measure of the internal degradation of the microstructural properties of the material (Johnson, 2001; Windels & Van Den Abeele, 2004). That is, in NRUS, the resonant frequency(ies) of an object is studied as a function of the excitation level. As the excitation level increases, the elastic nonlinearity is manifest by a shift in the resonance frequency. In Fig. 33 and Fig. 34 a result of this method is shown; according to experimental evidence (Van Den Abeele et al. ,2000; Van Den Abeele et al. ,2001; Windels & Van Den Abeele, 2004) the sample under a sweep load centered on one of its natural modes shows different behavior of structural response depending on the status of sample: intact or damaged.

$$\frac{\partial \sigma}{\partial \varepsilon} = E(1 - \beta \varepsilon - \delta \varepsilon^2 + \alpha \Delta \varepsilon \dots)$$

Where :

- $\alpha \propto \frac{f_0 - f}{f_0}$
- f_0 : Central frequency
- f : Frequency after shift
- α, β and δ : Non linear parameters

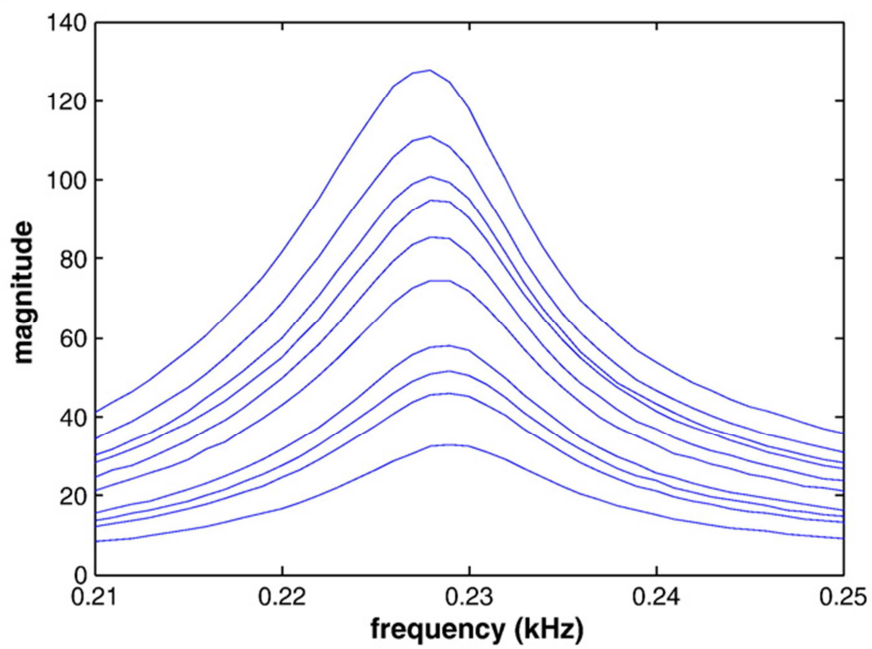


Fig. 33: A result of NRUS : healthy material

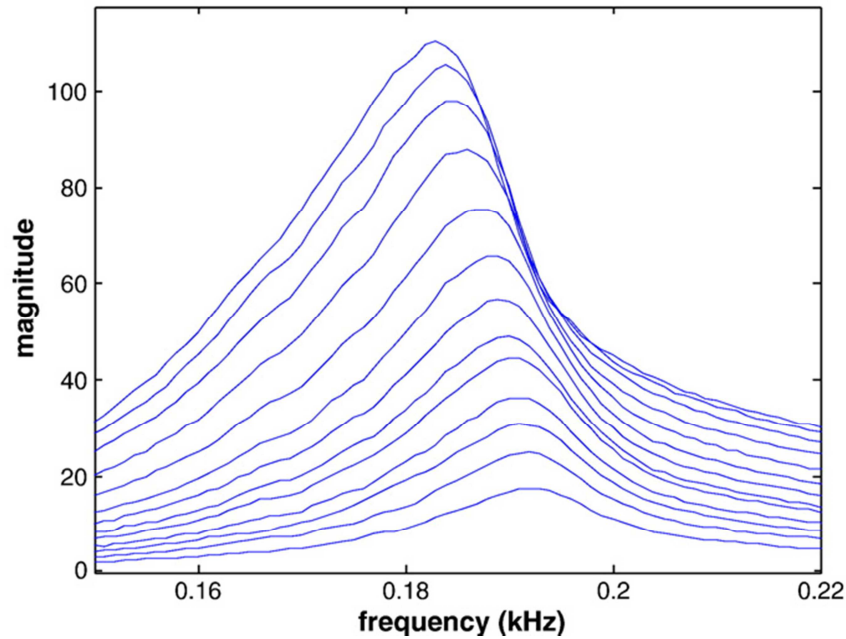


Fig. 34: A result of NRUS: damage material

Currently, NRUS is being actively applied in characterization of various materials, concrete (Payan et al., 2007), fiber reinforced plastic composites (Meo, 2008) as well as metallic material. Several tries to apply NRUS to medical diagnosis (Muller et al., 2005) are undergoing, and defect imaging (Van Den Abeele et al., 2001) by NRUS is also under investigation.

4. Evaluation of damage in cement based materials by non linear acoustic

Previous experiments show that the linear acoustic methods are practical to detect damage from a relatively high cracking, but it is clear that the linear acoustic techniques are less effective for detection micro cracks concrete.

However, the nonlinear acoustic measurements, which are interested in the consequences of changes in elastic properties, are more likely to detect small damage in materials.

The excitement of an environment induced a modification that could lead to the appearance of unknown phenomena such as linear acoustic modulation frequency, harmonic generation, the time lag of the ultrasonic wave, etc. Note that the micro cracks and the cracks as those generated by the damage increase the non-linearity in the cement based materials.

The difference between linear and nonlinear acoustic methods rests on a supposition about the frequency components of propagating waves. These techniques were used to characterize various

types of damage, such as compressive loading (Van Den Abeele & De Visscher, 2000; Shaha & Ribakov, 2010) and alkali–silica reaction (Les´nicki et al. 2011; Y. Boukari et al. 2015; F. Moradi-Marani et al. 2014; A.S. Kodjo et al., 2011).

4.1. Mechanical damage

The majority of studies carried to investigate the impact of mechanical damage on linear and nonlinear acoustics and shows the relevance of the latter.

Van Den Abeele, and De Visscher (2000), using both linear and nonlinear (amplitude - dependent) acoustical experiments on a reinforced concrete (RC) beam in which damage is gradually induced by means of static loading tests, show that the relative value of the nonlinearity parameter α (due to the shift of the frequency) increases drastically by a factor of 200 as function of the induced damage in the RC beam. Also, they concluded that the relative expansion of the non- linearity is far more sensitive to damage than the linear material properties (Fig.35). This is specifically important when examining the early phases of deterioration where reduction of linear wave speed is hardly measurable ($D < 0.1$).

For $D > 0.2$, it appears as if the change in the nonlinearity reaches a point of saturation when the micro cracks coalesce to form a crack that is visible at the surface. At this point the change in linear properties may be used as damage indicators, since they probably are more sensitive to macro cracks.

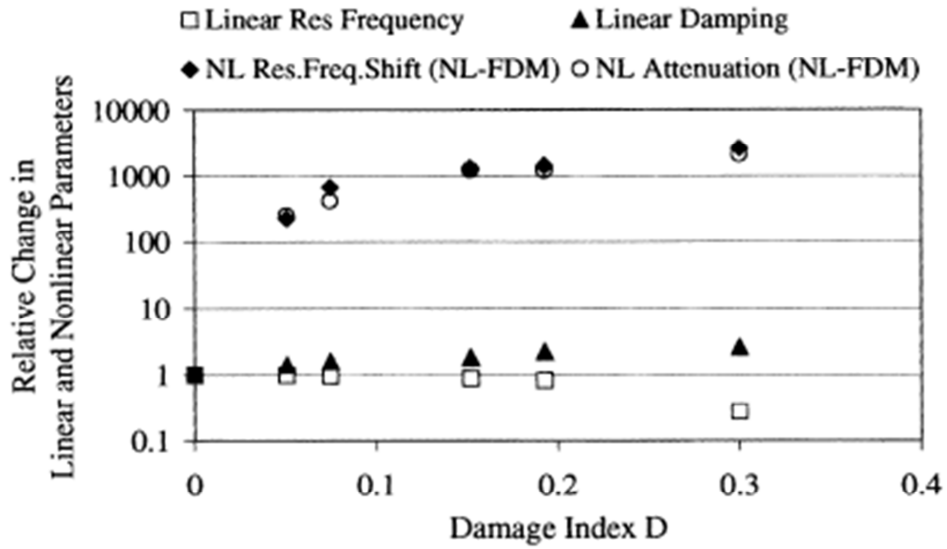


Fig. 35: Relative changes of the linear and nonlinear characteristics derived from SIMONRAS analysis of an RC beam as function of damage due to consecutive loading steps

Moreover, Shaha and Ribakov (2010) show that the acoustic emission activity and the nonlinear acoustic were found very sensitive to change in the applied loading events and w/c. Acoustic emission events increase significantly as damage progresses. Additionally, the increase in acoustic emission events was higher for high w/c concrete compared to low w/c one. Attenuation has also increased with increase in damage. The changes in attenuation, however, are greater for low w/c concrete than for high w/c one (Fig.36).

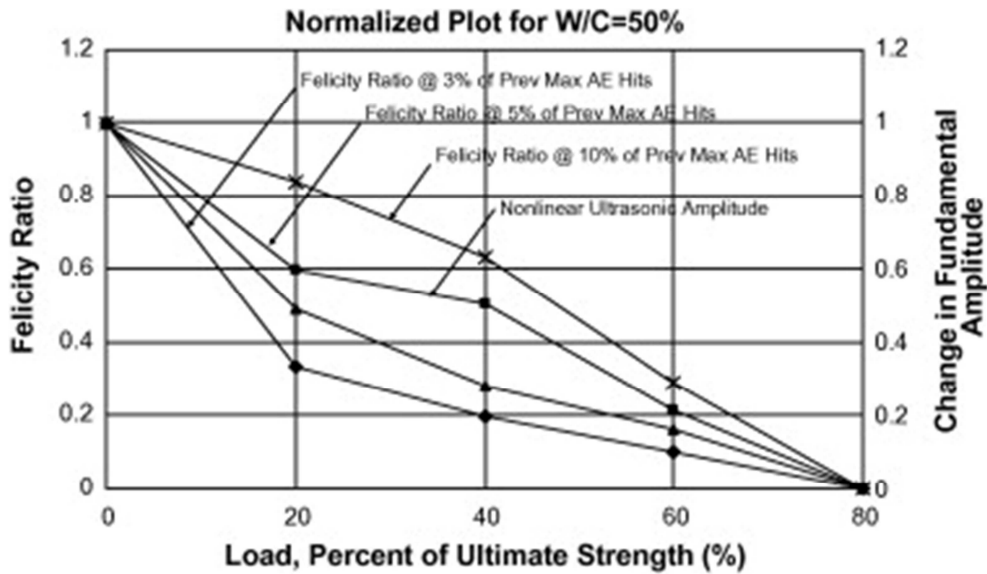


Fig. 36: Acoustic emission parameter and nonlinear acoustic parameter vs. the applied load (w/c = 50%) (Shaha and Ribakov (2010))

Antonaci et al (2010) reported that the nonlinear indicator seems to offer some advantages in monitoring damage evolution. In fact, degradation induced by quasi-static load is not expected to have a uniform growth. The existence of different phases in damage evolution is consistent with results from other techniques used in monitoring the progression of damage in concrete. Indeed, the nonlinear indicator (Fig.37) allows distinguishing three stages in the evolution of damage, none of which is enlightened by the linear indicators:

- ✓ 0 to 30% of the failure load: early damage occurs, with formation of micro-cracks and a sudden change of the performances of the material.
- ✓ 30% to 70% of the failure load: micro-cracks begin to coalesce in larger cracks and only a few new micro-cracks are formed. This corresponds to a slight increase of the nonlinearity, with consequent moderate decrease of the performances of the material.
- ✓ 70% to failure: micro-cracks coalesce into macro-cracks. The nonlinear indicator suddenly increases. This increasing of the nonlinear parameter can be interpreted as an indication of imminent failure. In the other hand, the linear indicators do not show any similar precursor sign.

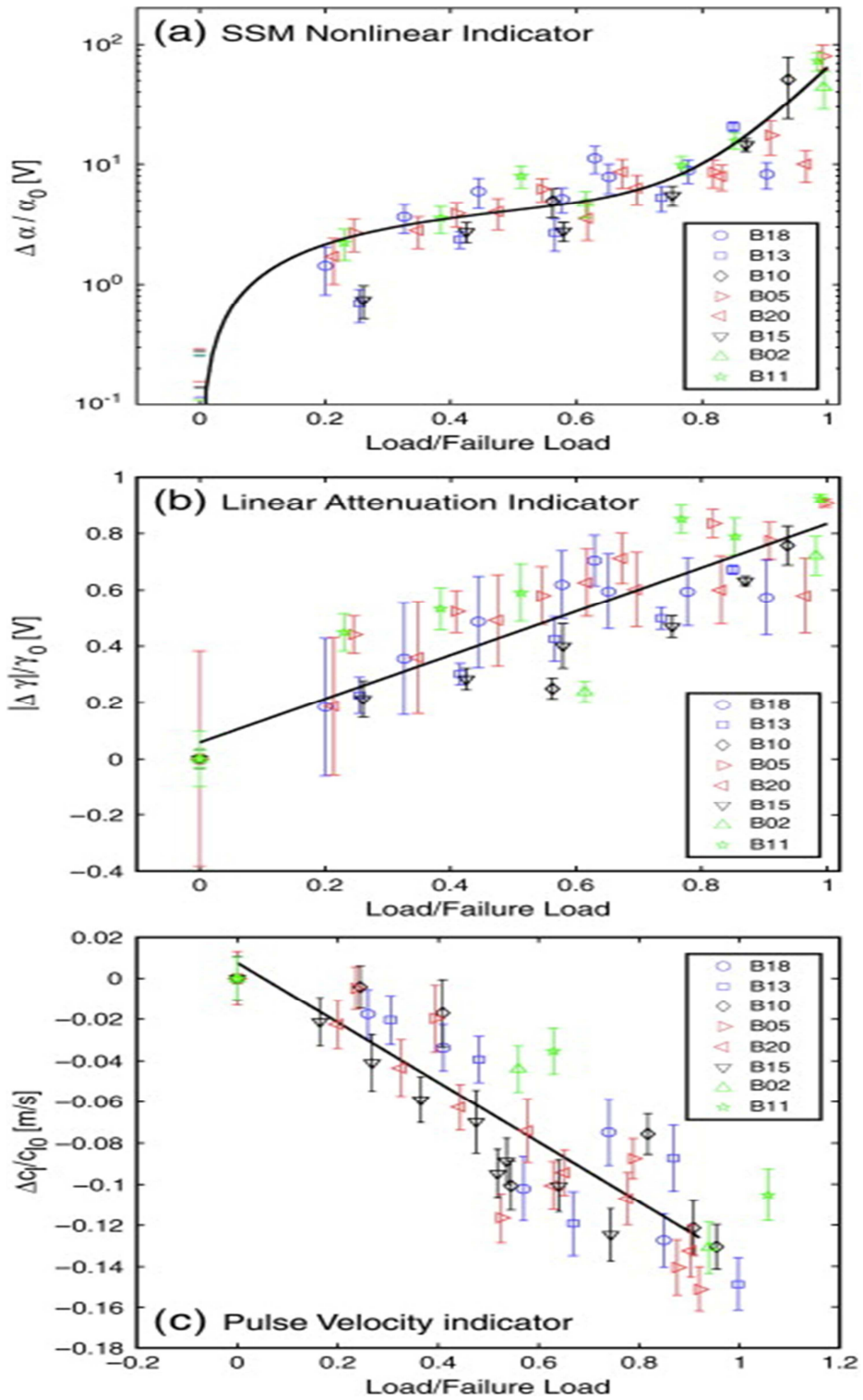


Fig. 37: Superposition of results from different specimens. (a) The variation of α for different specimens leads to the definition of a curve that describes the different stages of damage evolution. (b) and (c) point out that linear indicators show a linear evolution of damage (Antonaci et al (2010))

4.2. Thermal damage

After an overview on the detection of mechanical damage by the nonlinear acoustic, this section will be dedicated to studying the effect of thermal damage on nonlinear acoustic parameters.

Thermal damage to concrete includes the formation of contact-type defects based on physicochemical changes, which are a dominant factor in heat damage.

Park et al. (2014) in his study evaluated the shift of resonance frequency after exposing concrete structures to fire. The experimental study was performed on 100 concrete samples with different mix proportions and fire scenarios.

At two specific peak temperatures (200 °C and 400 °C), the non linear parameter (Fig.38) increased sharply compared to other temperatures, so these ranges of temperatures, in particular, seem to cause contact-type defects in concrete. We conclude that nonlinear resonance vibration can be used as an essential method to evaluate fire-damaged concrete.

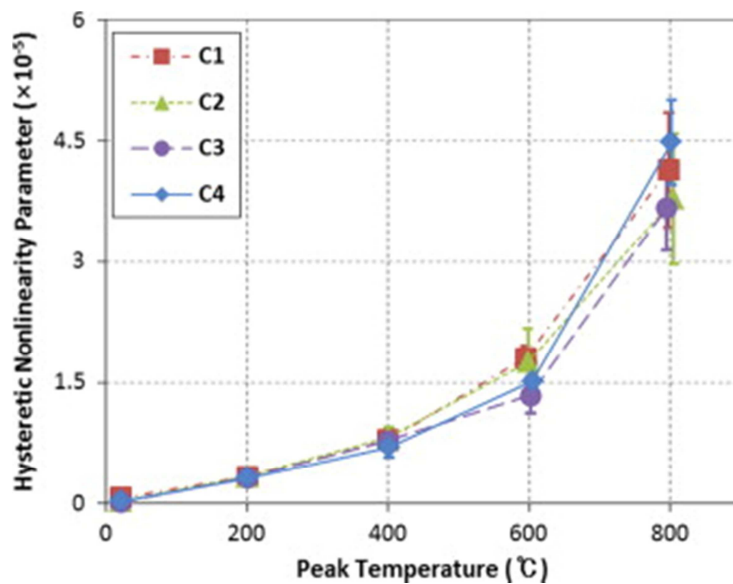


Fig. 38: Total results of the hysteretic nonlinearity parameter according to the peak temperature to which fire-damaged concrete had been exposed (Park et al. (2014)).

Moreover, Meo et al. (2014) attempts to visualize the thermal damage and characterizes the thermally damaged concrete using a nonlinear ultrasonic method. Thermal damage in concrete structures was induced and the nonlinear parameters were measured as a function of the damage. A visible shift in resonance frequency (Fig.39) was observed and the nonlinear parameter

measured as a function of the damage temperature, showed a dynamic range ten times greater than the variation velocity of the ultrasonic waves.

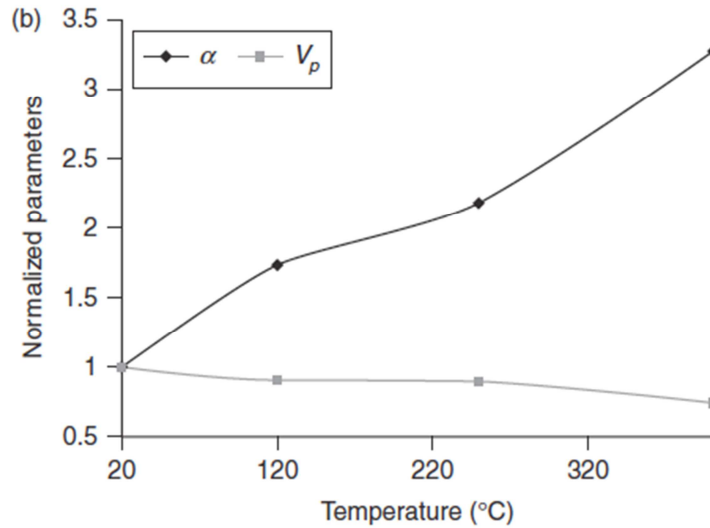


Fig. 39: Relative variation of the nonlinear parameter and velocity of pressure waves as a function of the damage temperature (Meo et al. (2014))

Conclusion

Cement based materials is an micro inhomogeneous material. It includes inhomogeneities larger than a distance between atoms. In addition, the study of its damage through acoustic waves is produced from the emission of waves whose wavelength is larger than the size of these irregularities. These two phenomena characterize micro inhomogeneous materials. However, since the material starts to deteriorate, the nonlinearity is a whole new dimension and becomes largely dominant compared to the nonlinearity of the material before degradation. Thus, for very little damage states developed, one can easily detect non-linear phenomena, whereas this is not allowed by the use of linear acoustic methods.

Chapter 5: Definition of the project

1. Context of the study

For twenty years, the characterization of materials by ultrasonic sound has progressed through the study of nonlinear phenomena.

This development of control health applications is directly related to the discovery that although very different from each other (rocks, concrete, polycrystalline metals, tired materials...) nonlinear elasticity of a large number of materials, was mainly due to contacts (grains, cracks...) within it. Thus, because of these contacts, these materials have a huge nonlinearity (several orders of magnitude compared to a solid mono-crystalline or fluid) is very sensitive to structural changes they undergo (fatigue, water uptake...). Thus, the importance of non-linear macroscopic effects, measured from the change in function of the excitation level of various acoustic parameters (speed, attenuation, spectral content, resonance frequency...), is an excellent indicator of the amount of degradation of existing micro cracks in the material and the durability.

The aging of infrastructure generates significant investment because of the so large number of structures damaged and very high costs of repair. Indeed, there is an explosion in the budget to repair these structures in order to ensure the reclamation and maintenance of its quality.

The life of cement-based structure is very often linked to the ability of the cement-based materials to prevent the penetration of aggressive agents in the porous network. This ability of cement-based materials against the intrusion of these agents is characterized by physical quantities: the permeability, porosity...

Cracking is a key parameter for durability of cement structures. But the coupling between cracking and the durability is complex, because the cracks can be evolutive. Their location and geometry (crack opening) may vary as a result of internal stresses (alkali-aggregate reaction, freeze-thaw) or external (mechanical loads, thermal cycling). The self-healing mechanisms may also contribute to changing the geometrical properties of cracks (length, breadth and openness) and consequently the transport mechanisms in the cracking plane.

Approaches to take account of cracking on the kinetics of degradation of cement structures and the prediction of its life span are still relatively poorly developed. This lack of reliable and efficient tools stems in particular from poor understanding of the mechanisms and kinetics of self-healing of the cracks in the cement matrices.

2. Problematic

This research project aims to study and characterize the damage and degradation in the mortar using the nonlinear acoustic and it contains essentially two related axes:

✚ **A first part:** to study the effect of thermal damage on nonlinear acoustic parameters in mortar. Indeed, thermal cracking induced by a temperature gradient represents a problem in the cement-based materials. For a multi-phase material, the deformation equity arising from the heterogeneity deformations of the phase components inevitably cause cracks in the composite, even if it is under a uniform temperature field. Also, this type of cracking reduces significantly the strength and elastic modulus of the mortar. However, the overall thermal cracking process (initiation, propagation and linkage of cracks) and stress related to distributions under high temperatures are difficult to quantify experimentally, mainly due to the limitation of equipment and complex structure of a composite material. So, the goal is to characterize the sensitivity of the heat damage in mortar by the nonlinear acoustics using the higher harmonics generation approach. Moreover, the effect of the cracking on the nonlinear parameter and his limits. In addition, the impact of the porosity and W/C ratio on the cracking by finding a correlation between those parameters. Besides, compare the response of the linear and non-linear acoustic of detecting damage and the limitations of each approach.

✚ **A second part:** to follow the phenomenon of self-healing in mortar by nonlinear acoustics. Indeed, the presence of cracks is one of the important factors affecting the durability of the mortar, especially in terms of resistance or transfer properties. The self-healing of cracks is a physicochemical phenomenon having a positive impact on the sustainability issues. So, the goal is to create a controlled cracks (mechanical damage) on mortar and follow the closing/clogging of the crack size due to the self-healing by the nonlinear acoustics using the shift resonance and higher harmonics generation approaches. Besides, comparing the evolution of the airflow (measured by the permeability tests) and nonlinear parameters according to the healing. In addition, seeing the effect of the initial crack size on the parameters (α , β) and the airflow. Moreover, identify the limitations of the nonlinear acoustic approaches against the permeability tests.

3. Objectives

In the framework of this project, the objectives are:

❖ **In the first part:**

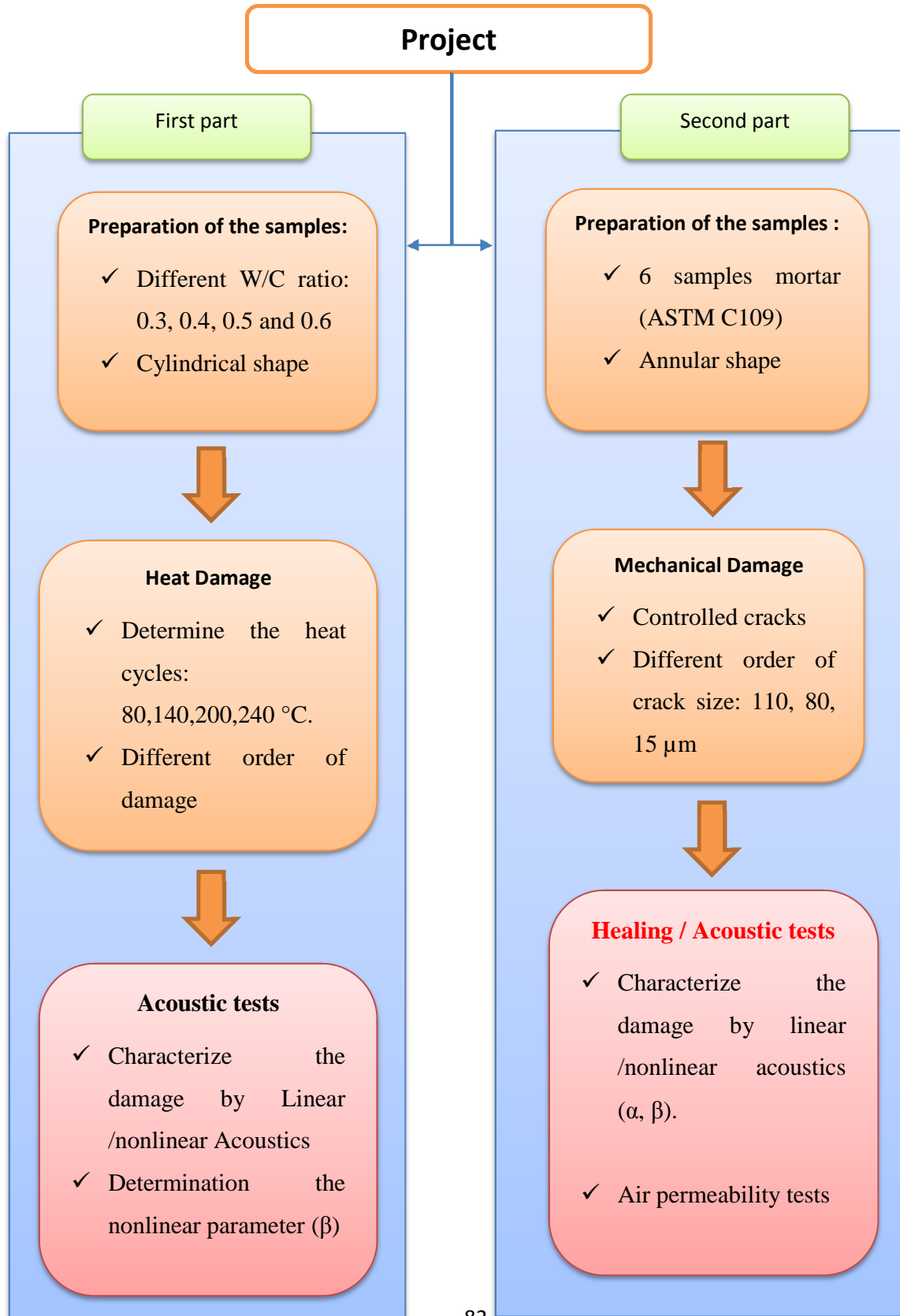
- Define the heat cycles to create cracking in the mortar.
- Choose initially the nonlinear acoustic method which will be used to characterize the heat damage: Higher Harmonic Generation.
- See the effect of the damage, porosity, W/C on the nonlinear and linear acoustic parameters.
- Estimate the level of damage in the mortar according to the propagation of cracks by non-linear and linear acoustic parameters.
- Coupling of mechanical and acoustic measurements to follow the cracking.

❖ **In the second part:**

- Choose initially the nonlinear acoustic method that will be used to characterize the self-healing: Shift Resonance and Higher Harmonic Generation.
- Correlating mechanical measurements and permeability to monitor acoustic cracking and self-healing of the mortar.
- See the effect of the crack size on the nonlinear and linear acoustic parameters.
- Establishing a comparative study of the evolution of acoustic and elastic parameters and geometric for different types of cracking properties.
- Creating a numerical model for the permeability tests to find a numerical relationship between crack size vs. air flow and validate the experimental results.

The experimental is divided into two parts (presented in the next scheme):

Experimental Procedure



Chapter 6:
*Heat damage: Protocol, results and
discussion*

Introduction

In this chapter we are basically interested in the effect of the heat damage on the velocities and the non-linear parameter β in mortar.

However, it would be interested to see the variation of the velocities, the modulus of Young and β according to the temperature, porosity and saturation. Thus, in this section, the experimental procedure of specimens' preparation and heat protocol are presented. Then, as first a step, we analyse the results obtained by the linear acoustic and as second step we analyse those of the nonlinear parameter β .

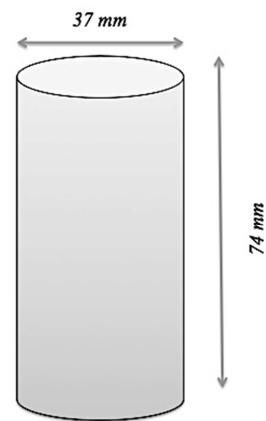
1. Experimental procedure

1.1. Mortar sample preparation and generation of heat treatment

In order to obtain various samples with different porosities, mortar samples were fabricated with four different water/cement (w/c) ratios: 0.3; 0.4; 0.5 and 0.6. The corresponding cement mass densities are reported in Fig.44, and some samples are shown in Fig.40 (a). The samples are cylinders with a diameter of 37 mm and a height of 74 mm (Fig.40 (b)). They are cored from larger slabs of a Portland cement (CEM I 52.5N) preserved in limewater and then rectified to obtain parallel end faces. Several heat treatment techniques were applied in mortar in previous studies (Fu et al. 2004; Xu et al. 2003; Joshua et al. 2007; Lion et al. 2005). In this work, it was chosen to impose the temperature variations used by Xu et al. (2003), as illustrated in Fig.41. The reference case considered in this study is the case of a saturated ambient temperature T_0 lying between 23°C and 30 °C (it was most often equal to 25°C in the laboratory). To prepare damaged mortar, the sample was first put in the oven for 120 min, during which temperature was progressively raised up (In order to avoid heat shocks) to a maximum temperature T_{max} . The samples were then maintained at temperature T_{max} for 60 min. Then, samples were exposed to ambient temperature. Advection heat exchanges with the atmosphere made the sample temperature decrease. For each ratio w/c, heat damaged samples were studied for four maximum temperatures (80°C, 140°C, 200°C and 240°C), and compared to a sound sample. As a result, five samples were prepared for each ratio w/c studied.



a)



b)

Fig. 40: Samples of mortar

- a) Different values of w/c
- b) Dimensions

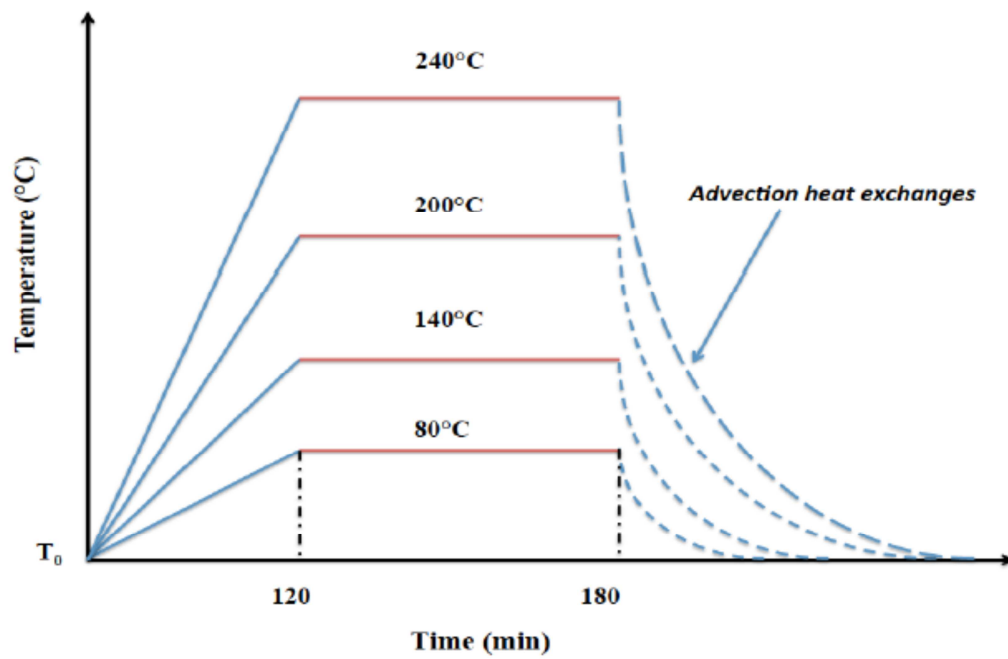


Fig. 41: Time evolution of temperature during heat treatment.

1.2. Porosity and density

Porosity was measured by the gravity method, using vacuum saturation. This is a well-established technique, as it has the benefit to be fast and easy to apply. Furthermore, it is considered to deliver an effective approximation of porosity of materials such as mortar or concrete. It consists of submitting the sample to a moderate oven drying at a temperature of 60 °C. The drying is stopped when the weight of the sample persists constant, which is achieved when its variation does not exceed 0.01% (Fig.42). The weight of the dried sample, symbolized as M_{dry} , is then measured with a precise balance. Afterwards, the specimen is immersed under vacuum in a container filled with distilled water. The weight of the sample is measured at different times until it becomes stable; the sample is then considered as fully saturated with water and its weight denoted as M_{sat} . In addition, the volume of the sample (V) was precisely measured with a pycnometer. Then, porosity (Fig.43) is calculated by this formula :

$$p = \frac{M_{sat} - M_{dry}}{\rho_w V}$$

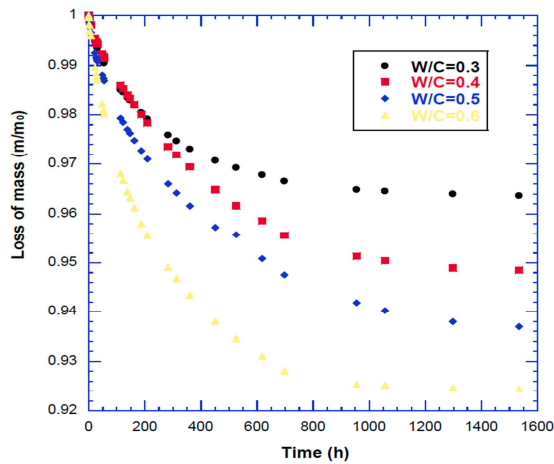


Fig. 42: Loss of mass

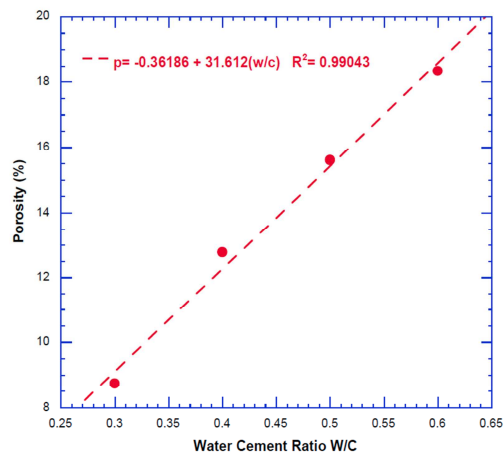


Fig. 43: Porosity vs. W/C

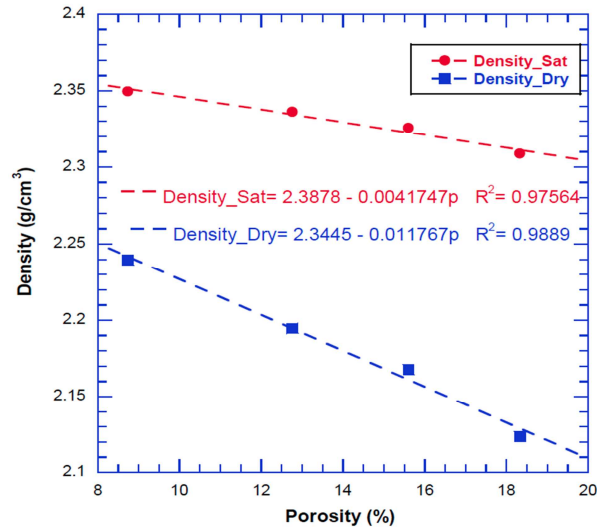


Fig. 44: Density vs. Porosity

All the results in this part are determined by taking the average of three experimental tests. The results (Fig.42) show that the variable kinetics of relative mass is related to the w/c. We note a stabilization of the latter at the end of 66 days for all samples.

Fig.43 show the variation of porosity with w/c ratio for the mortar for a linear trend curves. As expected, the results show an increase in the porosity of the mortar according to the ratio w/c. As an example, porosity increases from 9% to 21% when the w/c ratio goes from 0.3 to 0.6. These results are consistent with those obtained by other researchers (Baroghel-Bouny, 2001).

In the Fig.44, we determine the density because we need these values to determine the dynamic modulus of Young.

2. Linear acoustic

2.1. Experimental device

Broadband ultrasound spectroscopy was used to obtain ultrasonic parameters of the samples. This technique can be applied either in transmission mode, with a pair of transducers, one transmitter and one receiver (as used in this study), or in pulse-echo mode with a single transducer working as both transmitter and receiver. The transmitted ultrasonic pulse is wideband, with a 1 MHz central frequency and a 60% bandwidth. As the analysis is performed in the frequency domain, ultrasonic parameters are estimated from 0.6 to 1.2 MHz. A Panametrics 5055 pulser-receiver is used to send a high voltage pulse to the transmitter and to amplify the received signal. The

amplified signals are then acquired by a digital oscilloscope and transferred to a PC for further analysis (Fig.45). A thin layer of coupling agent is applied between the transducer face and the sample. It is either a silicone gel (Sofranel D coupling agent) for longitudinal waves or a highly viscous liquid (Sofranel SWC coupling agent) for shear waves. Pulse velocity is measured by estimating the flight time between the signal $S_2(t)$ and the reference signal $S_1(t)$ (Fig.46).

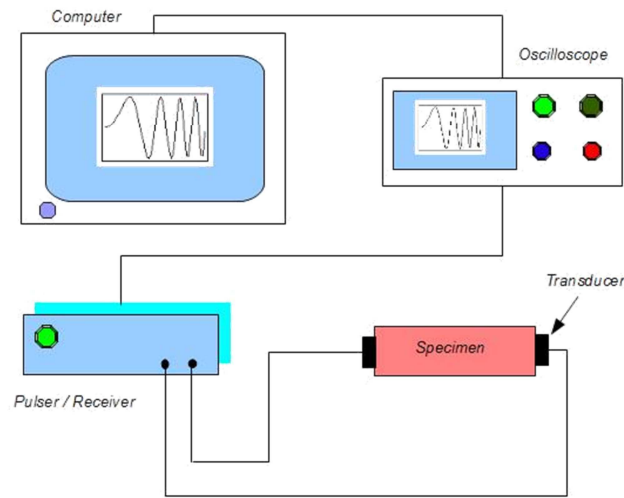


Fig. 45: Experimental device of linear acoustic

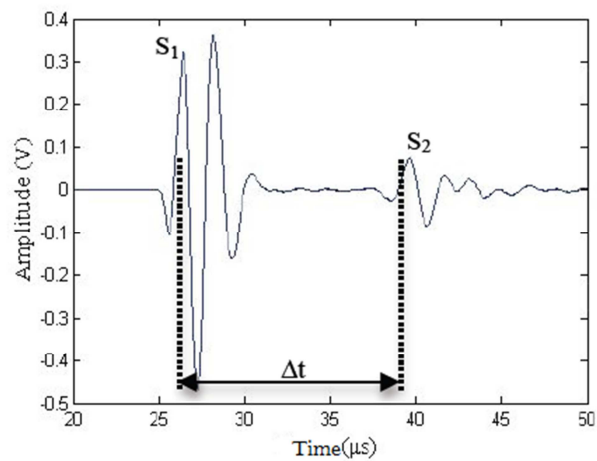


Fig. 46: Determination the time of flight

Linear Acoustic Methods were used extensively in the past at Ecole Centrale de Lille (ECL) in order to characterize the elastic and permeability properties of cement-based materials. This technique allows measuring the velocities (Longitudinal and Shear Velocities) of pulse waves emitted through a material sample. Assuming that the time-of-flight Δt (i.e. the time for the wave to cross the entire sample) can be measured in the laboratory (Fig.46), the wave velocity V is simply computed as:

$$V = \frac{L}{\Delta t}$$

In which L is the length of the sample. Mechanical properties (such as Young's modulus E and Poisson's coefficient ν) are related to wave velocities according to:

$$E = \frac{\rho V_L^2 (3V_L^2 - 4V_T^2)}{(V_L^2 - V_T^2)}, \quad \nu = \frac{1}{2} \frac{1 - 2 \left(\frac{V_T^2}{V_L^2} \right)}{1 - \left(\frac{V_T^2}{V_L^2} \right)}$$

Where V_L and V_T are longitudinal and shear velocities, and ρ is the mass density of the cement sample.

2.2. Effect of saturation

Initially, linear acoustic tests (longitudinal and shear velocities) were carried out on saturated and dry specimens. The following graph summarizes these results:

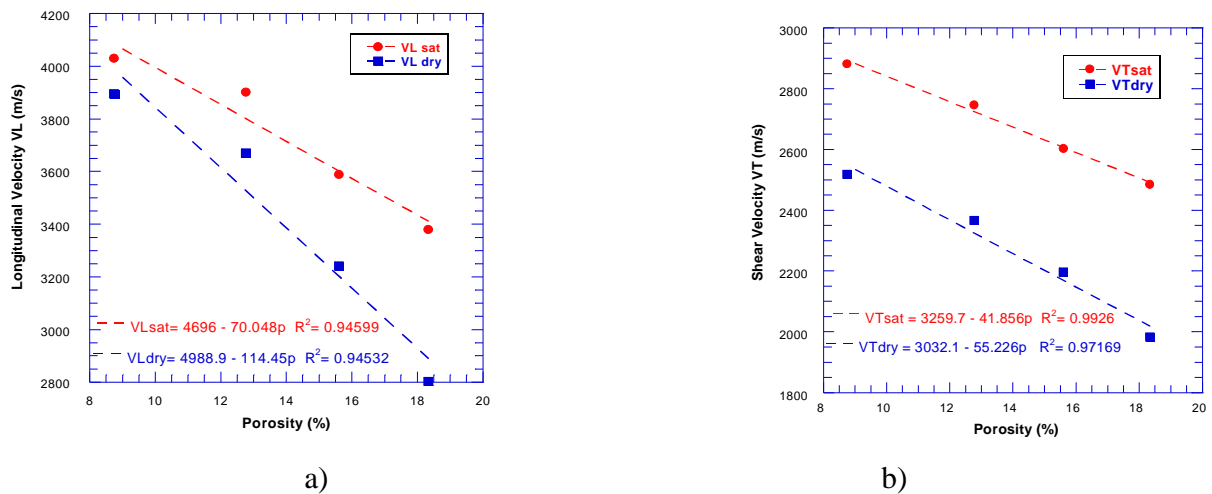


Fig. 47: The variation of the velocity for dry and saturated cases according to porosity

a) Longitudinal velocity b) Shear velocity

Fig.47 shows the ultrasonic pulse velocity versus porosity for longitudinal and shear wave, respectively. Again, the expected trend is observed: velocity of both waves decrease as porosity increase (negative slopes). All values of the regression coefficient R^2 are found to be higher than 0.9, which means that the measured variation of UPV versus porosity is correctly described by a linear relationship in the range of porosity considered. This was already observed by Ohdaira and Masuzawa (2000).

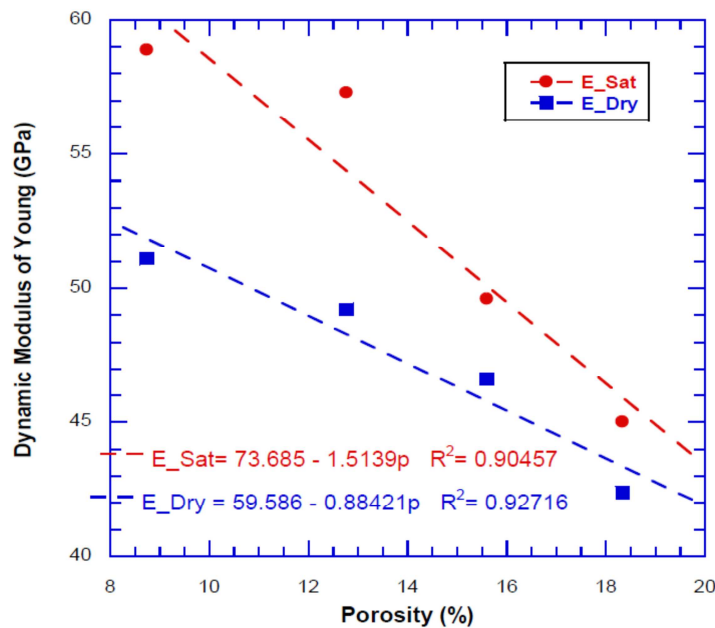


Fig. 48: Modulus of Young vs. Porosity

The relationship between Young's modulus and porosity p is taken in the form of a power law (Lafhaj, Z. et al (2006))

$$\left. \begin{aligned} E &= E_0 (1 - p)^a \\ VL &= VL_0 (1 - p)^b \\ VT &= VT_0 (1 - p)^c \end{aligned} \right\} \xrightarrow[\substack{\text{Low porosity} \\ p \ll 100\%}]{} \left. \begin{aligned} E &= E_0 (1 - ap) \\ VL &= VL_0 (1 - bp) \\ VT &= VT_0 (1 - cp) \end{aligned} \right\}$$

Tab 4: Correlation between porosity and linear acoustic parameters

Parameter $X=X_0(1-bp)$	Case	X_0	b	R^2
V_L	Saturated	4696	1.4097	0.94
	Dry	4988.9	2.2941	0.94
V_T	Saturated	3259.7	1.2840	0.99
	Dry	3032	1.8214	0.97
E	Saturated	73.685	2.0546	0.9
	Dry	59.586	1.4839	0.92

Tab.4 is filled using the trend curves in Fig.46, Fig.47 and Fig.48 to compare the proposed law and the experimental results.

All values of R^2 are found to be higher than 0.9, which means that the simple model describes correctly the behavior of UPV in the range of porosity values considered (8% to 19%).

The variations observed of the X_0 parameter (When $p=0$) according to the degree of saturation can be linked to certain processes, such as the gradual development of micro cracks during the drying phase (Baroghel-Bouny,1999). This affects the elasticity of the mortar and thus the velocity. The second explanatory of the process can be a rearrangement in the porous structure, resulting in a collapse of the gel pores and an expansion of capillary pores (Powers & Brownyard, 1947; Feldman & Sereda, 1968).

These observations are similar to those reported by Yaman et al (2002) for longitudinal waves in the saturated and dry concrete.

2.3. Effect of heat damage

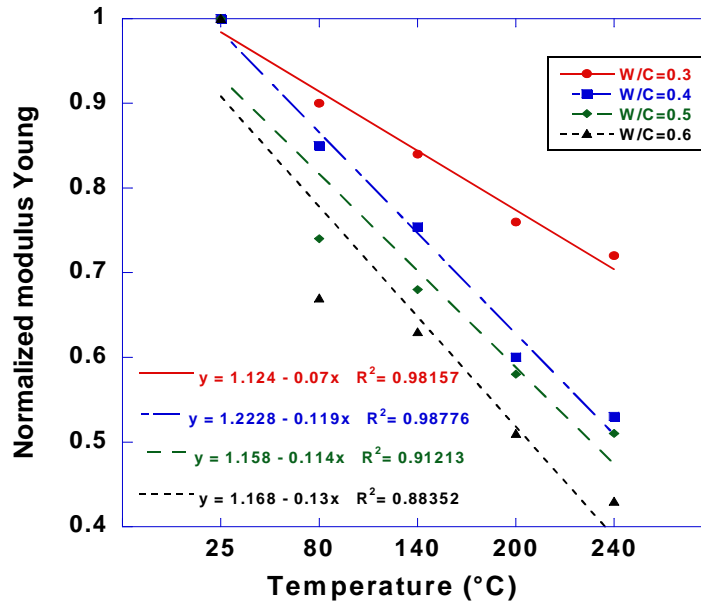


Fig. 49: Modulus of Young vs. Temperature

The evolution of mortar Young modulus with temperature is plotted in Fig. 49 for the four w/c ratios studied. The curves show that young's modulus decreases as temperature is raised, following a linear curve. From the slope of the curve showing the evolution of Young's modulus with temperature, it can also be noticed that higher w/c ratios tend to enhance the degradation process. As an example: for the same temperature 240°C, the normalized Young's modulus of the sample at ratio of w/c=0.6 is equal to 0.4, but for w/c=0.3, it is equal to 0.75, which is approximately the double value.

It may be noted also in the graph:

- Two curves for (W / C = 0.3 and 0.4) which are linear: the amount of water in these specimens is so small that the drying time is short, therefore the thermal damage begins quickly (just after 80).
- Two curves (W / C = 0.5 and 0.6) are not completely linear (between 25 and 140 °C): the amount of water in these samples is larger so the drying time is longer. The heat damage occurs after the 140 ° C.

Before this temperature is the phase drying and water evaporation.

We can remark also that the ultrasonic wave generated could not propagate through the severely damaged sample due to its high attenuation.

3. Nonlinear acoustic

3.1. Experimental device

A generator, controlled by a PC, was used to send a sine wave to the audio amplifier and the setup transformer in order to amplify the signal. The amplified signals were then transmitted through the sample and received by an accelerometer in the other side that linked to an acquisition card. Finally the data will be transferred to a PC for further analysis (Fig.50). A thin layer of coupling agent was applied between the transducer's face and the sample. Fig.51 represents the principle of measurement of beta using the peaks corresponds to the multiple of the initial frequency.

The non-linear parameter β is measured using the eq.4. Actually, a train wave is sent by wave generator than we examine the variation between the first and the second harmonics. The graph (Fig.52) shows an example of β . It can be remarked that non-linear parameter is not equal to zero (as shown in the figure), which prove the heterogeneity of the samples and the presence of the cracks in the cement structure.

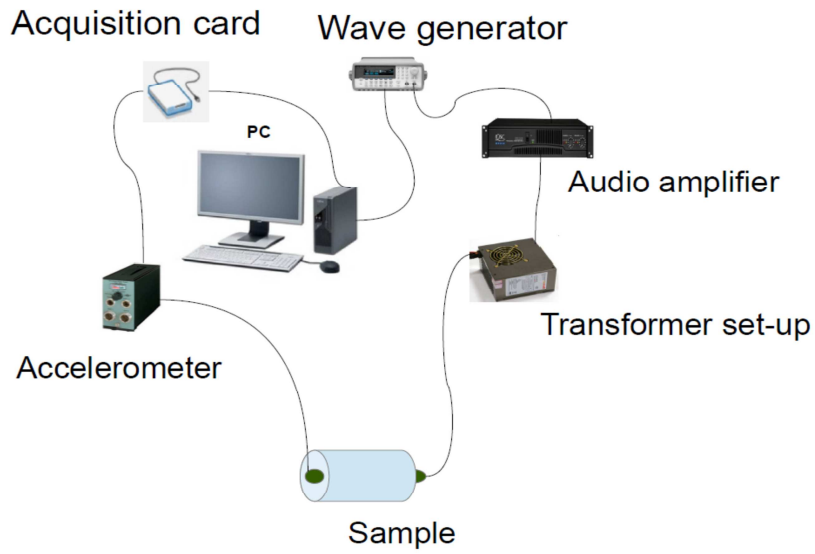
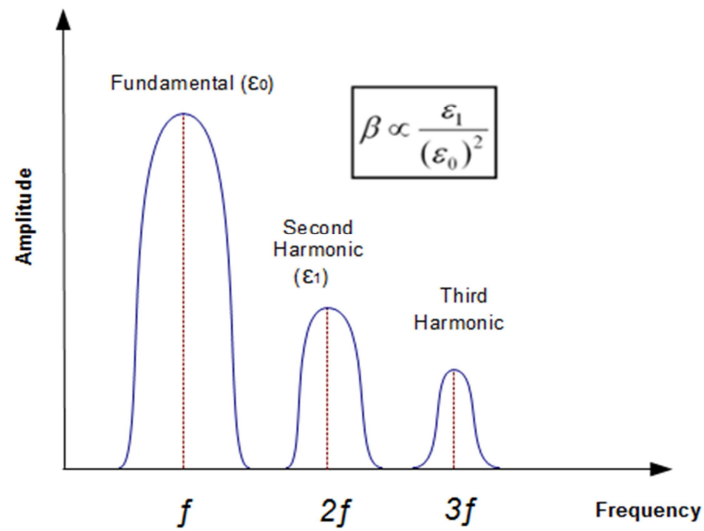


Fig. 50: Experimental device of the nonlinear acoustic waves



Fourier spectrum of the received signal after transmission and relation to β

Fig. 51: Principle of the High Harmonic Generation technique

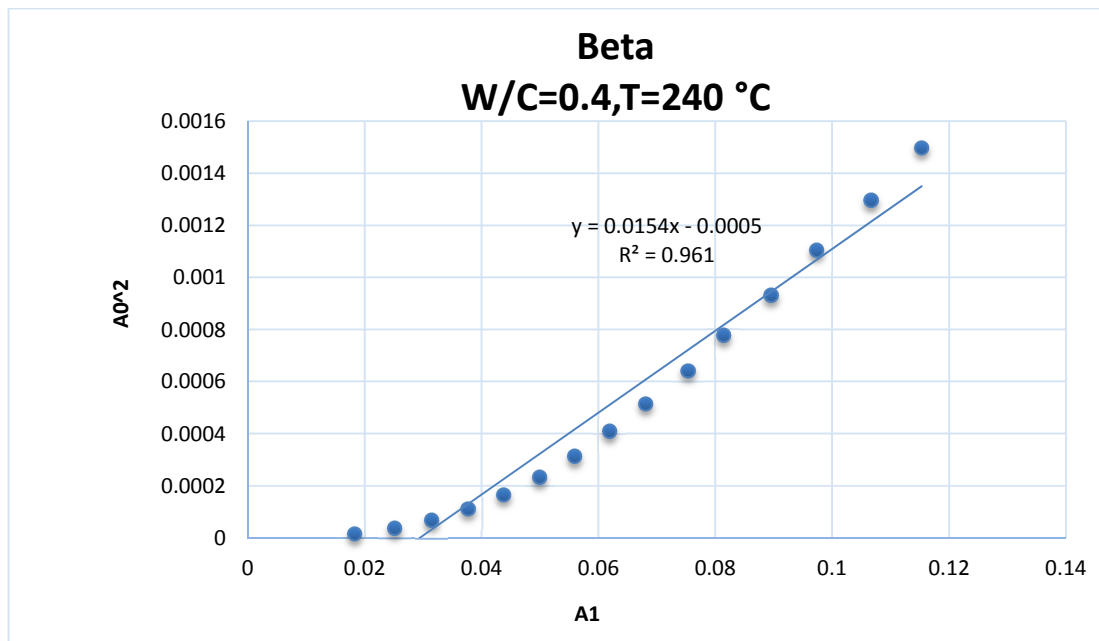


Fig. 52: Example of determination of nonlinear parameter beta

3.2. Effect of saturation

Initially, nonlinear acoustic tests were carried out on saturated and dry specimens. The following graph (Fig.53) summarizes these results of nonlinear parameter. The influence of w/c on the nonlinear parameter β is studied for the extreme water saturation states (Dry and Sat).

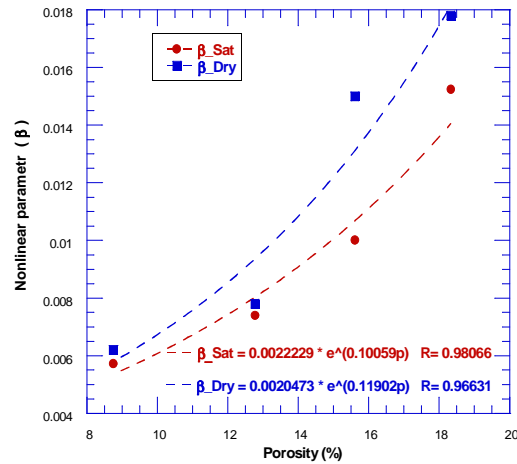


Fig. 53: Evolution of the Non-Linear Parameter β with porosity for dry and saturated specimens

Two essential observations appear:

- The first is that porosity rate has a notable influence on the nonlinear parameter into the usual w/c range and consequently the porosity (3 times between w/c=0.3 and 0.6).

Payan et al. (2010) shows that w/c has not an impact on the parameter α . Although, this study demonstrate that the parameter β is sensitive to the variation of porosity (means w/c). This can be explained by the difference between the nonlinear parameters α and β because α is measured by the shift resonance and β is measured by the higher harmonics generation.

- The second is that water saturation has also an influence on the nonlinear parameter: this influence is not significant for low porosity ($p < 14\%$), but it becomes significant for a high porosity, which demonstrated by Payan et al. (2010).

3.3. Effect of heat damage

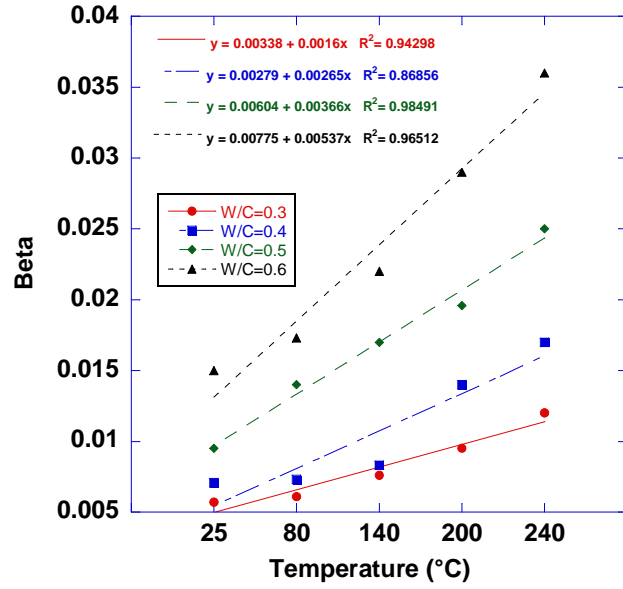


Fig. 54: Evolution of the Non-Linear Parameter β with Temperature (linear trend)

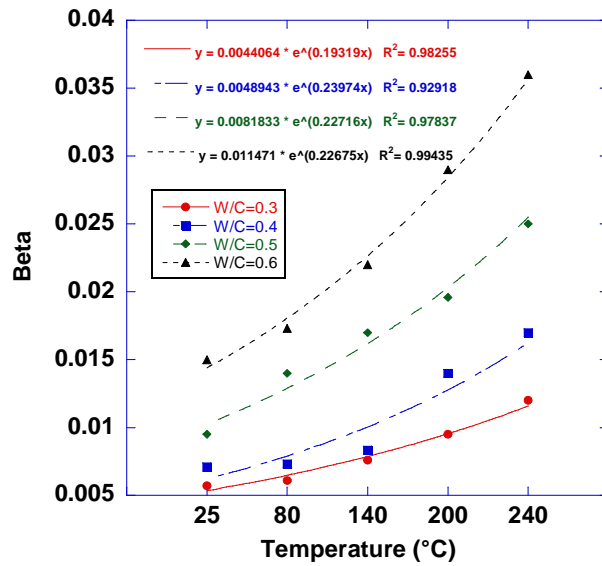


Fig. 55 : Evolution of the Non-Linear Parameter β with Temperature (exponential trend)

The graphs (Fig.54, Fig.55) show the evolution of the nonlinear parameter β according to temperature, for the three values of w/c under study. It can be observed that the nonlinear parameter is affected by both temperature and water cement ratio. For a given value of water content a significant increase of β with increasing temperature or damage degree. As an example, an increase of β , for w/c=0.5, is about 40% when temperature increases from 140°C to 240°C, yet this increase is about 20% when temperature rise from 25°C to 140°C. After plotting the trend curves an exponential function is established between the temperature and non-linear parameter. The nonlinear parameter β is also sensitive to the ratio w/c, i.e. to porosity.

Conclusion

This part included a special attention to various experimental techniques that were necessary to evaluate the heat treatment in the mortar. Indeed, the linear acoustic tests show that the velocities and dynamic modulus of Young decreases according to the porosity linearly.

In addition, the saturation has an impact on the velocities, while the velocities for a saturated mortar are higher than a dry one.

In order to quantify the heat treatment, linear acoustic tests were done and showed that the velocities decrease after the thermal damage. Moreover we can observe a linear loss of the modulus of Young.

In the other hand and using the nonlinear acoustic tests, the nonlinear parameter beta was determined by the higher harmonic generation technic. The measurements showed that beta increases linearly with porosity especially for the higher porosity and sensitive to the saturation of the mortar.

The study showed also that the beta is a good indicator to quantify the heat treatment. Indeed, the nonlinear parameter rises linearly according to the temperature.

Chapter 7:
*Self-Healing: Protocol, results and
discussion*

Introduction

This chapter is dedicated to study the self-healing phenomenon by the non-linear acoustic waves. First of all, the specimen's preparation and the cracking system are presented.

Then, experimental tests of permeability used to quantify the mechanical damage and to follow the self-healing process are explained.

Besides, it is interested to utilize both linear and non-linear acoustic waves tests to characterize the mechanical damage and the self-healing and find a correlation between the crack size and alpha and beta.

Finally, the nonlinear parameters alpha and beta are related to damage index in order to observe the effect of the damage on these parameters.

1. Specimens preparation

The test pieces of mortar are a ring shape (Fig.56) with an opening in the center to allow insertion of the cracking mechanism controlled: the expansive core.

All test of mortar samples are reinforced with a steel ring having a circular section of 4.8 mm and an inner diameter of 95.2 mm (Fig.57). This ring acts as an internal reinforcement for simulating the behaviour of a composite tensile reinforced concrete. It allows preserving the overall coherence after the cracking of the test.

The cylindrical molds, comprising a cylindrical insert into the center, have been completed in two layers using a slight vibration after the introduction of each of the layers.

The upper surface of the test piece is then leveled and a rigid impermeable plate of plastic covers the mold for approximately 24 hours.

Immediately after the release (Fig.56), the samples are kept in a humid chamber maintained at 23 °C and 100% relative humidity. Before starting the cracking, the upper surface of the specimen (referred to the leveling of fresh concrete) was polished or, if necessary, corrected by a precision machining using a diamond-grinding wheel mounted on industrial tower.



a)



b)

Fig. 56 : An example of a specimen

a) After molding

b) After the release from the mold

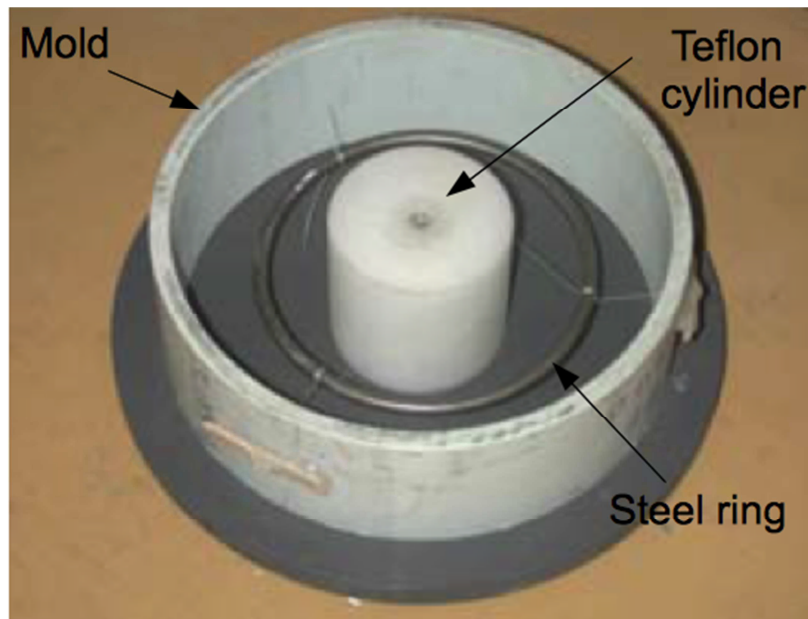


Fig. 57: A mold to make a specimen

In order to follow the evolution of the crack size, airflow and the effect of the self-healing by permeability tests and acoustic methods, the following experimental process was established (Fig.58).

After the preparation of the specimens, they are cracked and the crack size will be determined by the video microscope and permeability tests. Then, the samples will be placed in the humid chamber to begin the self-healing process. After a specified period time, the airflow and the crack size will be measured again by the permeability tests.

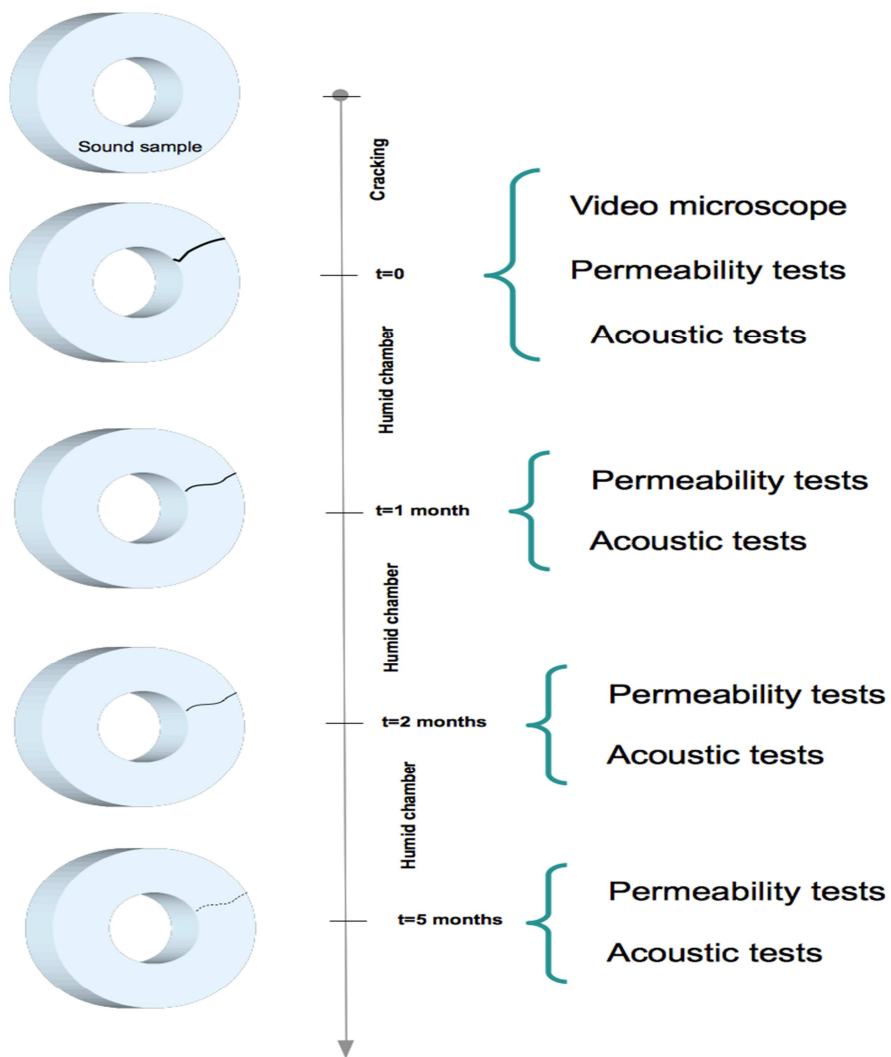


Fig. 58: Experimental process

The mortar specimens were cracked by the application of a deformation controlled traction generated by the expansive core (Fig.59).

The expansive core consists of a truncated core made of steel, which slides within six conical steel petals.

A thin ring retains all petals against the internal core and acts as a cushion between the deformable expansive core and the inner surface of mortar specimens.

The controlled cracking is affected by tightening the assembly: bolt and nut made of high strength steel, which forces the core penetration within the petals (Fig.60).

This process increases the diameter of the ring, which leads to a deformation of the internal diameter of the specimen mortar.

Controlled cracking (crack opening) is obtained by adjusting the deformation of expansive core.

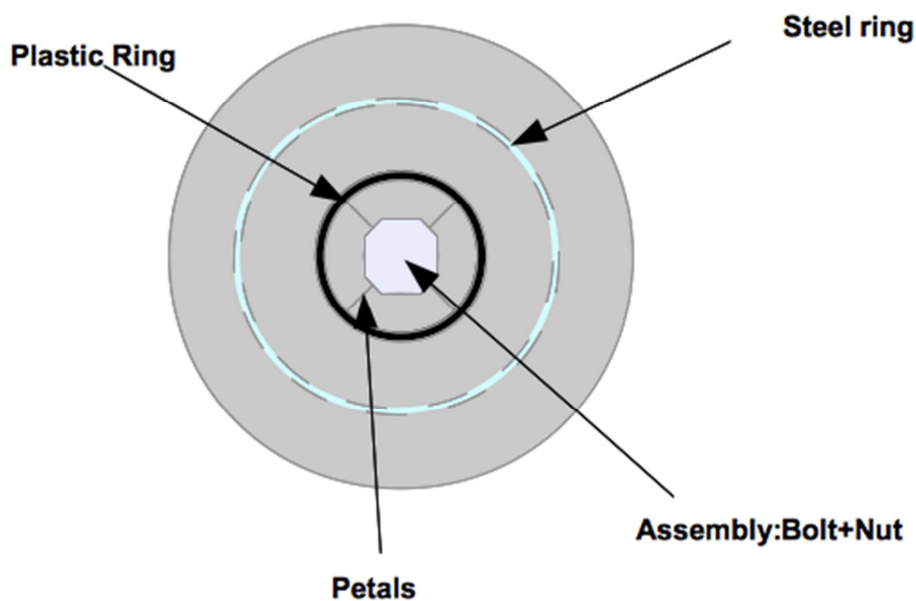


Fig. 59: Specimen with the expansive core

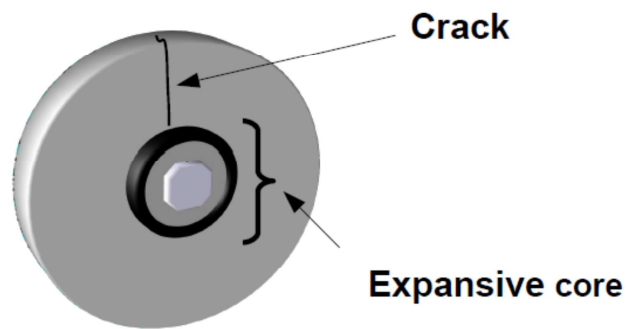


Fig. 60: Crack created by the expansive core

2. Airflow and permeability tests

The development of self-healing, and its effect on the transport properties in a crack, was quantified using a cell of air permeability by following of the variation of the airflow of the crack (Fig.61).

This cell is specifically designed for use with a mortar specimen cracked by an expansive core. It allows a precise measurement of the airflow through a single crack under well-controlled flow conditions (constant temperature and pressure gradient). The absolute pressures upstream and lateral are kept constant. The downstream volume flow (liter / minute) is measured by a digital flow-meter. Cracks were established 28 days after manufacturing the specimens.

During cracking by the expansive core, several cracks can form in the same specimen. So, in this case, an aluminium tape is applied to the upper face of the test. This waterproof film is previously cut to create a thin opening directly to the right crack (that we want to study) and cover all the others crack.

This technique is used to force the passing of the airflow through a single crack. Hence, for each size of crack, the airflow was measured. Ismail (2006) demonstrates that this aluminium plate has not an impact on the tests.

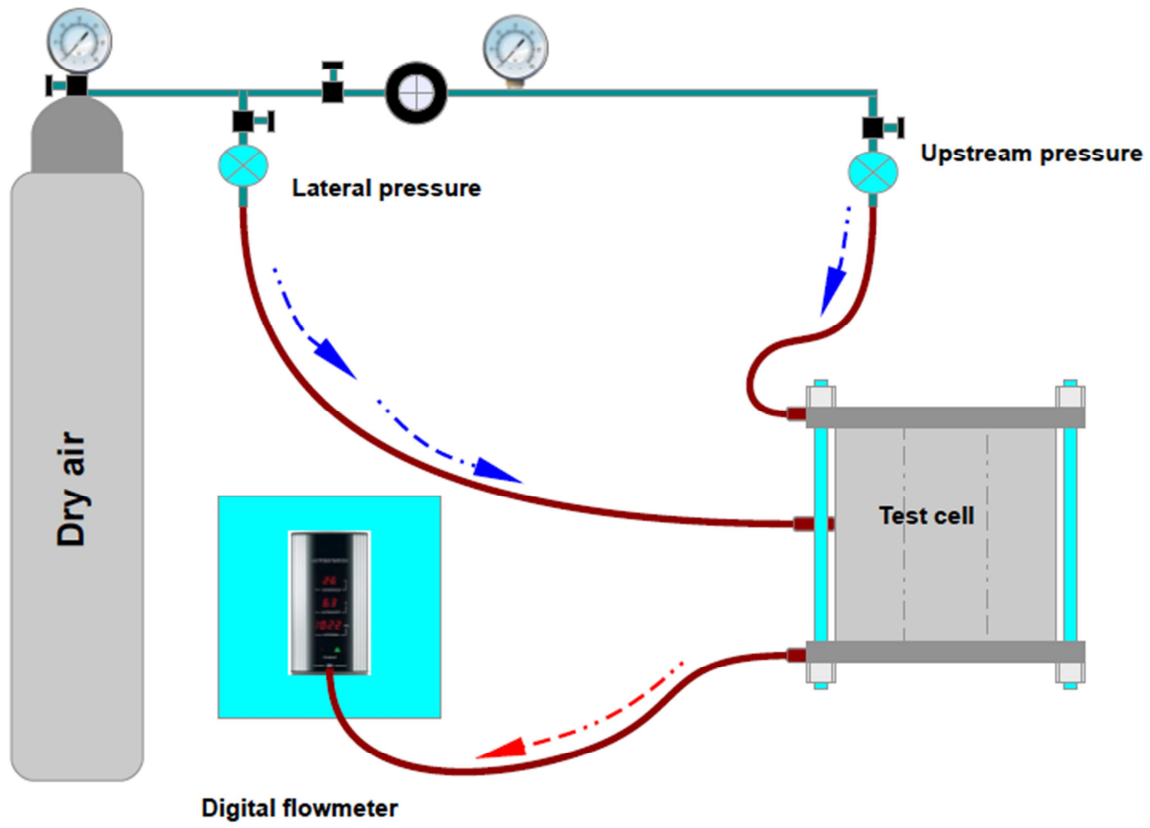


Fig. 61: A cell of air permeability

The initial opening of a crack was measured with a video-microscope (images with high resolution) with graphical tools for performing geometric measurements (length, surfaces, etc..). The opening of a crack is the average of 5 measurements distributed over the top and bottom faces of the specimen (Fig.62)



Fig. 62: Initial crack taken by a video microscope (in the order of 100 μm)

The experimental results made on nineteen cracks (Fig.63) in the laboratory show that there is a polynomial correlation between the flow and the initial opening of the crack (empirical relationship).

$$Q = 8 * 10^{-6} * w^3 - 8 * 10^{-4} * w^2 + 0.0356 * w \quad \text{Eq.5}$$

Q: Airflow measured by the cell of the permeability (L/ min)

W: apparent opening measured by a video microscope (μm)

This relationship will be used later to estimate the apparent aperture of a crack in healing. Indeed, from an experimentally measured airflow (Q) by a test of a permeability, the apparent opening (w) can be estimated using the last equation. This type of relationship is consistent with the flow model proposed by Ismail (Ismail, 2006).

The apparent opening is an indirect estimate of the actual opening of a crack being self-healing. This value is however very useful because it is not possible to measure the actual opening of a crack after self-healing. Indeed, during storage in a humid chamber, after the initial cracking, the formation of secondary hydrates and carbonation in the crack and on the external surfaces of the specimens make practically impossible the precise location of the cracks lips

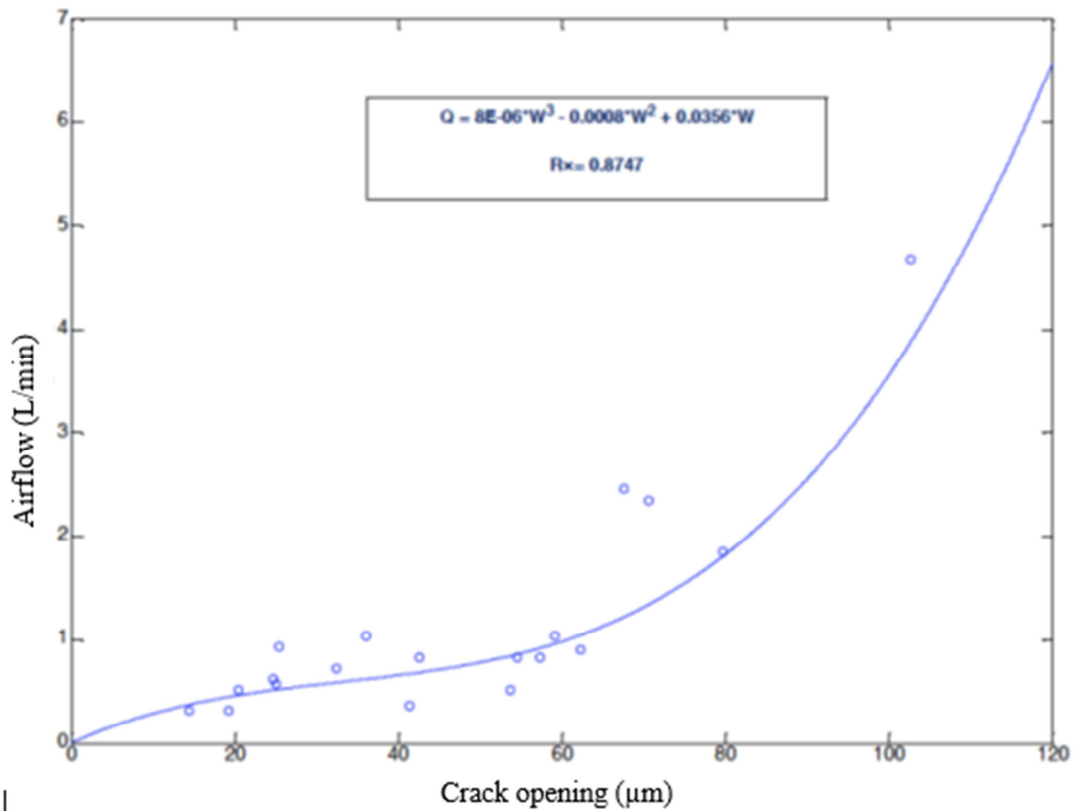


Fig. 63: Initial crack size Vs. Airflow

3. Results: Self-healing effect

After the measurement of the initial crack by the permeability tests for each sample, the samples are placed in a humid chamber for one month. The specimens were subjected to drying at 40° C for 24 hours before starting the airflow measurement. This treatment facilitates the evaporation of water into the crack, and reduces the risk of contamination of the cell permeability and flow meters. Then, the airflows are measured again after 2 and 5 months by the cell permeability. Then, from the values of the airflow and using the equation $Q=f(w)$ the size of cracks are calculated (See Fig.64, Fig.65). We can't use the video-microscope because during storage in a humid chamber (after the initial cracking), the formation of secondary hydrates and carbonation in the crack and on the external surfaces of the specimens make practically impossible to precise the lips cracks location.

3.1. The evolution of the airflow

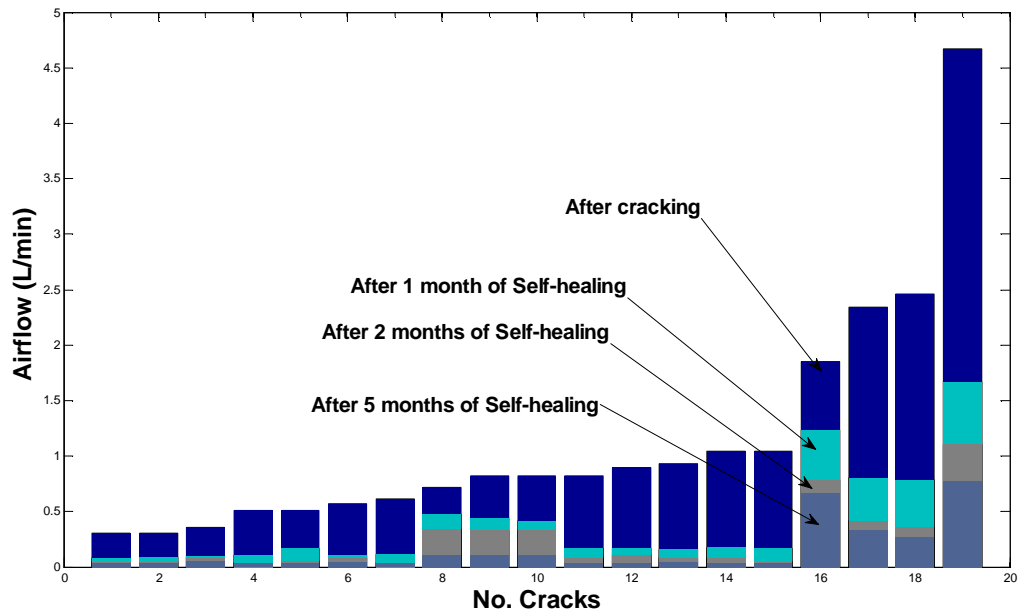


Fig. 64: The evolution of the airflow before and after self-healing in humid chamber for all the cracks

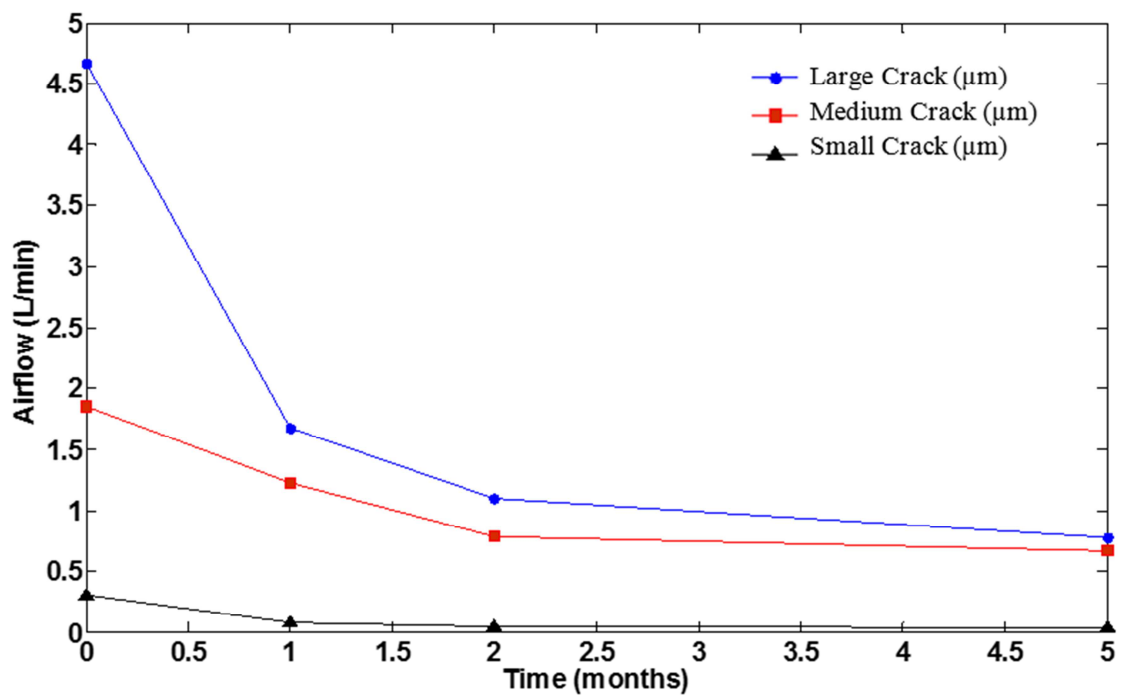


Fig. 65: The variation of the airflow for different cracks Vs. Time

The curves represent the effect of the self-healing on the airflow after 1, 2 and 5 months in the humid chamber.

Fig.64 shows the evolution of airflows as a function of storage time in the humid chamber after the initial cracking. All the airflows decrease according to time, regardless of the initial opening of the crack. This general pattern demonstrates the existence of a self-healing mechanism that gradually fills the volume of cracks and opposes the passage of air. So, the airflows are reduced after self-healing, which shows that moisture plays a major role in closing cracks.

While, the self-healing of small cracks is greater than that of big cracks. Thus, the decreasing of the airflow is more remarkable for the big cracks.

The analysis of the slope of the curves versus time indicates that the kinetics of self-healing is most important during the first month after the initial cracking. Between 1 and 5 months, flows continue to decrease, but about flows 4 times lower than that measured during the first month. The opening of the initial crack influences the evolution of the airflow. In general, the decreasing of airflows is more quickly in the first month for the higher initial cracks. (Fig.65).

To further analyse the influence of the self-healing on the evolution of flows versus time, the histogram (Fig.64) is plotted to express the proportion of airflow of each stage (after 1 month, after 2 months and after 5 months) comparing to the initial airflow (after cracking).

The flow of medium and small cracks (**$Q < 2.5 \text{ L/min}$**) decreases significantly more quickly during the first month of self-healing. After 2 and 5 months, the decreasing continues slowly. So, the results show that the crack is thinner, the flows decline rapidly during the first month and become slow after 2 and 5 months of storage and tend to zero.

During the first month, the formation of hydrates and carbonation fill part of the volume of the crack. Subsequently, this phenomenon continues, but much slower, probably because of the significant obstruction of the crack limiting the supply of CO_2 and moisture for the further reactions.

For larger cracks (**$Q > 4 \text{ L/min}$**), the relative rate gradually decreases over time. After five months, the final flow rate is 25% of the initial flow.

Clogging is more gradual because the volume to be filled is bigger. Even after one month, the crack is still relatively few and closed. Moisture and CO_2 are always available in large quantities to continue the reactions of hydration and carbonation during the 4 months.

3.2. The evolution of the crack size

The apparent crack was determined for all samples after each step of self-healing (After cracking, after 1 month, 2 and 5 months). These apparent openings (W) were calculated using the experimental relation $Q=f(W)$, by inserting the experimental airflow (Q), then extracting the roots of the polynomial (Fig.63). The analysis of the evolution of the apparent crack allows more precise quantification of the self-healing mechanisms in the cracks.

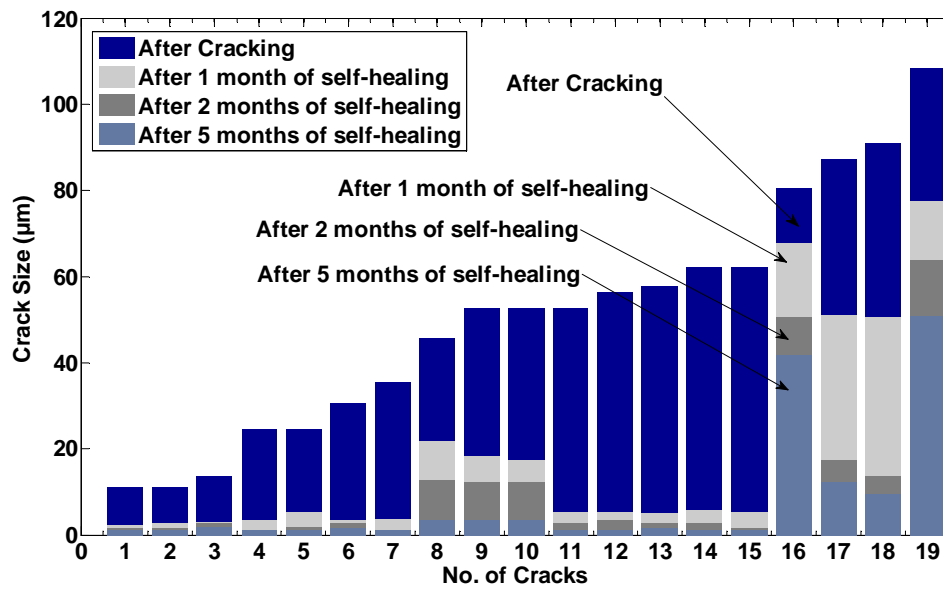


Fig. 66: The evolution of the size of crack before and after self-healing in humid chamber

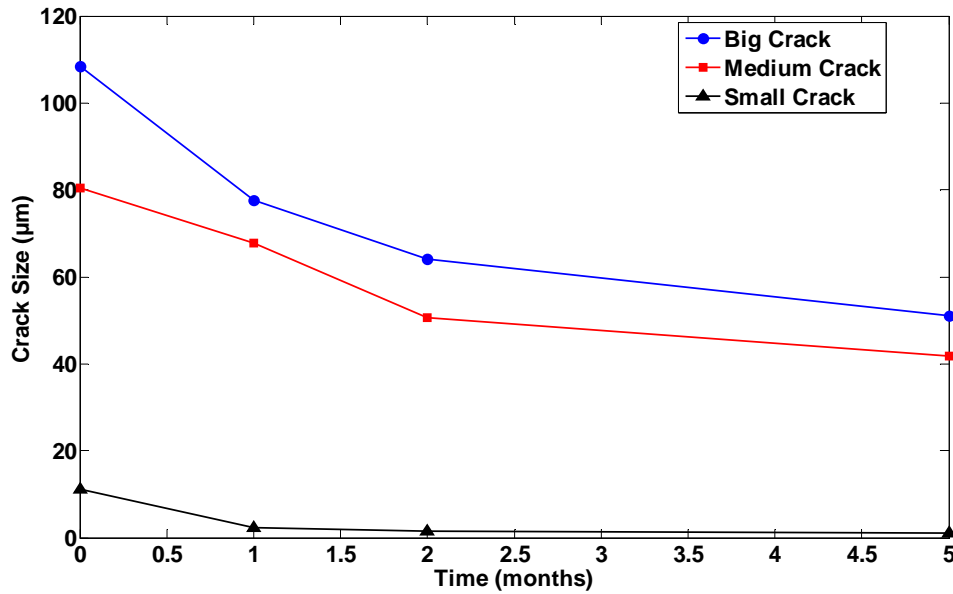


Fig. 67: The variation of the crack size for different cracks Vs. Time

Figure 67 presents the evolution of the apparent opening function of time for 3 types of cracks. As in the case of the flows, the kinetics of the apparent opening is variable in time. It is much faster during the first month after cracking. The healing rate is about 45 microns / month during the first month. This rate varies relatively slightly with the initial opening of the crack (38-56 microns / month). Between 1 and 3 months of storage after cracking, the average rate of healing decreases very significantly to an average rate of about 6 microns / month. Between 1 and 3 months, the healing rate is strongly influenced by the opening of the crack. It is higher for the crack of 254 microns (14 microns / month) but very low for small crack 41 microns (1 micron / month). As an example for the big crack, the healing in the first month is equal to 30 micron and in the fifth month is 5 micron.

4. Linear acoustic waves

After the measurement of the initial velocity by the acoustic tests for each sample, the samples are placed in a humid chamber to trigger the self-healing process. Then, the velocities are measured again after 1, 2 and 5 months.

The cracks are placed between the two transducers as shown in the Fig.68. An example of a longitudinal velocity is shown in the graphs (Fig.69+Fig.70)

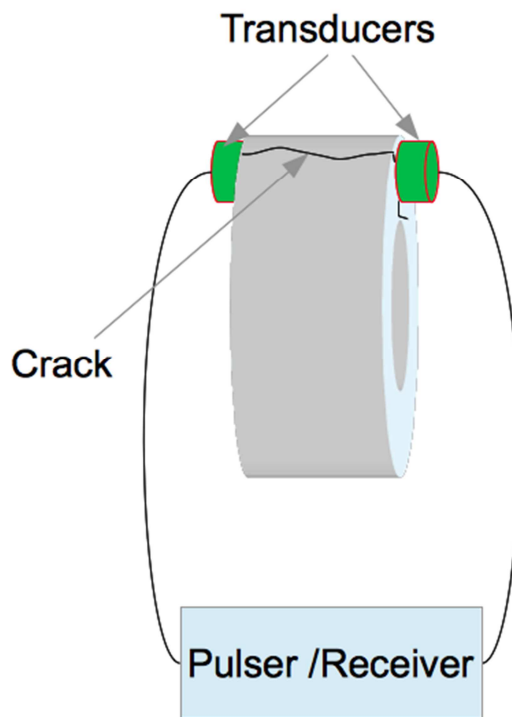


Fig. 68: The crack is placed between the two transducers

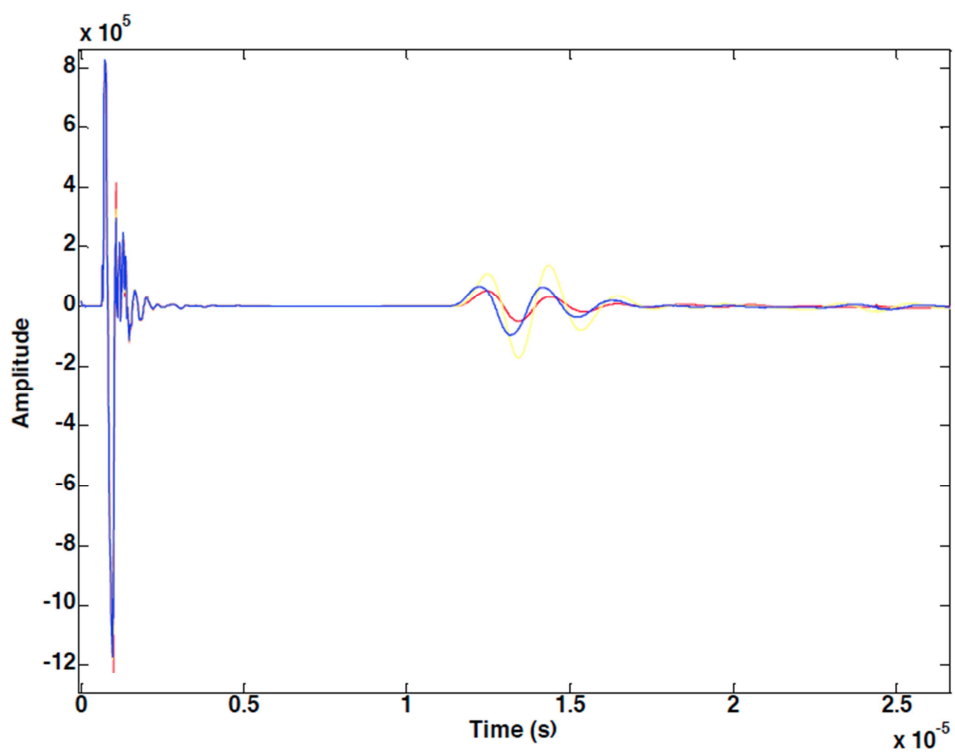


Fig. 69: Example of velocity measurement

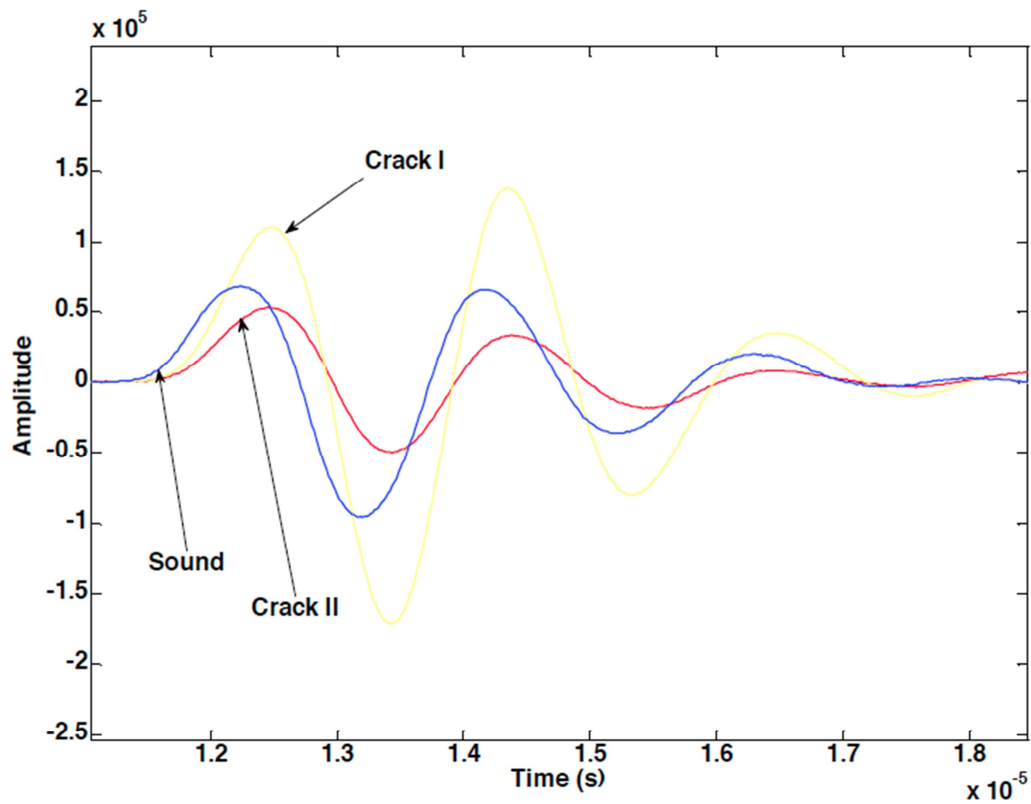


Fig. 70: Zoom for the previous example of velocity measurement

Since the specimens contains many cracks so we define a Velocity for each sample which represents the average of all velocities measured for all the cracks in one sample. In the next table, we presented the specimens with their initial cracks.

Tab 5: Number of cracks on each sample and crack size measured via video-microscope

Initial cracks		
	Crack N°	Crack Size (micron)
Sample 1 (3 cracks)	1	11
	2	13
	3	11
Sample 2 (4 cracks)	1	24
	2	35
	3	24
	4	30
Sample 3 (2 cracks)	1	108
	2	80
Sample 4 (3 cracks)	1	52
	2	45
	3	52
Sample 5 (5 cracks)	1	57
	2	62
	3	56
	4	62
	5	52
Sample 6 (2 cracks)	1	90
	2	87

4.1. Effect of self healing on longitudinal velocity

Figures (From fig.71to Fig.76) show the variation of the velocity during the self-healing process. Globally, it is observed that the curves show an increasing in the first month then a negligible variation of velocity after 2 and 5 months. This growth can be linked to the kinetics of self-healing which is most important during the first month after the initial cracking. For example, it can be noted a variation of 2% in the velocity after one month of healing.

Indeed, after cracking, the volume of crack is empty (filled by air) and after self-healing the same volume will be filled step by step due to the hydration of cement. Or the acoustic velocity is greater in the solid than the air.

The results show a good correlation between airflow and velocity in the first month but this correlation is neglected after 2 and 5 months So, we can conclude that velocity is a good indicator for self-healing.

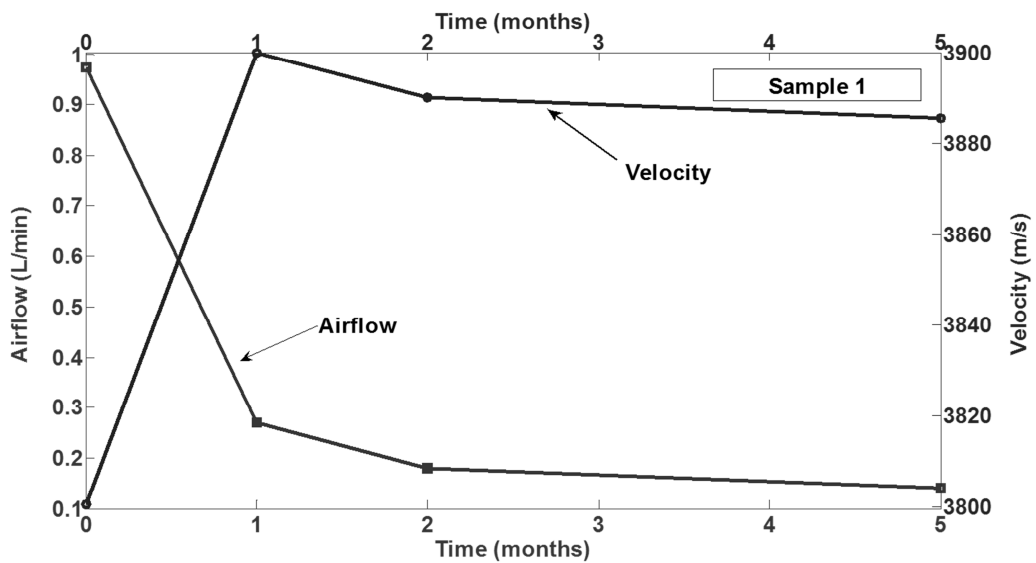


Fig. 71: The variation of the velocity vs. time for the sample N° 1

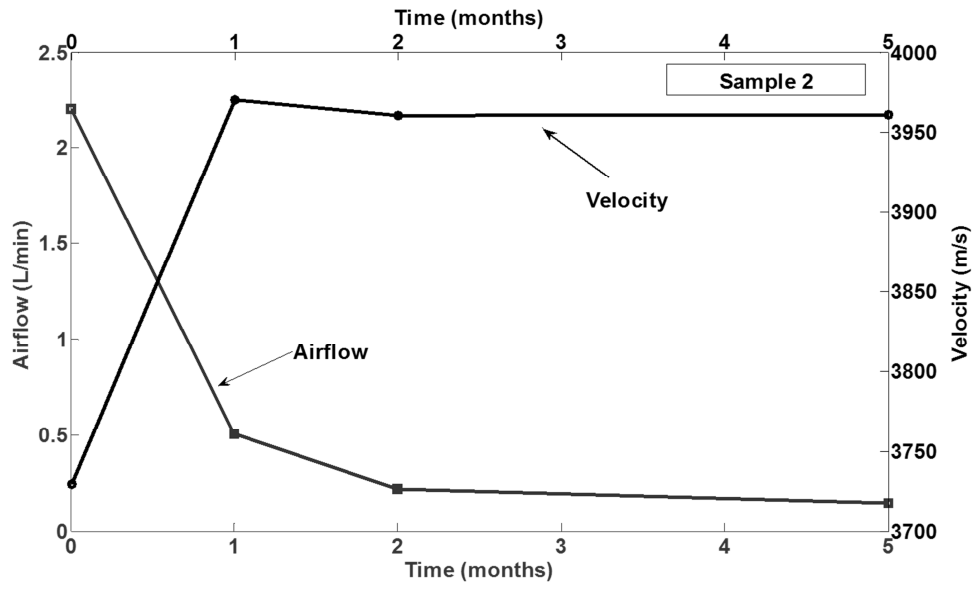


Fig. 72: The variation of the velocity vs. time for the sample N° 2

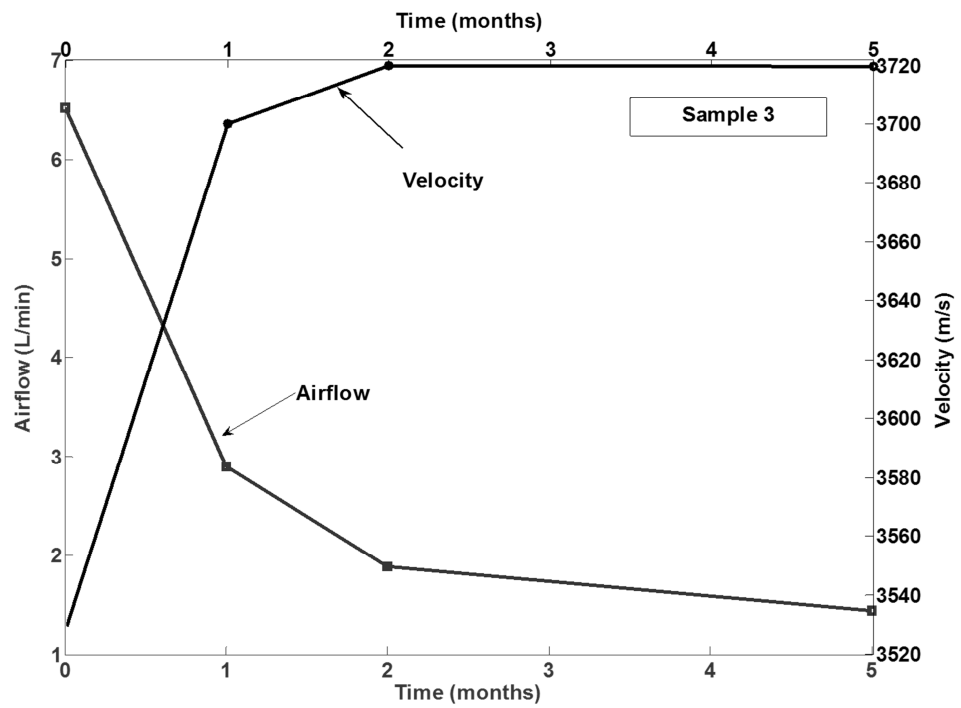


Fig. 73: The variation of the velocity vs. time for the sample N° 3

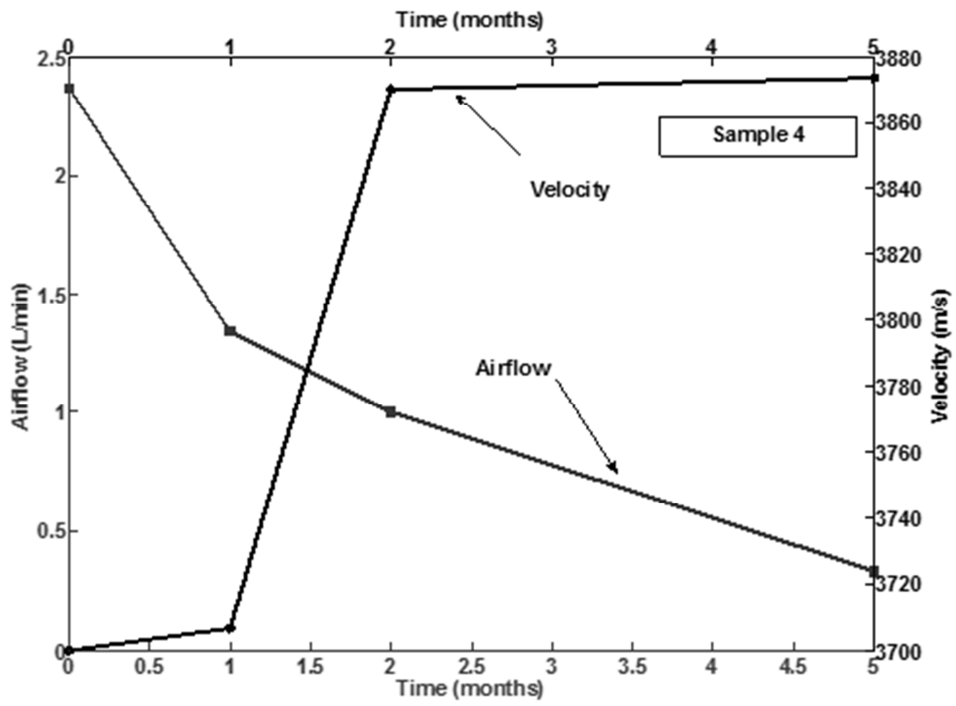


Fig. 74: The variation of the velocity vs. time for the sample N° 4

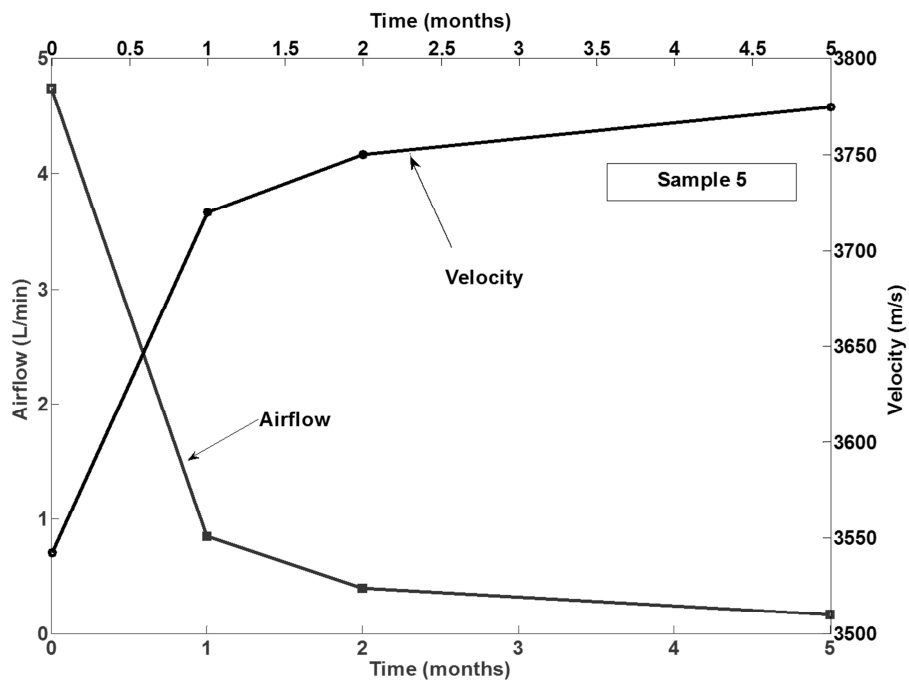


Fig. 75: The variation of the velocity vs. time for the sample N° 5

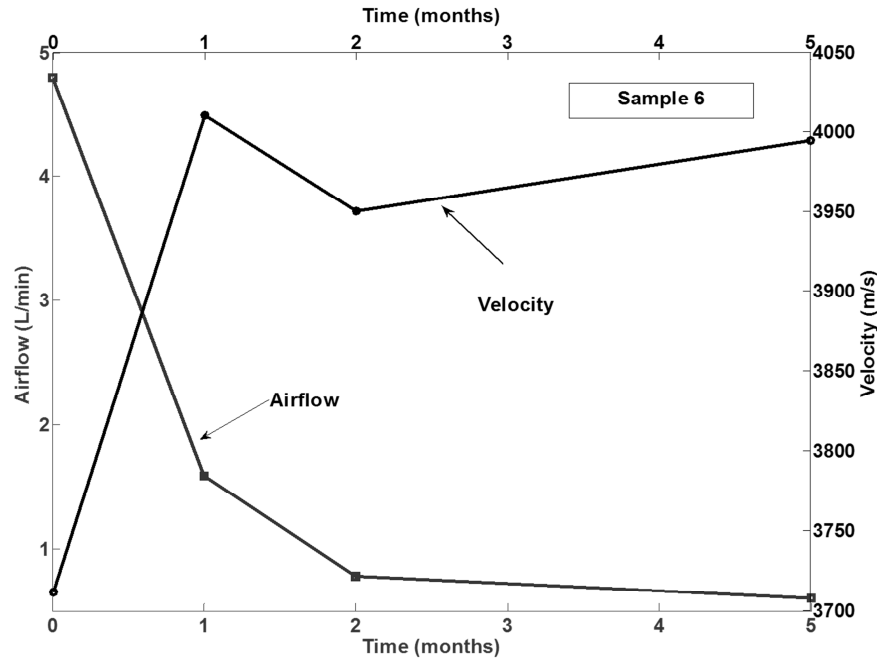


Fig. 76: The variation of the velocity vs. time for the sample N° 6

5. Nonlinear acoustic waves

5.1. Choice of resonance frequency

In non-linear acoustic, the choice of the frequency range is one of these challenges, which must be chosen according to the tested materials. In the case of homogeneous materials (like the majority of metallic materials), we have only to choose the frequency so as to obtain a wavelength less than the size of the defects to be detected. In the case of non-homogeneous materials (such as cement-based materials), this consideration becomes complex because there are several types of particles (eg. Fine aggregate, cement hydrated phases) and several types of irregularities which sizes are not known with precision. In this case, defects are "invisible" to the low frequency waves because they are inferior to the sent wavelength. This shows that it is important to find the appropriate frequency ranges for the type of characterization referred.

In addition, the frequency of resonance depends on the form of the specimens. For the sample form (cylinder, cube...) it is easy to determine the frequency of resonance. It's normally linked to the mechanicals, physic characteristics. In the case of an annular specimen, the

determination of the resonance frequency becomes so difficult. To solve this problem, we need a numerical simulation. To do this, we choose FEM Lab 2D as a software (Fig.77) and a triangular mesh (Fig.78)

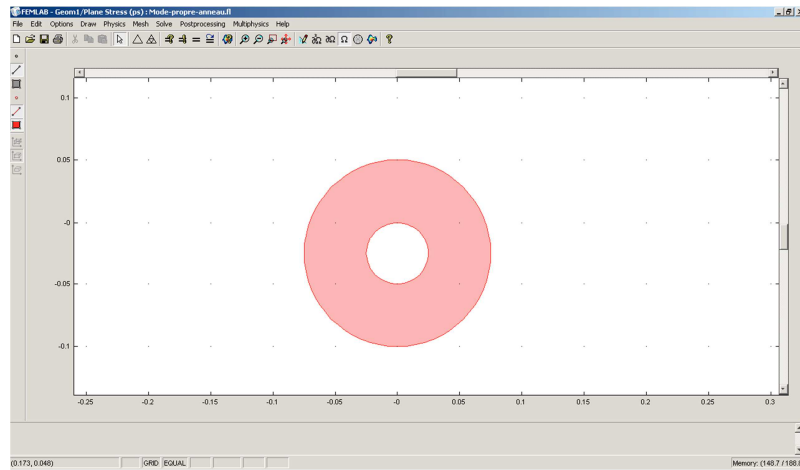


Fig. 77: Definition of the domain of the resolution

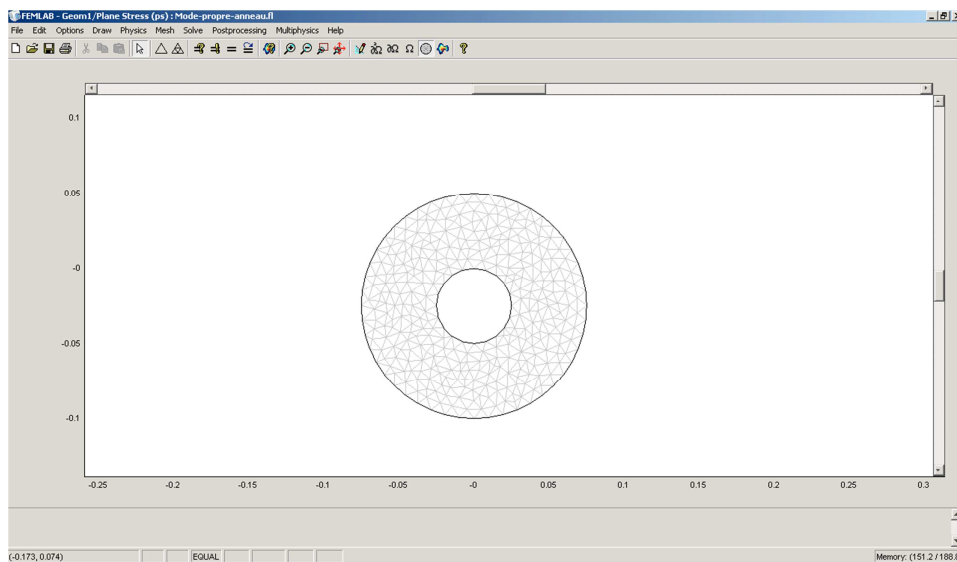


Fig. 78: Triangular Mesh

After simulation, two frequencies are chosen for 12 and 15 KHz (Fig.79+Fig 80). This choice is based essentially on the clearness of the experimental curves.

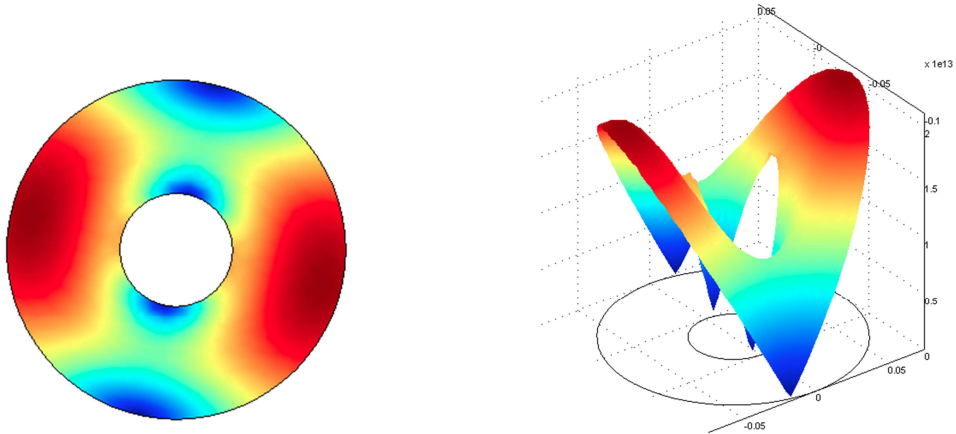


Fig. 79: Frequency of resonance 12 KHz

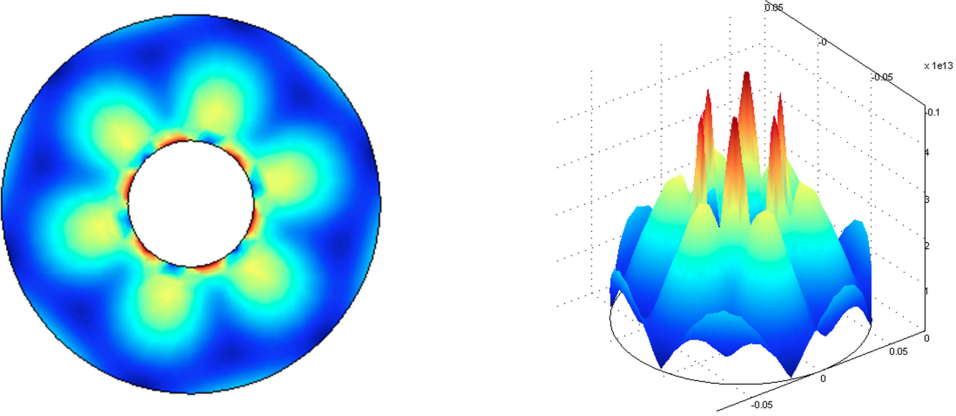


Fig. 80: Frequency of resonance 15 KHz

Examples of experimental shift resonance

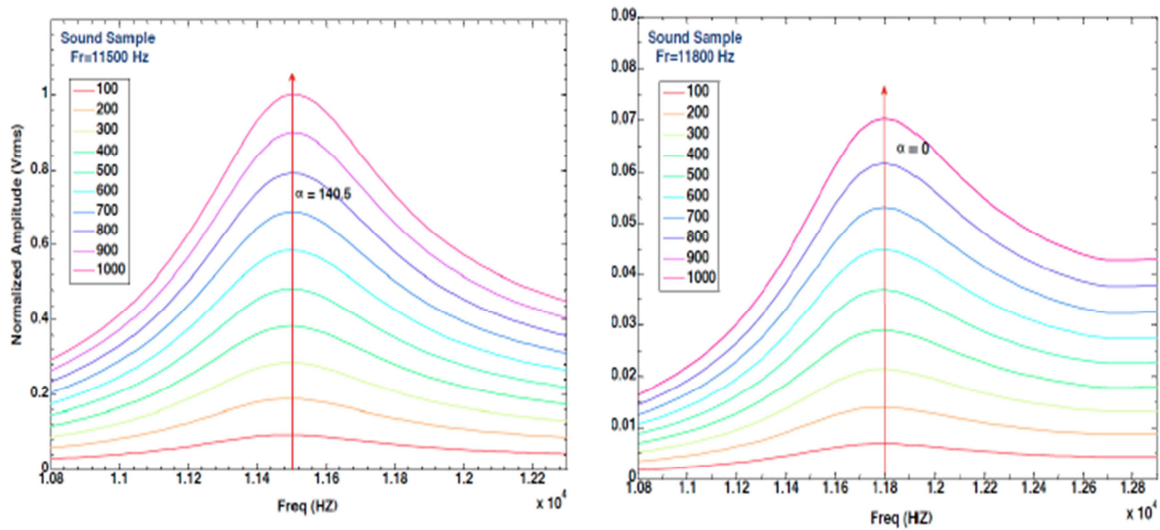


Fig. 81: Shift resonance of a sound sample

The curve of resonance (Fig.81) of the sound sample shows that the sound mortar shift is not necessarily equal to zero, which implies that mortar structure admits already negligible nonlinearity. This type of nonlinearity comes from the inhomogeneity structure of mortar.

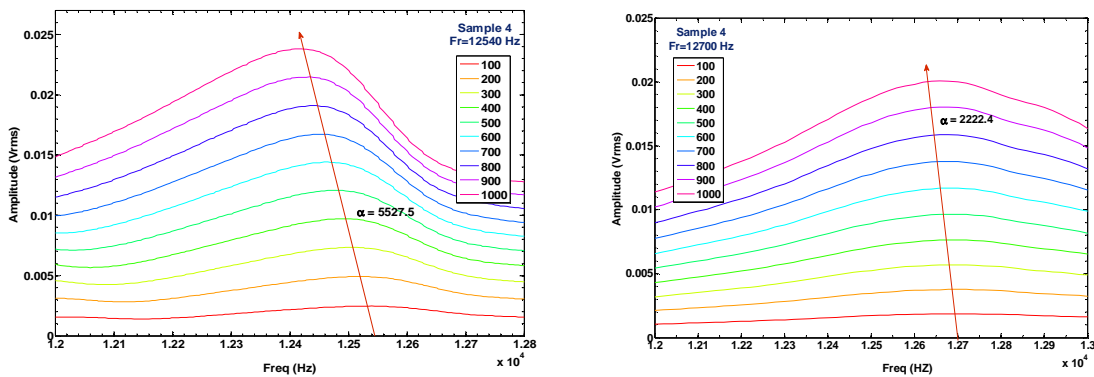


Fig. 82: Shift resonance before and after self-healing for a cracked sample

The curve of resonance (Fig.82) for a damaged sample shows that the shift decrease after self-healing which improve the:

- Existence of self-healing phenomena
- The technique of the shift resonance is able to detect the self-healing

5.2. Evolution of non-linear parameter "Alpha" for 12 KHZ

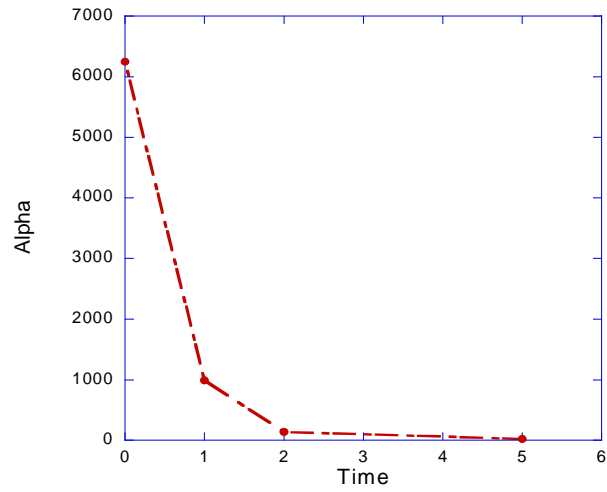


Fig. 83: The variation of the alpha vs. time for the sample N° 1

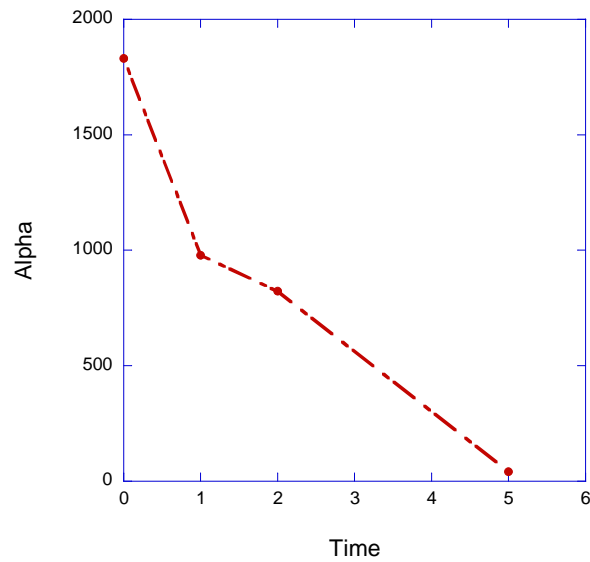


Fig. 84: The variation of the alpha vs. time for the sample N° 2

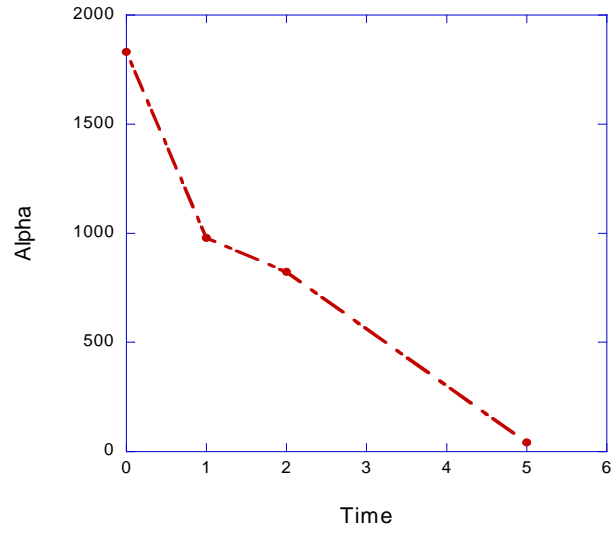


Fig. 85: The variation of the alpha vs. time for the sample N° 3

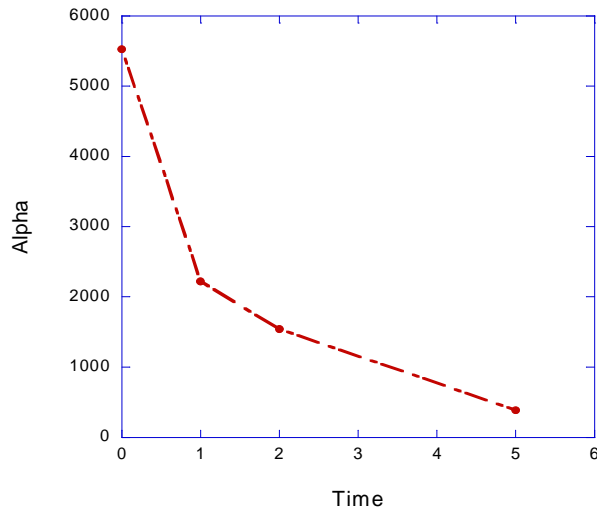


Fig. 86: The variation of the alpha vs. time for the sample N° 4

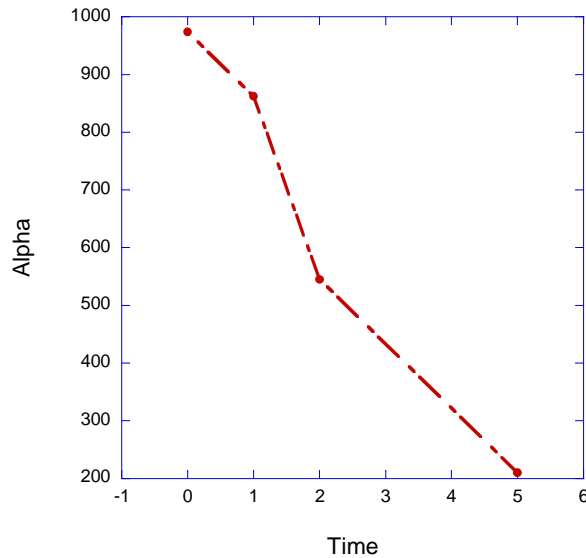


Fig. 87: The variation of the alpha vs. time for the sample N° 6

The graphs (From Fig.83 to Fig.87) show the evolution of alpha according to time. As expected, Alpha decreases with time. The values of alpha decrease significantly and more quickly during the first month of self-healing. After 2 and 5 months, the decline continues slowly. So, the results show that when the crack is thinner, alpha decline rapidly during the first month and become slow after 2 and 5 months of storage and tend to zero. In general, at the end of the self-healing process, alpha does not reach the value 0 which confirms that the crack is not completely healed. It can be noted also the big difference between the values of initial alpha and after 5 months which can reaches to times five in some cases. This difference can prove the high sensitivity of alpha to follow the self-healing phenomena.

5.3. Relationship between airflow and Alpha

In order to see the effect of the self-healing on alpha, the figures (From Fig.88 until Fig.91) are plotted. The figs show the variation of the non-linear parameter alpha with airflow. The alpha increases according to the airflow.

In general, alpha reminds small for the small airflow (small crack size) but increases exponentially when the airflow increases (big crack size). So the non-linear parameter alpha represents a good indicator to follow the self-healing phenomena.

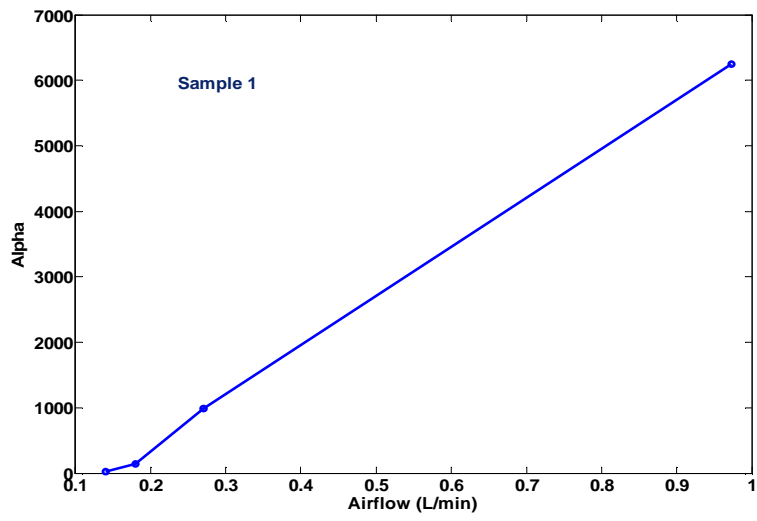


Fig. 88: The variation of the alpha vs. airflow for the sample N° 1

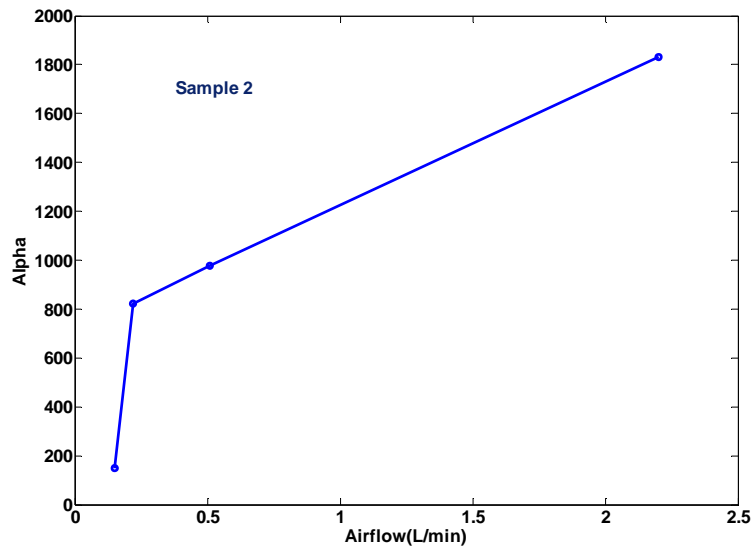


Fig. 89: The variation of the alpha vs. airflow for the sample N° 2

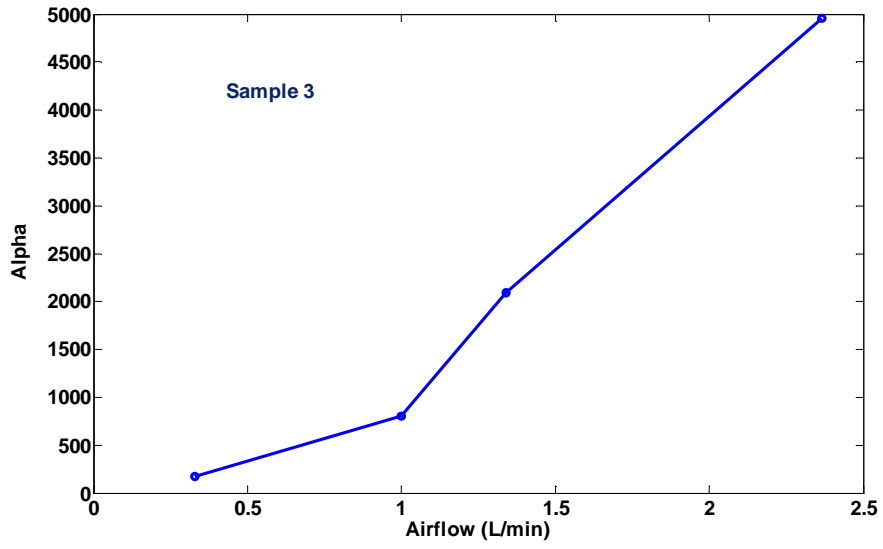


Fig. 90: The variation of the alpha vs. airflow for the sample N° 3

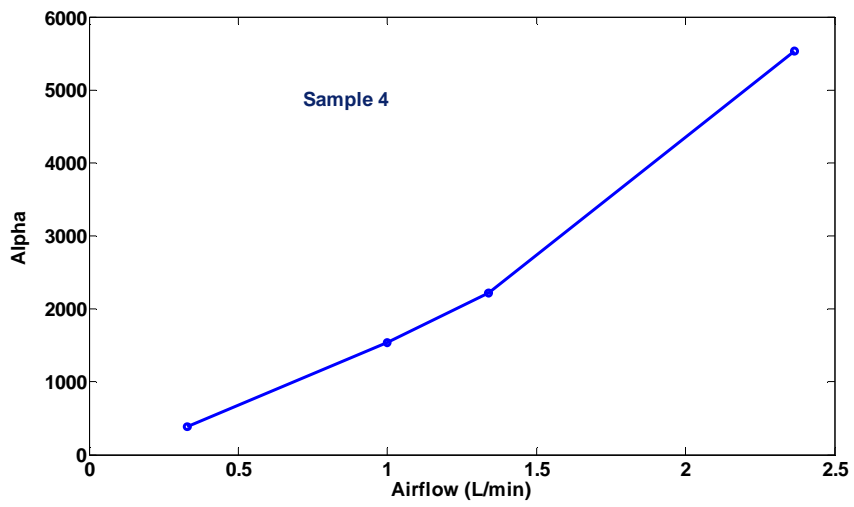


Fig. 91: The variation of the alpha vs. airflow for the sample N° 4

6. Correlation between non-linear parameter and airflow

6.1. Correlation: Alpha 12 KHz and airflow

For the purpose of seeing the impact of the airflow on the non-linear parameter alpha 12, we plot all the results corresponds to “alpha 12 KHz” in the same graph. The figures (Fig.92, Fig.93) show the variation of the alpha according to the airflow. In overall, the non-linear parameter increases with the airflow. In the first figure we see that that we have some **critical points due to** the experimental errors. So, we make another figure that contains only the correct points. The points that don't respect the shape curve will be neglected but for each case we will keep the different curves. .

The critical points can due to:

- The experimental errors: in fact the tests of the nonlinear acoustic tests are sensitive to the noise although the tests are done in secure room.
- The accelerometer and the transducer should be placed on the same place during all the tests (after cracking, 1 month, 2 month and 5 month of self-healing).
- After retrieving the samples from the humid room, they are dried for 24 hours. Maybe, the samples are not dried in the same way.
- During the data processing, the non-linear parameters are determined by trend curves and by FFT and in general these numerical treatments are based on same assumptions.
→ Such and other effects can produce errors in the values of the non-linear parameters.

In fig.93, we can remark the existence of three zones:

- ✓ For airflow < 1 L/min: the values of alpha doesn't exceed 1500: So for the small crack (< 60 micron) we can deduce that the values of non linear parameter are less than 1500.
- ✓ For $1 < \text{airflow} < 5$: the values of alpha reaches 2000: So for the crack size between 60 and 110 micron we can deduce that the values of non linear parameter can reaches 2000.
- ✓ For the airflow > 5 : the values of alpha reaches 5000: So for the big crack (crack size > 110 micron), we can deduce that the values of non-linear parameter can reaches 5000.

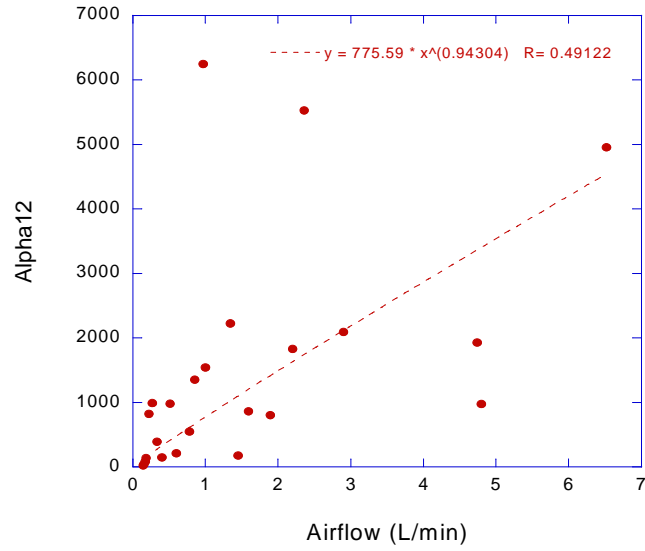


Fig. 92: The variation of the alpha 12 vs. airflow with an exponential approximation

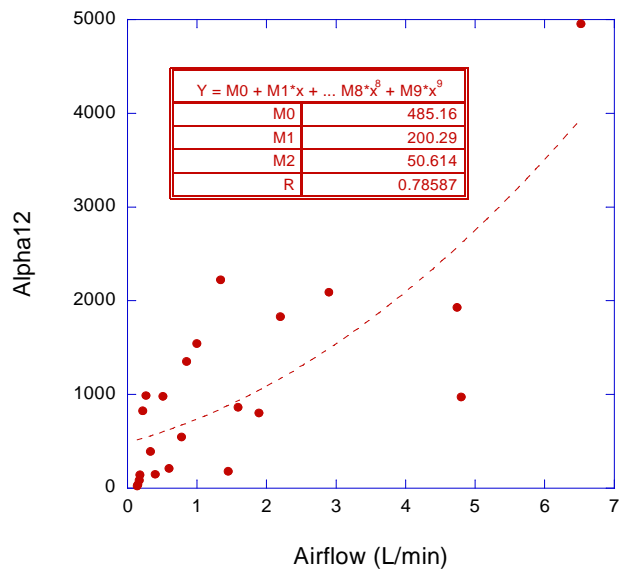


Fig. 93: The variation of the alpha 12 vs. airflow with a polynomial approximation

6.2. Correlation: Beta 12 KHz and airflow

For the purpose of seeing the impact of the airflow on the non-linear parameter beta 12, we plot all the results corresponds to “beta 12 KHz” in the same graph. The figures (Fig.94+Fig.95) show the variation of the beta according to the airflow. In overall, the non-linear parameter increases with the airflow. In the first figure we remark that we have some critical points due to the experimental errors. So, we make another figure that contains only the correct points. These values are determined by neglecting the points that doesn't respect the shape curve. In the second figure we can remark the existence of two zones:

- ✓ For airflow <1 L/min: the values of beta doesn't exceed 30: So for the small crack (<60 micron) we can deduce that the values of non linear parameter are less than 30.
- ✓ For $1 < \text{airflow} < 3$: the values of beta reaches 40: So for the crack size between 60 and 95 micron, we can deduce that the values of non linear parameter can reaches 40.
- ✓ For the airflow >5: the values of alpha reaches 65: So for the crack size bigger than 85 micron we can deduce that the values of non-linear parameter can reaches 65.

→ As conclusion concerning the variation of the beta 12 and alpha 12, we note that alpha is more sensitive to the self-healing than beta. Indeed, the evolution is more speed for the change of the crack size. As an example, the slope of the alpha curve is equal to 50 is bigger than the slope of beta curve that equal to 8.

So, we can deduce that the alpha 12 and beta 12 are good indicators to follow the self-healing but the shift resonance technique is more efficient than the higher harmonic generation.

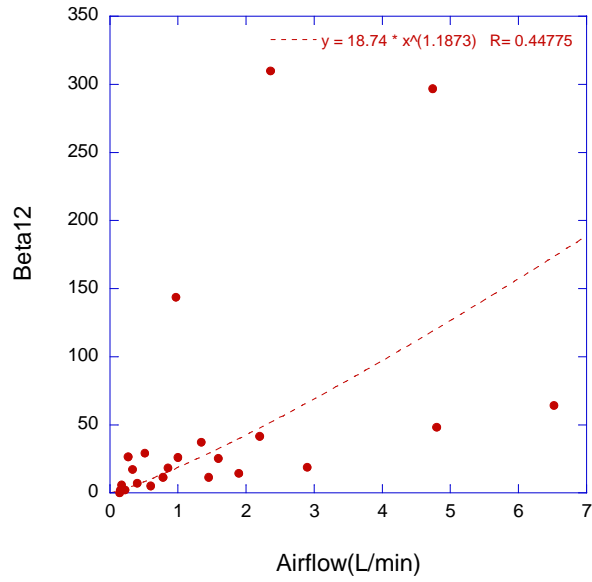


Fig. 94: The variation of the beta 12 vs. airflow

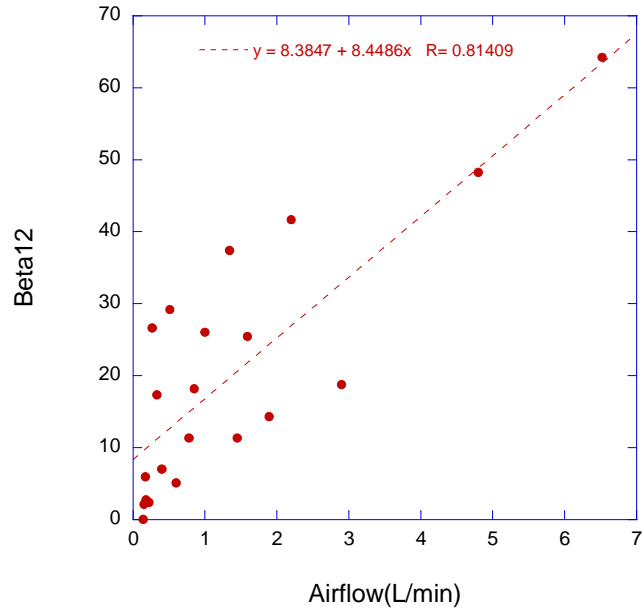


Fig. 95: The variation of the beta 12 vs. airflow

6.3. Correlation Alpha 15 KHz and airflow

For the purpose of seeing the impact of the airflow on the non-linear parameter alpha 15, we plot all the results correspond to “Alpha 15 KHz” in the same graph. The figures (Fig.96, Fig.97) show the variation of the beta according to the airflow. Overall, the non-linear parameter increases with the airflow. In the first figure we view that we have one critical point due to the experimental errors. In the second figure we can observe the existence of two zones:

- ✓ For airflow <3 L/min: the values of alpha doesn't exceed 2000: So for crack size between 0 and 95 micron, the values of alpha are less than 2000.
- ✓ For the airflow >3: the values of alpha are higher than 2000: So for the crack size bigger than 100 micron, the values of alpha are between 2000 and 4500.

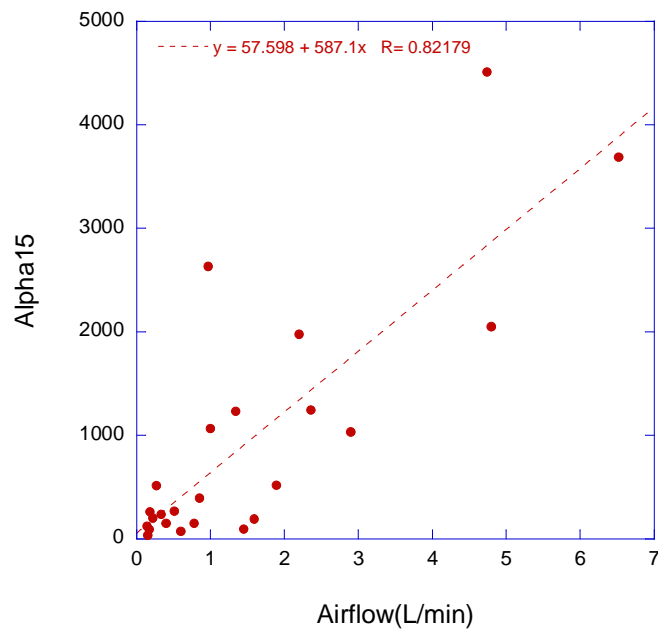


Fig. 96: The variation of the alpha 15 vs. airflow

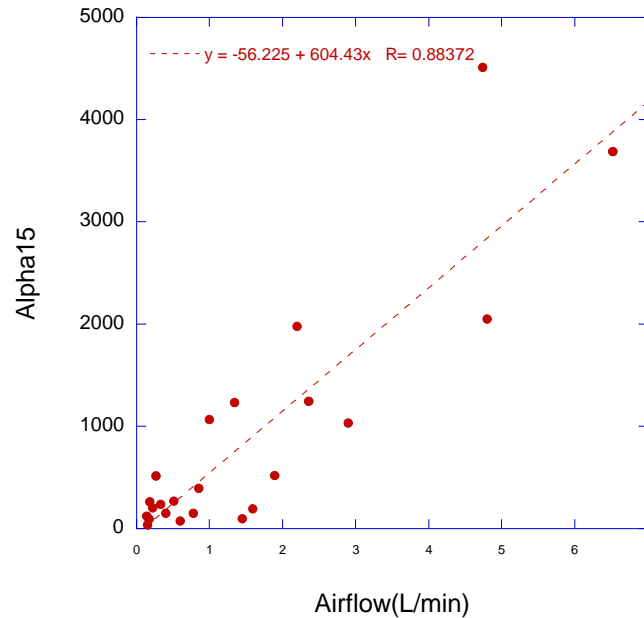


Fig. 97: The variation of the alpha 15 vs. airflow

6.4. Correlation Beta 15 KHz and airflow

For the purpose of seeing the impact of the airflow on the non-linear parameter beta 15, we plot all the results correspond to “Beta 15 KHz” in the same graph. The figures (Fig.98+Fig.99) show the variation of the beta according to the airflow. In overall, the non-linear parameter increases with the airflow. We can observe the existence of two zones:

- ✓ For airflow <3 L/min: the values of beta are fewer than 50: So for crack size between 0 and 95 micron, the values of beta are between 0 and 50.
- ✓ For the airflow >3: the values of beta are bigger than 50: So for the crack size bigger than 100 micron we can deduce that the values of non-linear parameter are superior than 50 and can reaches 250.

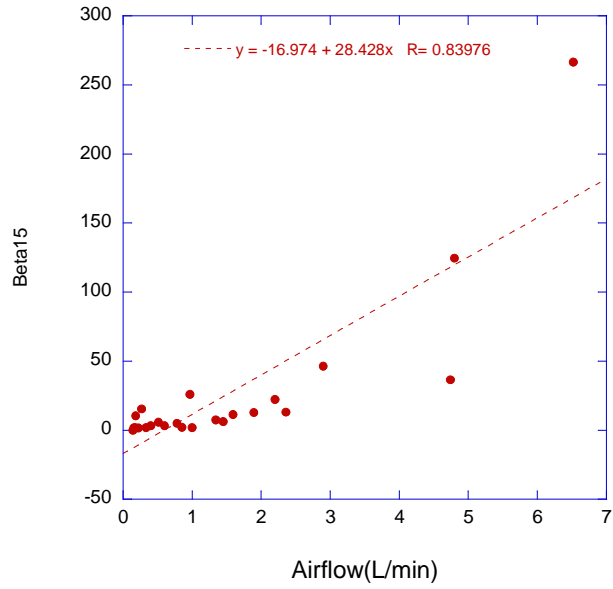


Fig. 98: The variation of the beta 15 vs. airflow with a linear approximation

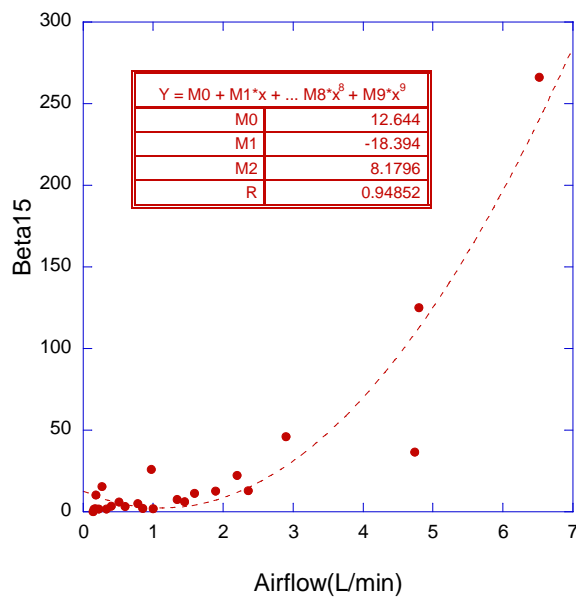


Fig. 99: The variation of the beta 15 vs. airflow with a polynomial approximation

→ As a conclusion concerning the variation of the beta 15 and alpha 15, both the non-linear parameters increases according to the crack size and the air flow. We also note that alpha is more sensitive to the self-healing than beta. Indeed, the evolution is more speed for the change of the crack size. As example, the gradient of the alpha curve is equal to 604 is bigger than the gradient of beta curve that equal to 28.

So, we can deduce that the alpha 15 et beta 15 are a good indicators to follow the self-healing but the shift resonance technique is more efficient than the higher harmonic generation.

We can observe also that the non-linear parameters of 15 KHz give us as a good correlation between the crack size and alpha /beta than the nonlinear parameters of 12 KHz. So the frequency of resonance corresponds to 15 KHz is more sensitive to characterize and follow the damage than 12 KHz.

7. Correlation between non-linear parameter and damage index

We looked for a correlation between the airflow/crack size and the non-linear parameters, but that results are related to our case study. So, to obtain a general relation ship, we defines a damage index:

$$I = \frac{W}{P_{moy}} = \frac{W}{2\pi r}$$

Where:

- w: Crack size
- r: Mean radius of the annular specimen (Fig.100)
- I : index damage ($\mu\mathbf{m}/\mathbf{m}$)

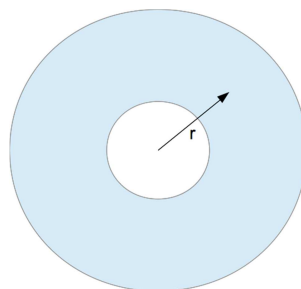


Fig. 100: Mean radius of the annular specimen

If the specimen contains more than one crack, we determine the total airflow (the sum of each airflow) then using the relation $Q=f(w)$, we calculated the appropriate crack size.

In the interpretation of the results, we define $I_r=200 \mu\text{m}/\text{m}$ as the break value of the mortar.

7.1. Correlation Alpha 12 KHz and damage index

Fig.101 shows the evolution of the Alpha 12 with damage index. The non-linear parameter increases in function the damage index according to polynomial function of 2nd degree. Based on the breakdown value, two zones can be defined:

- Before the breaking (Damage Index < 200): alpha 12 is less than 1000. So for the small crack (<60 micron) the value of alpha 12 doesn't exceed 1000.
- After the breaking (Damage Index >200), alpha 12 is bigger than 1000. So for the medium crack size (>60 micron) the value of alpha are superior than 1000.

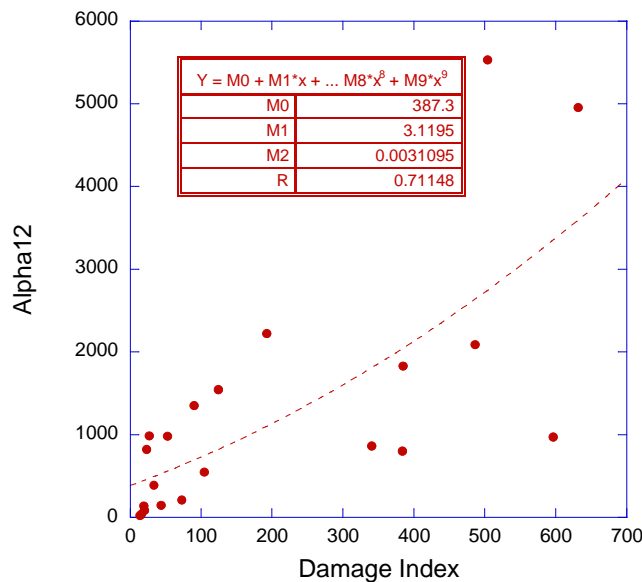


Fig. 101: Alpha 12 Vs. Damage Index

7.2. Correlation Beta 12 KHz and damage index

Fig.102 shows the evolution of the Beta 12 with damage index. The non-linear parameter increases in function the damage index according to polynomial function of 2nd degree. Based on the breakdown value, two zones can be defined:

- Before the breaking (Damage Index < 200): beta 12 is less than 25. So for the small crack (<60 micron) the value of beta 12 doesn't exceed 25.
- After the breaking (Damage Index >200), beta 12 is bigger than 25. So for the medium and big crack (>60 micron) the value of beta are superior than 25.

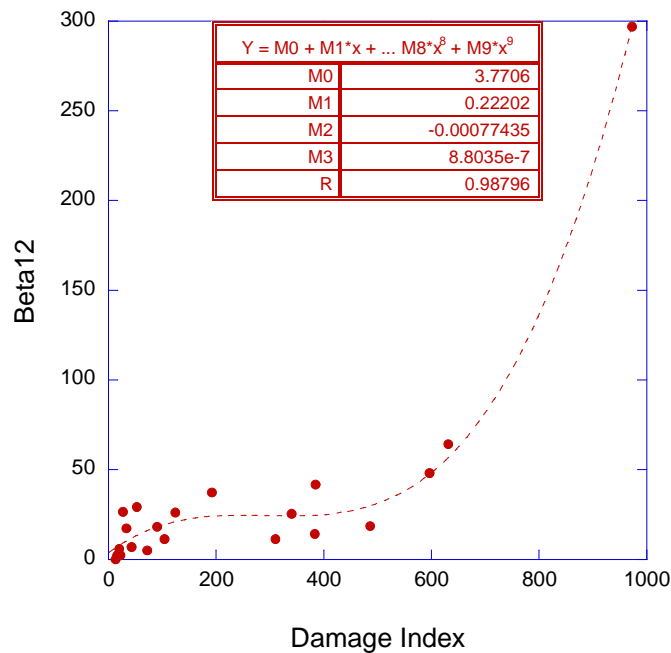


Fig. 102: Beta 12 Vs. Damage Index

→ As a conclusion concerning the variation of alpha 12 and beta 12 according to damage index, both the non-linear parameters increases according to the index damage with a polynomial function of a 2nd degree. We note also that “alpha 12” is more sensitive to detect damage than “beta 12”. Indeed, the evolution is more speed for the change of damage. As an example, the gradient of the alpha curve is equal to 0.003 is higher than the gradient of beta curve that equal to 10^{-6} .

To obtain a better correlation between index damage and nonlinear parameters, we need more experimental tests with different crack size.

7.3. Correlation Alpha 15 KHz and damage index

Fig.103 shows the evolution of the Alpha 15 with damage index. The non-linear parameter increases in function the damage index according to polynomial function of 2nd degree. Based on the breakdown value, two zones can be defined:

- Before the breaking (Damage Index < 200): alpha 12 is less than 500. So for the small crack (<60 micron) the value of alpha 12 doesn't exceed 1000.
- After the breaking (Damage Index >200), alpha 12 is bigger than 500. So for the medium crack size (>60 micron) the value of alpha are superior than 500.

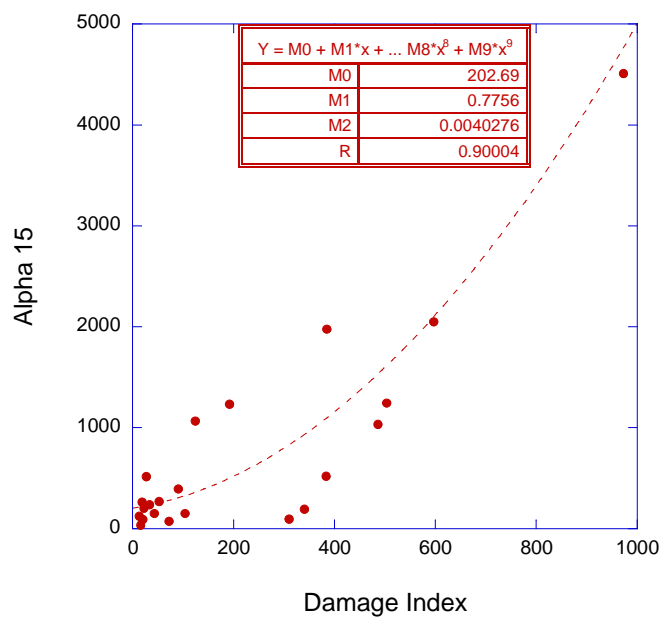


Fig. 103: Alpha 15 Vs. Damage Index

7.4. Correlation Beta 15 KHz and damage index

Fig.104 shows the evolution of the Beta 15 with damage index. The non-linear parameter increases in function the damage index according to polynomial function of 2nd degree. Based on the breakdown value, two zones can be defined:

- Before the breaking (Damage Index < 200): beta 15 is less than 10. So for the small crack (<60 micron) the value of beta 12 doesn't exceed 10.
- After the breaking (Damage Index >200), beta 15 is bigger than 10. So for the medium and big crack (>60 micron) the value of beta are superior than 10.

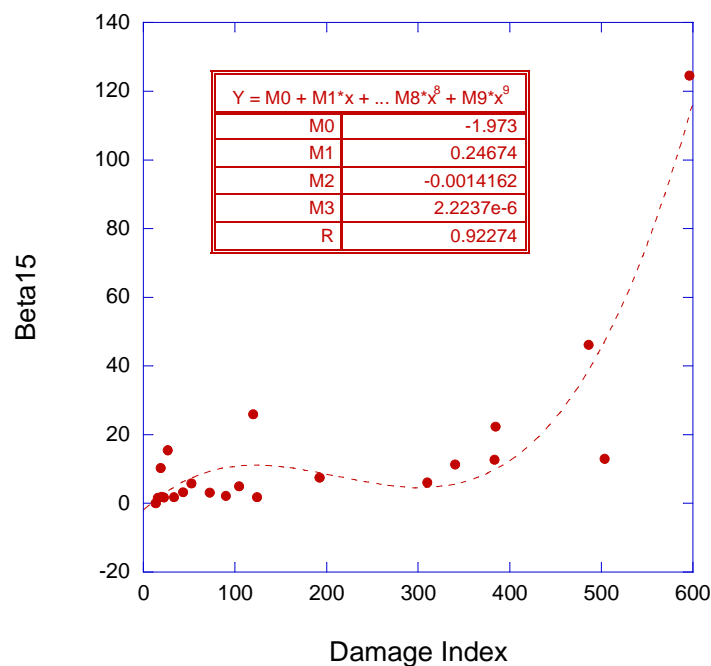


Fig. 104: Beta 15 Vs. Damage Index

→ As a conclusion concerning the variation of the beta 15 and alpha 15, both the non-linear parameters increases according to the index damage. We note also that alpha is more sensitive to the damage than beta. Indeed, the evolution is quicker for the change of index damage. As example, the gradient of the alpha curve is equal to 0.003 is higher than the gradient of beta curve that equal to $2 \cdot 10^{-6}$.

So, we can deduce that the alpha 15 and beta 15 are good indicators to characterize mechanical damage but the shift resonance technique is more pertinent than the higher harmonic generation.

Conclusion

This part included a special attention to various experimental techniques that were necessary to evaluate the self-healing in the mortar. Indeed, the crack size is correlated by a polynomial function to the airflow by a permeability tests. In addition, these tests demonstrated that the kinetics of self-healing is influenced by the initial opening of a crack.

On the other hand, both linear and non linear were used to characterize the self-healing phenomena. Indeed, ultrasonic longitudinal velocities increase during the healing process and show the presence of self-healing phenomenon and the crack close gradually. Moreover, the nonlinear parameters alpha and beta decreases during the healing process, which indicate that the residues of damage decrease progressively.

We succeed to establish a correlation between the nonlinear parameters (alpha and beta) and airflow in the form of a linear and polynomial functions.

Then, aiming to propose a general correlation based on the experimental results, we defined a damage index that will be correlated the non-linear parameters. Indeed, we achieve to define correlations in the form of polynomial function of 2nd degree.

Chapter 8:
Numerical modelling

Introduction

To determine the relationship between crack size and airflow, many experimental tests of permeability were done which take a lot of time. So our objective in this part is to modelize the permeability tests and find a numerical correlation between the crack size and the airflow. Then this relationship allows avoiding permeability tests and link directly the airflow to crack size.

In this chapter we will define the problem, then determine the equations of Navier-Stokes and fix the boundary/initial conditions. Finally, we will discuss the difference between the numerical and experimental results.

1. Problem

During the last part, the equation between Airflow and crack size was determined by a permeability tests. Our objective in this chapter is to model this experience in order to find a numeric correlation between theses parameters. In the beginning, we suppose that the crack can be modelling by two parallel plates (Fig.106). Then, we fix the boundary and initial conditions (Fig.107). Finally, we solve the equations of motions depends on velocity (vertical and horizontal) and the pressure.

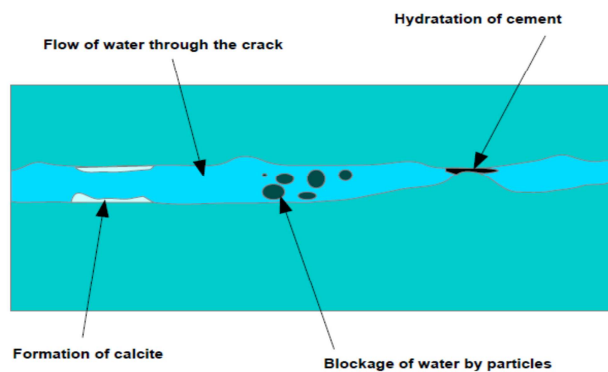


Fig. 105: Schema of the crack

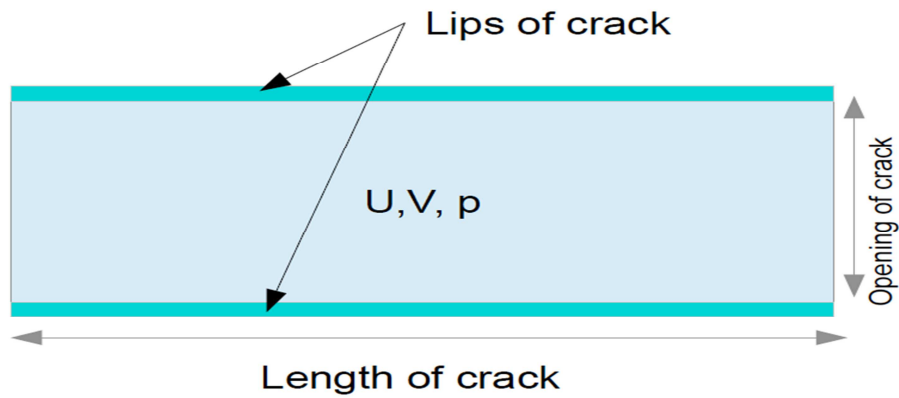


Fig. 106: Domain of the resolution

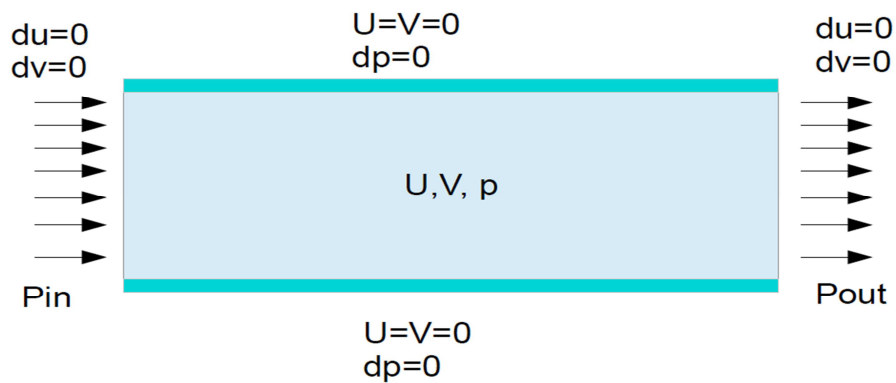


Fig. 107: Boundary conditions

2. Equations and model

After determination of the Navier-Stokes equations between the two lips of crack, we need to fix some hypothesis.

Hypothesis:

We suppose that:

- The two lips of cracks are parallel
- The velocities are equal to zero near the lips.
- The air is an incompressible fluid ($\Delta\rho = 0$) which means that $\rho = \rho_0$

We start with the incompressible Navier-Stokes equations in conservative form:

$$U_{,x} + V_{,y} = 0 \quad (1)$$

$$U_{,t} + (UU)_{,x} + (VU)_{,y} = \frac{-1}{\rho} p_{,x} + \nu(U_{,xx} + U_{,yy}) \quad (2)$$

$$V_{,t} + (UV)_{,x} + (VV)_{,y} = \frac{-1}{\rho} p_{,y} + \nu(V_{,xx} + V_{,yy}) - g \quad (3)$$

Where:

- $(A_{,x}) = \frac{\partial A}{\partial x}$
- $(A_{,t}) = \frac{\partial A}{\partial t}$
- ρ : Density of the air
- ν : Viscosity
- g : Gravity (neglected value)
- U : x-Velocity (m/s)
- V : y-velocity (m/s)
- p : Pressure (Pa)

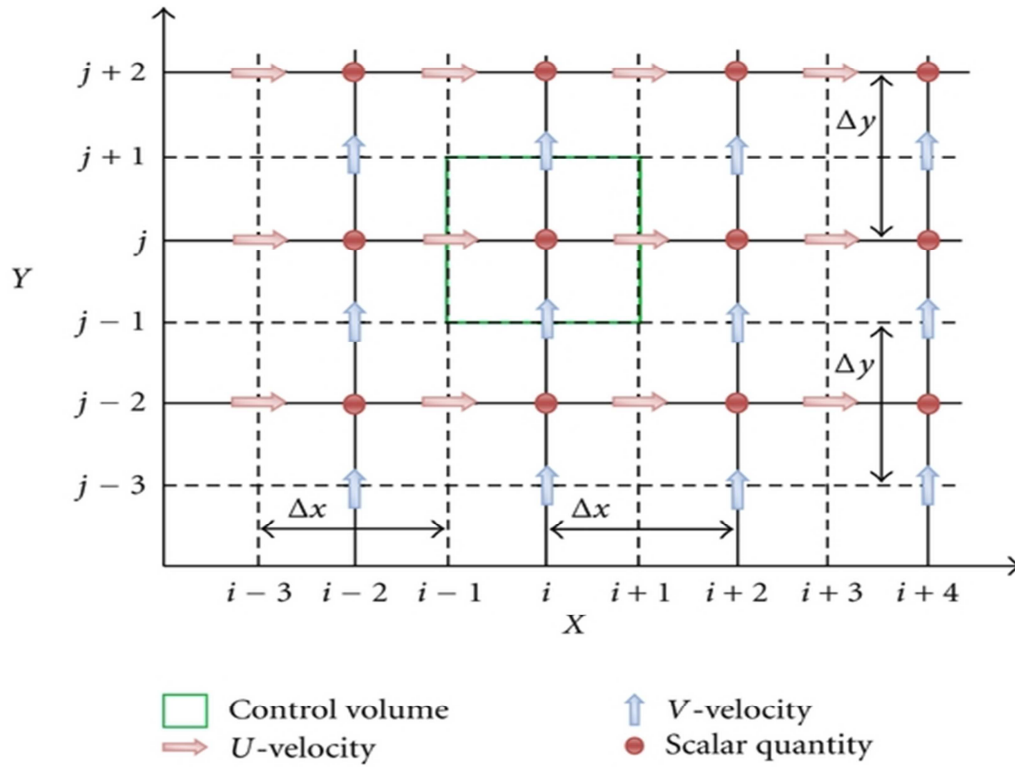


Fig. 108: Meshing of domain of resolution

We want to discretise these equations in space. We will apply central differences. The discretised parts of the Navier-Stokes equations are (without pressure term, which will be added in the pressure correction equation):

$$U_{,x} = \frac{U_{i+1,j} - U_{i-1,j}}{2h_x}$$

$$U_{,y} = \frac{U_{i,j+1} - U_{i,j-1}}{2h_y}$$

$$V_{,x} = \frac{V_{i+1,j} - V_{i-1,j}}{2h_x}$$

$$V_{,y} = \frac{V_{i,j+1} - V_{i,j-1}}{2h_y}$$

$$U_{,xx} = \frac{U_{i+1,j} - 2U_{i,j} + U_{i-1,j}}{h_x^2} \quad (4)$$

$$U_{,yy} = \frac{U_{i,j+1} - 2U_{i,j} + U_{i,j-1}}{h_y^2}$$

$$V_{,yy} = \frac{V_{i,j+1} - 2V_{i,j} + V_{i,j-1}}{h_y^2}$$

$$V_{,xx} = \frac{V_{i+1,j} - 2V_{i,j} + V_{i-1,j}}{h_x^2}$$

We insert the last equation in equation Eq.1:

$$\frac{U_{i+1,j} - U_{i-1,j}}{2h_x} + \frac{V_{i,j+1} - V_{i,j-1}}{2h_x} = 0$$

$$u_{j,t} + u_{jj} \frac{u_{i+1,j} - u_{i-1,j}}{2h_x} + v_{jj} \frac{u_{j+1} - u_{j-1}}{2h_y} = \nu \left(\frac{u_{i+1,j} - 2u_{i,j} + u_{i-1,j}}{h_x^2} + \frac{u_{j+1} - 2u_{j,j} + u_{j-1}}{h_y^2} \right)$$

$$v_{j,t} + u_{jj} \frac{v_{i+1,j} - v_{i-1,j}}{2h_x} + v_{jj} \frac{v_{j+1} - v_{j-1}}{2h_y} = \nu \left(\frac{v_{i+1,j} - 2v_{i,j} + v_{i-1,j}}{h_x^2} + \frac{v_{j+1} - 2v_{j,j} + v_{j-1}}{h_y^2} \right) - g$$

Navier-Stokes equations discretised in space and time

We start from (6) and (7), but first write it a little bit different: We will discretise these equations in time with the use of the Euler method for time discretisation. We will first calculate a guess for the velocity and use the pressure from the old time level. After that we will update the pressure with the use of equation (1) and calculate the velocities for the new time level.

The Euler scheme is given as:

$$U^* = U^n + F_u(U^n, V^n)$$

$$V^* = V^n + F_v(U^n, V^n)$$

3. Results

3.1. Convergence of the solution

We chose as a condition of stop:

$$|Velocity_i - Velocity_{i-1}| < \varepsilon = 10^{-6}$$

Where: $Velocity = \sqrt{U^2 + V^2}$

The following figures (Fig.109+110) shows the convergence of the velocity solution in time.

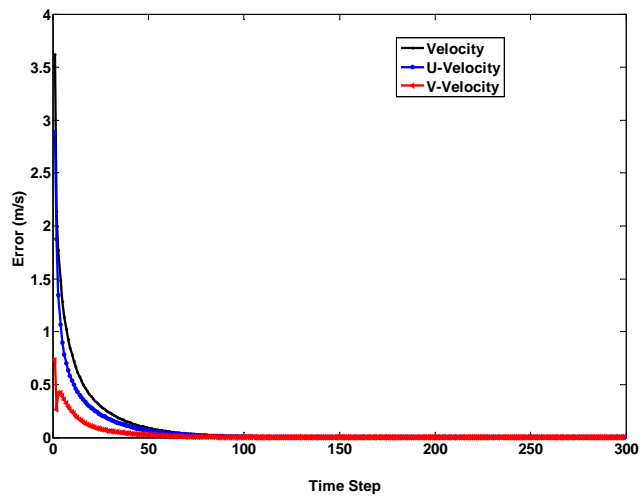


Fig. 109: The convergence of the solution in time

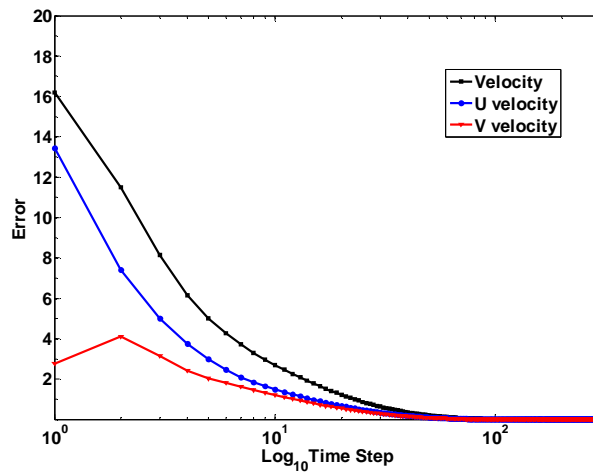


Fig. 110: The convergence of the solution in time (Logarithmic scale)

3.2. Pressure

The figure (Fig.111) shows the variation of the pressure in the crack for two types of meshing. The first one for 10 nodes and the second is 40 nodes. We increase the number of nodes to concentrate the mesh and to obtain a more accurate result. This remark can be observed in the difference between the pressure corresponds to first and the second case. Certainly, the second curve is smoother than the first curve. The pressure is not exactly linear as supposed by Poiseuille.

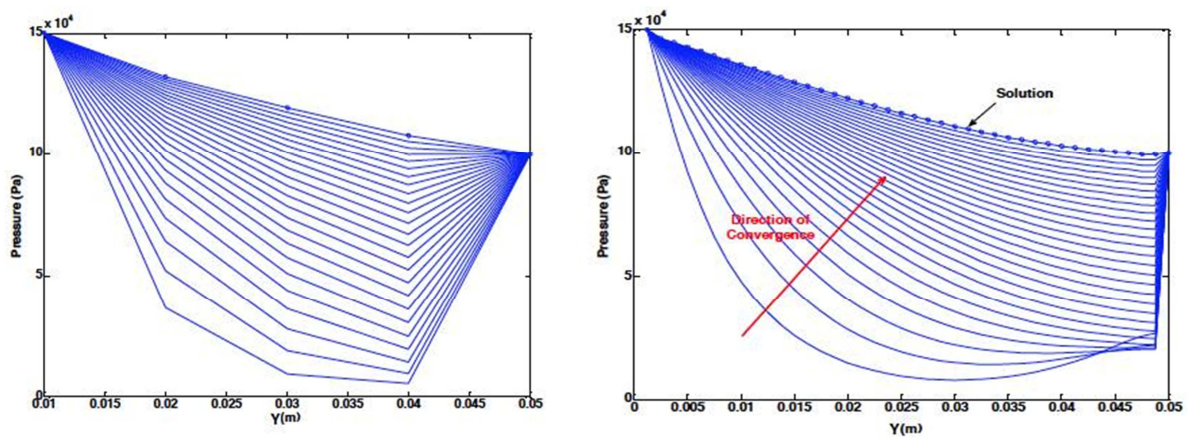


Fig. 111: Variation of the pressure in the crack

3.3. Vertical velocity

As shown in the fig.112, the vertical velocity is symmetric. We can also verify our results by the boundary conditions (velocity=0 near to the lips). The values of vertical velocity appear neglected comparing to the horizontal velocity. Indeed, the max for the vertical velocity is equal to 0.2 m/s or for the horizontal velocity it is equal to 20 m/s means times 100 (Fig.114). In general, in the literature, the vertical velocity is neglected so our results confirm this assumption.

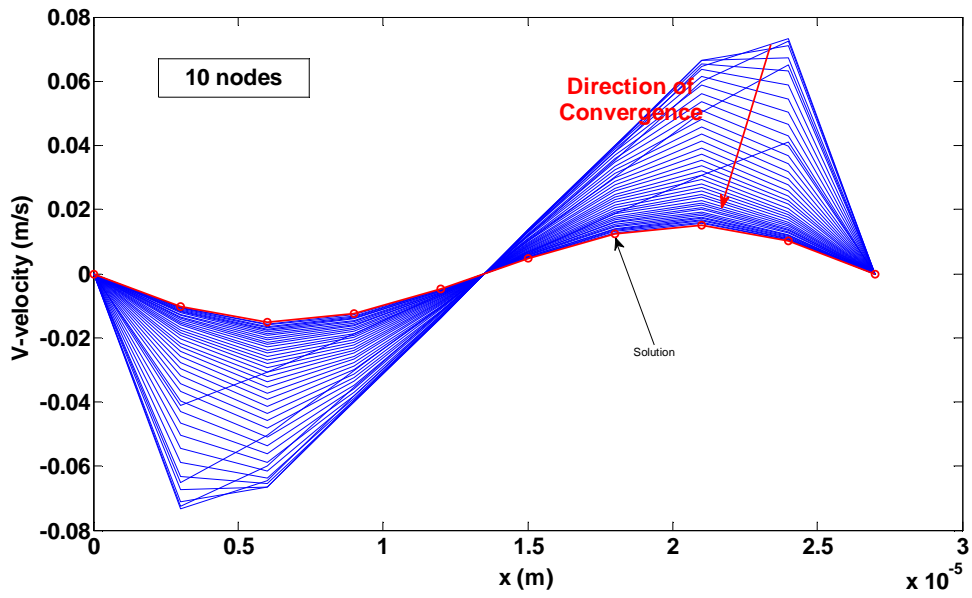


Fig. 112: Convergence of the V-velocity in the crack (10 nodes)

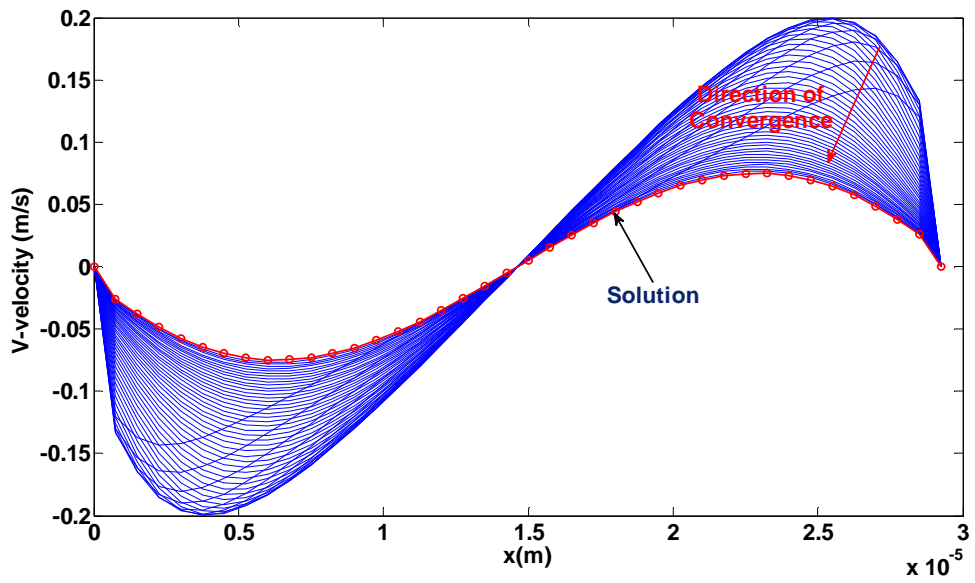


Fig. 113: Convergence of the V-velocity in the crack (40 nodes)

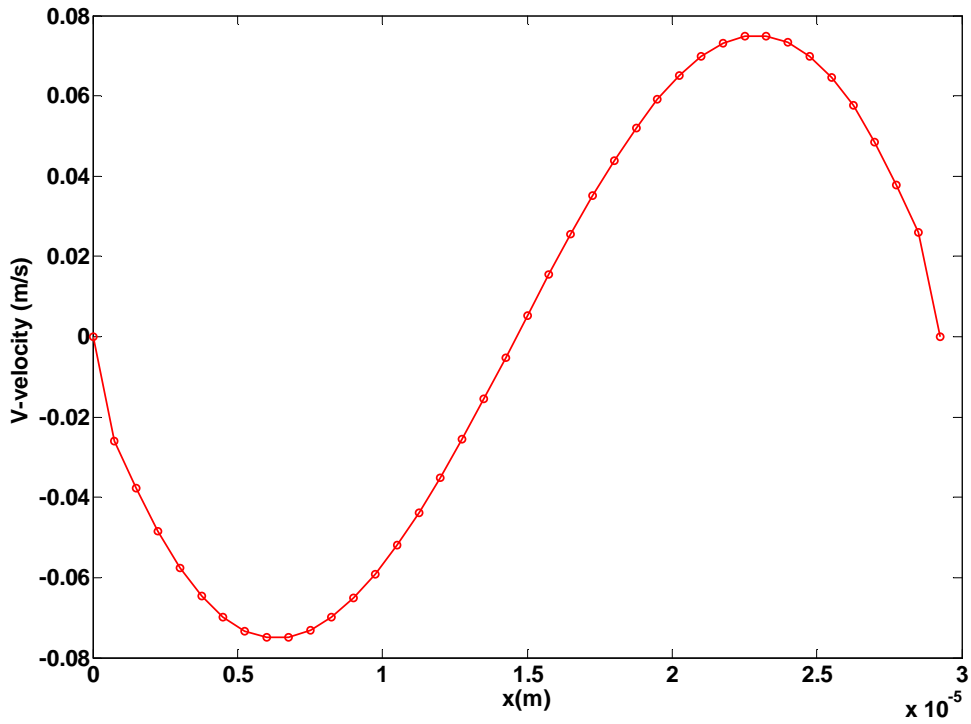


Fig. 114: Convergence of the V-velocity in the crack (10 nodes)

3.4. Horizontal velocity

The numerical program allows calculating the horizontal velocity too (This velocity is more important because from it flow will be calculated). The velocity starts from zero until reaching the establishment of flow (the convergence).

For the mesh, forty nodes are already enough to get an appropriate result (Fig.116).

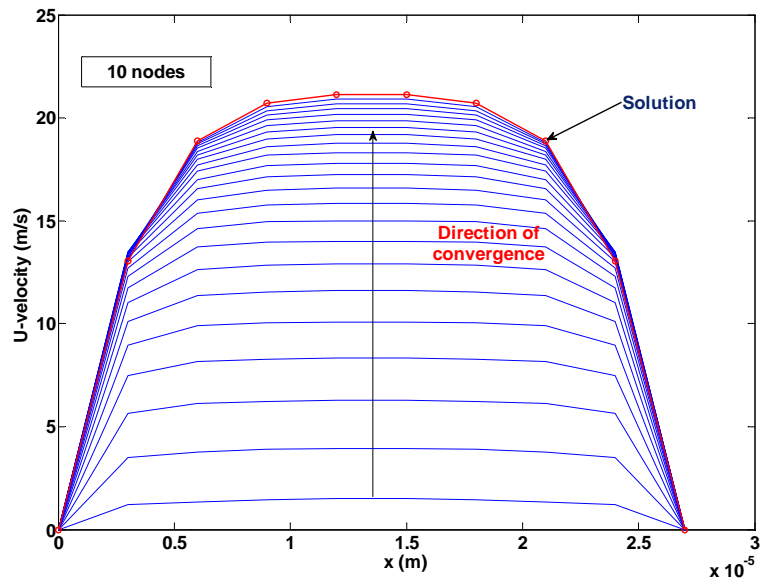


Fig. 115: Convergence of the U-velocity in the crack (10 nodes)

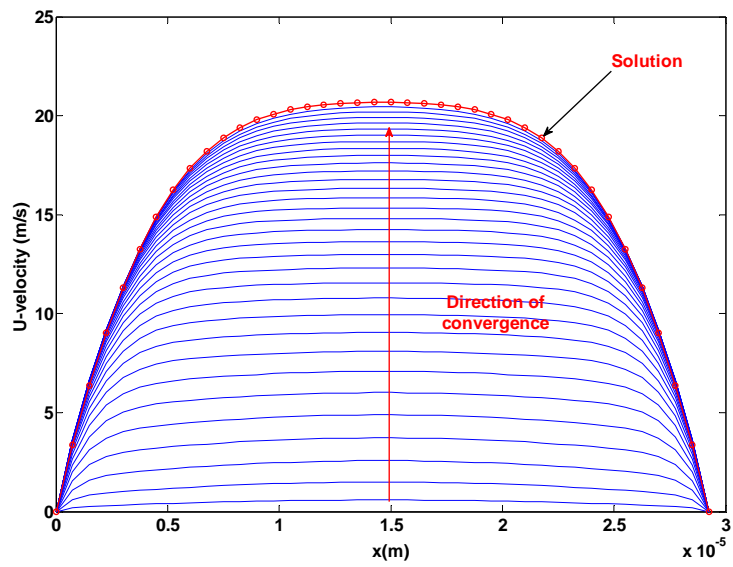


Fig. 116: Convergence of the U-velocity in the crack (40 nodes)

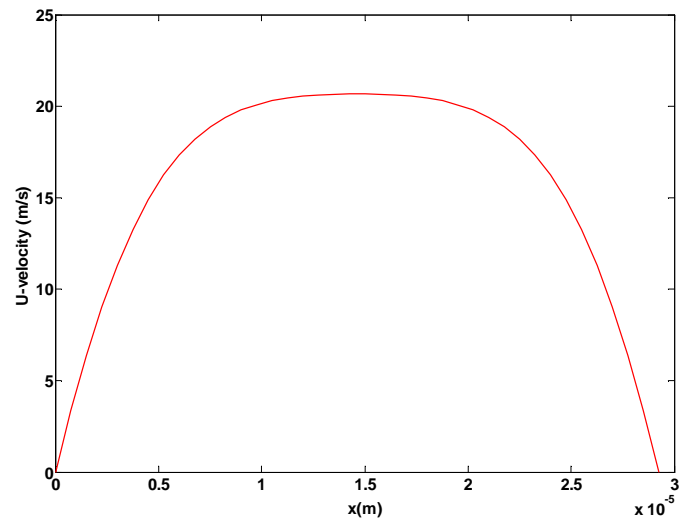


Fig. 117: Convergence of the V-velocity in the crack (10 nodes)

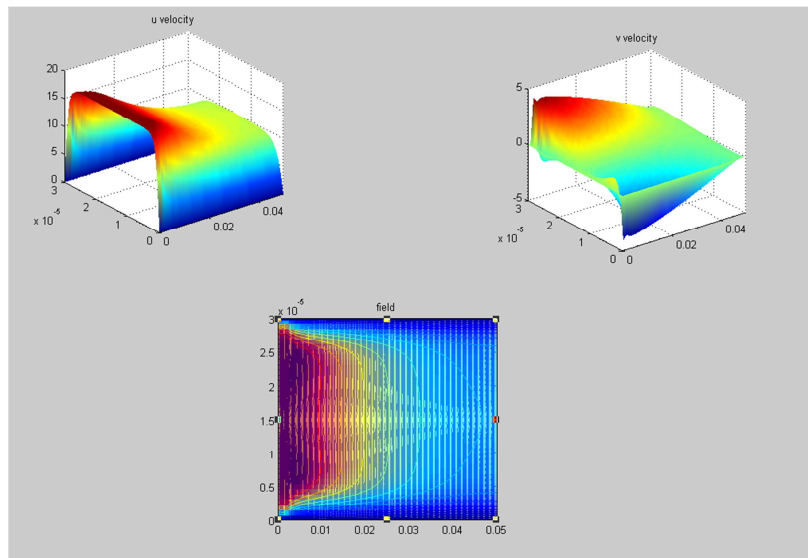


Fig. 118: Curve 3D of velocities (U and V) and velocity field in the crack before the flow establishment

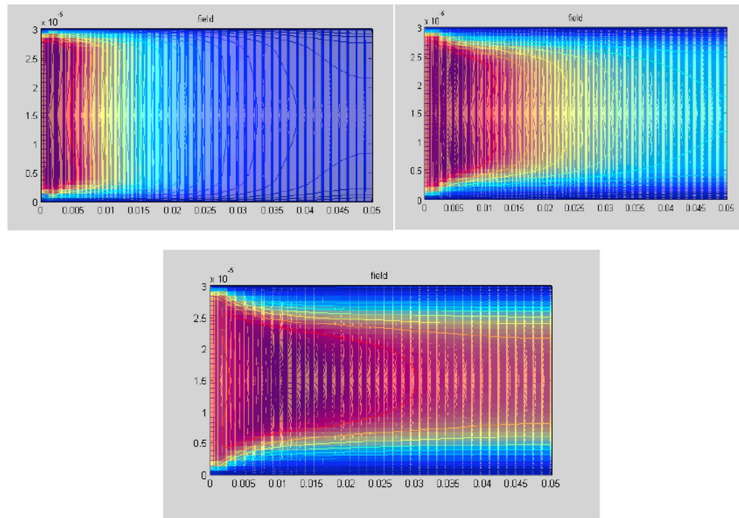


Fig. 119: The establishment of the flow in the crack in time

4. Comparison between numerical and experimental airflows

After the flow establishment and the calculation of the velocity, the airflow can be determined by this equation:

$$Q = \int U dx dy = b \int U dy$$

To do we need for each velocity the determination of an interpolation function.

After the integration of the interpolation function we obtain the following curve.

The fig.120 displays both the numerical and experimental evolution of the airflow according to crack size. It shows an increase of the airflow.

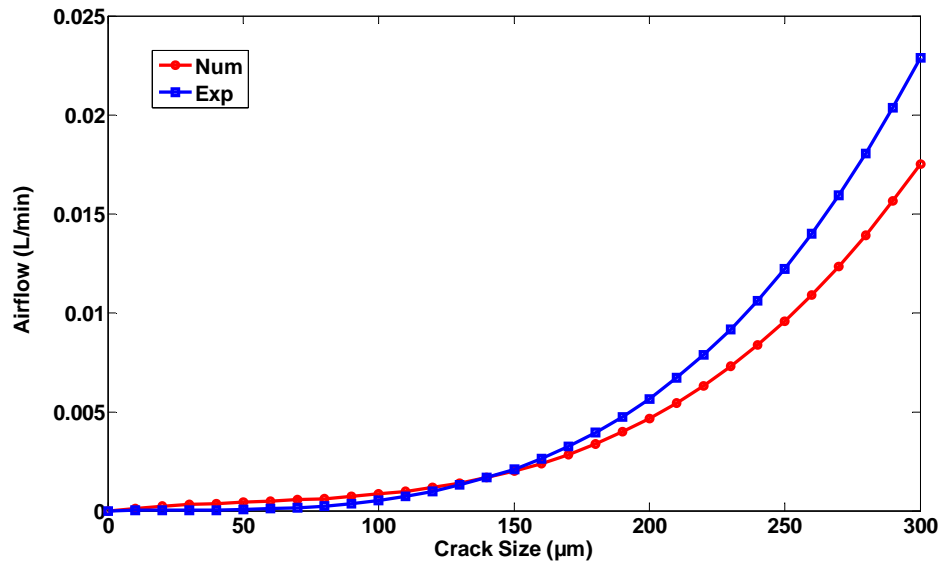


Fig. 120: Variation of the Airflow with crack size (experimental and numerical)

We observed two zones:

- Crack size < 150 micron: the experimental values are inferior to the numerical one which is due the neglecting of friction
- Crack size > 150 micron: the experimental values are inferior to the numerical one which is due the neglecting of friction.

The difference between the experimental and numerical results is due to:

The form of the crack size: in reality the crack is not a two paralleled plates as supposed in modelling.

In the modelling, we suppose that the velocity near to crack is equal to zero or the velocity.

Conclusion

Our objective in this part is to determine the relationship between crack size and airflow. We arrived model the permeability test by solving the Navier-Stockes equation by FVM.

The crack is supposed as two parallel plates and the initial / boundary conditions are fixed in accordance with the experimental tests. After meshing, pressure and velocities are calculated then the airflow was determined by integration the horizontal velocity and this process is repeatable each time by changing the crack size.

The numerical results (represented the airflow according to crack size) show a good agreement with the experimental measurements.

The results can be improved by improving the assumptions as an example:

- Changing the form of the crack such it represent the real crack
- Changing the boundary conditions of the velocities near to the lips of the crack

General Conclusion

The present work is expected to give new insights in the field of Non Destructive Testing Methods. In particular, this preliminary study could be used to detect the non-linear behavior of standard civil engineering materials (such as concrete, mortar and cement) in the early stages of damage. Non Linear Acoustic Methods are expected to enable earlier failure diagnosis and thus reduce maintenance costs of infrastructure.

In the first part: Mortar samples with different initial porosities were subjected to different temperature gradients in order to evaluate the effect of thermal damage on cement elastic properties, and to establish a relationship between damage, temperature and water content. It is assessed in the laboratory by measuring sample mass densities and wave velocities. Mass density tends to decrease with higher applied temperature gradients and with higher water contents. The Linear Acoustic Method allows relating wave velocities to Young's modulus. The variations of Young's modulus with temperature changes also show a linear trend. Although the Linear Acoustic Method is easy and fast to implement, it is limited to damage models assuming that the virgin material is linear elastic, which is not satisfactory for an inhomogeneous micro-material such as mortar. That is the reason why a nonlinear technic was used in order to use a more sophisticated damage assessment technique, based on the Higher Harmonic Generation Method. The experimental set up is described in this report. Experimental measurements provide evidence of an exponential growth of β with temperature gradient.

Several results have been showed in this first part:

- The linear acoustic tests show that the velocities and dynamic modulus of Young decreases according to the porosity linearly.
- The saturation has an impact on the velocities while the velocities for a saturated mortar bigger than a dry one.
- Linear acoustic tests were done and showed that the velocities decreases after the thermal damage moreover we can observe a linear loss of the modulus of Young.
- The nonlinear acoustic measurements showed that beta increases linearly with porosity especially for the higher porosity and sensitive to the saturation of the mortar.

- Beta is a good indicator to quantify the heat treatment. Indeed, the nonlinear parameter rises linearly according to the temperature.

In the second part: an annular specimens of mortar were subjected to different crack size in order to evaluate the effect of mechanical damage on mortar elastic properties and to follow the self-healing phenomena. The airflow and the size of crack are reduced after self-healing, which shows that moisture plays a major role in closing cracks. In the other hand, a nonlinear technic was used in order to use a more sophisticated damage assessment technique, based on the Shift Resonance and the Higher Harmonic Generation. The Experimental measurements provide evidence of a decay of alpha and beta with the self-healing.

In this part, several results have been demonstrated:

- The tests permeability showed that the kinetics of self-healing is influenced by the initial opening of a crack.
- Ultrasonic longitudinal velocities increase during the healing process and show the presence of self-healing phenomenon and the crack close gradually.
- The nonlinear parameters alpha and beta decreases during the healing process, which indicate that the residues of damage decrease progressively.
- Correlations between the nonlinear parameters (alpha and beta) and airflow in the form of a linear and polynomial functions were established.
- relationships between the nonlinear parameters (alpha and beta) and index in the form of polynomial function of 2nd degree were determined

Finally, a numerical part was done to model the relationship between the airflow and the crack size to find a numerical model that allows us to avoid testing permeability.

The numerical results (represented the airflow according to crack size) show a good agreement with the experimental measurements.

The results can be improved by improving the assumptions as an example:

- Changing the form of the crack such it represent the real crack
- Changing the boundary conditions of the velocities near to the lips of the crack

References

Ahn, T. H., Kishi, T. (2010), Crack self-healing behavior of cementitious composites incorporating various mineral admixtures, *Journal of Advanced Concrete Technology*, 8(2), 171-186.

Ankit, S., Francesco L. (2010), The existence of longitudinal or flexural waves in rods at nonlinear higher harmonics, *Journal of Sound and Vibration*, 329 1499–1506.

Antonaci, P. (2010), Monitoring evolution of compressive damage in concrete with linear and nonlinear ultrasonic methods, *Cement and Concrete Research* 40, 1106–1113

AFPC-AFREM, Méthodes recommandés pour la mesure des grandeurs associées à la durabilité.

Argouges, M., Gagné, R. (2009), Étude des mécanismes et de la cinétique de l'autocicatrisation dans des mortiers cimentaires fissurés, Dixième édition des Journées scientifiques du Regroupement francophone pour la recherche et la formation sur le béton (RF)2B, Cachan, France

Baroghel-Bouny, V. (2004), Conception des bétons pour une durée de vie donnée des ouvrages - Maîtrise de la durabilité vis-à-vis de la corrosion des armatures et de l'alcaliréaction – Etat de l'art et guide pour la mise en oeuvre d'une approche performantielle et prédictive sur la base d'indicateurs de durabilité, Document scientifique et technique de l'association Française de Génie Civile, p 252 .

Baroghel-bouny, V. (2005), Nouvelle approche performantielle et prédictive fondée sur les indicateurs de durabilité (Club Régional ouvrages d'Art, 08 déc. 2005, les sables d'Olonne, France), p 4.

Bray, D.E., McBride, D. (1992), *Nondestructive testing techniques*, John Wiley & Sons (Ed.), pp. 15-24.

Birks, A. S. (1991), *Nondestructive Testing Handbook 7: Ultrasonic Testing*, ASNT Handbook.

Clear, C.A. (1985), *The effects of autogenous healing upon the leakage of water through cracks in concrete - Technical report 559*, in, Cement and Concrete Association, Wexham Springs.

Carr, P. H. (1964), *Harmonic generation of microwave phonons in quartz*, *Physical Review Letters*, Vol. 13, No. 10, pp. 332-335.

Payan, C., Garnier, V., Moysan, J. (2010), *Effect of water saturation and porosity on the nonlinear elastic response of concrete*, *Cement and Concrete Research* 40 473–476.

Donskoy, D., Sutin, A., Ekimov, A. (2001), *Nonlinear Acoustic Interaction on Contact Interfaces and its use for Nondestructive Testing*, *NDT&E International*, Vol. 34, No. 4, pp. 231-238.

Edwardsen, E. (1999), *Water Permeability and Autogenous Healing of Cracks in Concrete*, *ACI Material Journal*, 96 ,448-454.

Ettemeyer, A. (2004), *Material and component validation by speckle interferometry and correlation methods* , 16th WCNDT 2004 – World Conference on NDT, Aug 30 - Sep 3, Montreal, Canada.

Fournier, N., Brousset, C. (2006), *ShapeView - A Portable Shape Measurement System* , 9th European Conference on Non-Destructive Testing, 25-29 sept., Berlin, Allemagne.

Fu, Y.F., Wong, Y.L., Tang, C.A., C.S. Poon (2004), Thermal induced stress and associated cracking in cement-based composite at elevated temperatures-Part I: Thermal cracking around single inclusion, *Cement Concrete Composite*. 26.

Feldman, R. F., Sereda, P.J. (1968), A model for hydrated Portland cement paste as deduced from sorption-length change and mechanical properties , *Mater. Struct.*, vol.6, p.509-520.

Moradi-Marani, F. Kodjo, S, Rivard, P., Lamarche, C. (2014), Nonlinear Acoustic Technique of Time Shift for Evaluation of Alkali-Silica Reaction Damage in Concrete Structures , *ACI Materials Journal* , Title No. 111-M52.

Guillaume, R. Samuel, C., Jean-Pierre, R., Marielle, D. (2008), Non-linear acoustic measurements to assess crack density in trabecular bone, *International Journal of Non-Linear Mechanics*, 43, 194 – 200.

Granger, S., Loukili, A. , Chanvillard, G. (2006), Caractérisation expérimentale du phénomène d'autocicatrisation des fissures dans le bétons, Paper presented at the XXIViemes Rencontres universitaires de génie civil 2006, La Grande-Motte, France.

Granger, S., Loukili, A. , Chanvillard, G. (2007), Experimental characterization of the self-healing of cracks in an ultra high performance cementitious material: Mechanical tests and acoustic emission analysis, *Cement and Concrete Research*, 37(4), 519-527.

Hearn, N. (1998), Self-healing, autogenous healing and continued hydration : What is the difference ? *Materials and Structures*, 31, 563-567.

Hellier, C.J. (2001), *Handbook of nondestructive evaluation* , McGraw – Hill (Ed.), p. 603.

Huber, R., Berger, R., (2006), Shearography as an Industrial Application Including 3D Result Mapping , 9th European Conference on Non-Destructive Testing, 25-29 sept., Berlin.

Homma, H. Mihashi, T. Nishiwaki (2009), Self-healing capability of fiber reinforced cementitious composites, *Journal of Advanced Concrete Technology*, 7, 217-228.

Hosoda, A., S. Komatsu, T. Ahn, T. Kishi, S. Ikeno, K. Kobayashi (2009), Self healing properties with various crack widths under continuous water leakage, in: A.e. al (Ed.) *Concrete Repair, Rehabilitation and Retrofitting II*, Taylor & Francis Group, London, , pp. 221-227.

Hikata, A., Chick, B. B., Elbaum, C. (1963), Effect of Dislocations on Finite Amplitude Ultrasonic Waves in Aluminum,” *Applied Physics Letters*, Vol. 3, No. 11, pp. 195-197.

Igarashi, S.I., Minoru, K. Tomoya, N. (2009), Technical Committee on Autogenous Healing in Cementitious Materials, Committee Report JCI-TC075B. Japan: Concrete Institute.

Ismail, M. (2006). Etude des transferts et de leurs interactions avec la cicatrisation dans les fissures pour prolonger la durée de service des infrastructures (ponts, centrales nucléaires) (Institut National des Sciences Appliquées de Toulouse, Toulouse).

Jacobsen, S., Marchand, J., Boisvert, L. (1996), Effect of cracking and healing on chloride transport in OPC concrete, *Cement and Concrete Research*, 26(6), 869-881.

Jacobsen, S., Marchand, J., Hornain, H. (1995). SEM Observations of the microstructure of frost deteriorated and self-healed concretes, *Cement and Concrete Research*, 25(8), 1781-1790.

Jacobsen, S., Sellevold, E. J. (1996), Self healing of high strength concrete after deterioration by freeze/thaw, *Cement and Concrete Research*, 26(1), 55-62.

Jhang, K. Y. (2000), Applications of Nonlinear Ultrasonics to the NDE of Material Degradation, *IEEE-UFFC*, Vol. 47, No. 3, pp. 540-548.

Jeong, H., Nahm, SH., Jhang, KY., Nam, YH. (2003), A Nondestructive Method for Estimation of the Fracture Toughness of CrMoV Rotor Steels based on Ultrasonic Nonlinearity, *Ultrasonics*, Vol. 41, No. 7, pp. 543-549.

Johnson, P. A. (2001), Resonant Nonlinear Ultrasound Spectroscopy, US Patent, No.6330827.

Jun, C. (2010), Rapid evaluation of alkali-silica reactivity of aggregates using a nonlinear resonance spectroscopy technique, *Cement and Concrete Research*, 40, 914-923.

Joshua, B. A. Elizabeth, V. Wilasa, (2007), Young's modulus of cement paste at elevated temperatures, *Cem. Concr. Res.* 37, 258.

Korotkov, A. S., Slavinskii, M. M., Sutin, A. M. (1994), Variations of Acoustic Nonlinear Parameters with the Concentration of Defects in Steel," *Acoustical Physics*, Vol. 40, Issue 1, pp. 71-74.

Kouzoubachian, C. (2006), Les principales méthodes utilisées en END, intérêts dans l'industrie », *Contrôles – Essais - Mesures*, Hors série n°1, pp. 15-19.

Kodjo S.A., Rivard, P., Cohen-Tenouji F., Gallias, J.L. (2011), Impact of the alkali-silica reaction products on slow dynamics behavior of concrete", *Cement and Concrete Research* 41 422-428.

Kishi, T., Tae-Ho, A., Akira, H. (2007), Self-healing behaviour by cementitious recrystallization of cracked concrete incorporating expansive agent. First International Conference on Self Healing Materials, Noordwijkaan Zee, The Netherlands.

Lauer, K.R., Slate, F.O. (1956), Autogenous Healing of Cement Paste, *Journal of the American Concrete institute*, 27, 1083-1097.

Les'nicki, K.J. et al. (2011), Characterization of ASR damage in concrete using nonlinear impact resonance acoustic spectroscopy technique, *NDT&E International* 44 , 721–727.

Li, V. C., Yang, E.H. (2007), Self-Healing in Concrete Materials, In S.van.der.Zwaag , *Self Healing Materials : An Alternative Approach to 20 Centuries of Materials Science* (pp. 161-193): Springer.

Li, M., Li, V.C. (2011), Cracking and Healing of Engineered Cementitious Composites under Chloride Environment, *ACI Materials Journal*, 108, 333-340.

Loving , M.W. (1936), Autogenous healing of concrete, *American Concrete Pipe Association, Bulletin No.13*.

Lion, M. et al. (2005). Experimental study on a mortar: Temperature effects on porosity and permeability: Residual properties or direct measurements under temperature, *Cement. Concrete. Research.* 35, 1937.

Lafhaj, Z. et al (2006), Correlation between porosity, permeability And ultrasonic parameters of mortar with variable water/cement ratio and water content, *Cement and concrete Research*, 36(4):625–33.

Meo, M. (2014), Nonlinear acoustic and ultrasound methods for assessing and monitoring civil infrastructures, *Sensor Technologies for Civil Infrastructures*, Pages 179–200.

Meo, M. et al. (2008), Detecting Damage in Composite Material Using Nonlinear Elastic Wave Spectroscopy Methods, *Applied Composite Materials*, Vol. 15, No. 3, pp.115-126.

Muller, M. et al (2005), Nonlinear Resonant Ultrasound Spectroscopy (NRUS) Applied To Damage Assessment in Bone, *The Journal of the Acoustical Society of America*, Vol. 118, No. 6, pp. 3946-3952.

NT BUILD 443 (1998) , Concrete, hardened: accelerated chloride penetration.

NT BUILD 492 (1999), Concrete, mortar and cement-based repair materials – Chloride migration coefficient from non-steady-state migration experiments.

NF EN 12390-8 (2001), Norme : Essai pour béton durci – partie 8 : Profondeur de pénétration d'eau sous pression, AFNOR.

Neville, A. (2002), Autogenous Healing: A Concrete Miracle , Concrete International, 24(11), 76-82.e , Materials and Structures, 31, 563-567.

Nanayakkara, A. (2003), Self-healing of cracks in concrete subjected to water pressure, Paper presented at the The Second International Synopsium New Technologies for Urban Safety of Mega Cities in Asia, Tokyo, Japan.

Na, J. K. et al. (1996), Linear and Nonlinear Ultrasonic Properties of Fatigued 410Cb Stainless Steel, Review of Progress in QNDE, Vol. 15, pp. 1347-1351.

P. Antonaci et al. (2010), Monitoring evolution of compressive damage in concrete with linear and nonlinear ultrasonic methods, Cement and Concrete Research 40.

Payan, C. et al. (2007), Applying Nonlinear Resonant Ultrasound Spectroscopy to Improving Thermal Damage Assessment in Concrete, The Journal of the Acoustical Society of America, Vol. 121, No. 4, pp. EL125- EL130.

Parker, Jr., et al. (1964), An ultrasonic optical determination of the third order elastic constant c_{111} for nacl single crystals, Applied Physics Letters, Vol. 5, No. 1, pp. 7-9.

Ramm, W., Biscopio M. (1995) , Autogenous healing and reinforcement corrosion in water penetrated separation cracks, 13th International Conference on Structural Mechanics in Reactor Technology (SMiRT 13), Porto Alegre, Brazil.

Reinhardt, H.W, Jooss M (2003) , Permeability and self-healing of cracked concrete as a function of temperature and crack width, *Cement and Concrete Research*, V. 33, No. 7, pp. 981-985.

Shull, PJ. (2002), *Nondestructive evaluation: Theory, techniques, and applications* , Marcel Dekker (Ed.), p. 848.

Shah, A.A., Ribakov Y. (2010), Effectiveness of nonlinear ultrasonic and acoustic emission evaluation of concrete with distributed damages , *Materials and Design* 31, 3777–3784.

Shah, A.A, Ribakov Y. (2009), Non-linear ultrasonic evaluation of damaged concrete based on higher order harmonic generation , 12 May 2009.

Scalerandi1, M. et al. (2008), Nonlinear acoustic time reversal imaging using the scaling subtraction method, *J. Phys. D: Appl. Phys.* 41.

Sukhotskaya, S. et al. (1983), Effect of autogenous healing of concrete subjected to periodic freeze-thaw cycles, Translated from *Gidrotekhnicheskoe Stroitel'stvo*, 6.

Schlangen, E et al. (2006), Crack healing of early age cracks in concrete, in: M.S. Konstantoudos (Ed.) *Measuring , Monitoring and Modeling Concrete Properties*, pp. 273-284.

Park S.J. et al. (2014), Nonlinear resonance vibration method to estimate the damage level on heat-exposed concrete , *Fire Safety Journal* 69, 36–42.

Powers T. C., Brownyard T.L. (1947), Studies of the physical properties of hardened Portland cement paste, *Journal of American Concrete Institute*, vol.43.

Straka, L. et al. (2008), Detection of Structural Damage of Aluminum Alloy 6082 Using Elastic Wave Modulation Spectroscopy, *NDT and E International*, Vol. 41, No. 7, pp. 554-563.

Sutin, A. M., Johnson, P. A. (2005), Nonlinear Elastic Wave Nde II. Nonlinear Wave Modulation Spectroscopy and Nonlinear Time Reversed Acoustics, *AIP Conference Proceedings*, Vol. 760, Issue 1, pp. 385-392.

Tae, H. , Kyung Y (2009), Experimental investigation of nonlinear acoustic effect at crack, *NDT & E International* 42 757–764.

Thurston, R. N., Brugger, K. (1964), Third-order elastic constants and the velocity of small amplitude elastic waves in homogeneously stressed media, *Physical Review*, Vol. 133, No. 6A, pp. A1604-A1610.

Turner, L. (1937), The autogenous healing of cement and concrete : its relation to vibrated concrete and cracked concrete, *International Association for Testing Materials ,Congress*, London (pp. 344-345).

Van Den Abeele. K., J. De Visscher (2000) , Damage assessment in reinforced concrete using spectral and temporal nonlinear vibration techniques, *Cement and Concrete Research* 30, 1453-1464.

Van Den Abeele, K., et al. (2001), Micro-Damage Diagnostics Using Nonlinear Elastic Wave Spectroscopy (NEWS), *NDT and E International*, Vol. 34, No.4, pp. 239-248.

Van Den Abeele, K. et al. (2000), Non-Linear Elastic Wave Spectroscopy (NEWS) Techniques to Discern Material Damage, Part I: Non-Linear Wave Modulation Spectroscopy (NWMS), *Research in Nondestructive Evaluation*, Vol. 12, No. 1, pp. 17-30.

Van Den Abeele, K. et al. (2000), Nonlinear Elastic Wave Spectroscopy (NEWS) Techniques to Discern Material Damage, Part II: Single-Mode Nonlinear Resonance Acoustic Spectroscopy, *Research in Nondestructive Evaluation*, Vol. 12, No. 1, pp. 31-42.

Van Den Abeele, K., et al. (2001) , Micro-Damage Diagnostics Using Nonlinear Elastic Wave Spectroscopy (NEWS), *NDT and E International*, Vol. 34, No.4, pp. 239-248.

Visscher, W. M. et al. (1991), On the Normal Modes of Free Vibration of Inhomogeneous And Anisotropic Elastic Objects, *The Journal of the Acoustical Society of America*, Vol. 90 No. 4, pp. 2154-2162.

Wallace, D. C. (1970) , *Solid State Physics*, Academic Press, pp. 301-404.

Windels, F., Van Den Abeele, K. (2004), The Influence of Localized Damage in a Sample on Its Resonance Spectrum, *Ultrasonics* , Vol. 42, No. 1-9, pp. 1025-1029.

Xu, Y.Y.L Y. et al. (2009), Influence of PFA on cracking of concrete and cement paste after exposure to high temperatures, *Cement Concrete Research*, 33.

Ying-Zi, Y. et al. (2005), Self -healing of engineered cementitious composites under cyclic wetting and drying, *Durability of Reinforced Concrete under Combined Mechanical and Climatic Loads (CMCL)*, Qingdao (China).

Yost, W. T. (1998), Nonlinear Ultrasonic Scanning to Detect Material Defects, US Patent, No. 5763642.

Yost, W. T., Cantrell, J. H. (1993), The Effects of Artificial Aging of Aluminum 2024 on its Nonlinearity Parameter, *Review of Progress in QNDE*, Vol. 12, pp. 2067-2073.

Y. Boukari et al. (2015), Combining nonlinear acoustics and physico-chemical analysis of aggregates to improve alkali–silica reaction monitoring, *Cement and Concrete Research* 67, 44–51.

Yaman I.O., Hearn N., Aktan H.M. (2002), Active and non-active porosity in concrete Part II: Evaluation of existing models , *Materials and Structures*, vol.35, p.110-116.

Yang, Y., et al. (2009), Autogenous healing of engineered cementitious composites under wet-dry cycles, *Cement and Concrete Research*, 39, 382-390.

Zhong, W., Yao, W. (2007), Influence of damage degree on self-healing of concrete, *Construction and building materials*.

Zagrai, A., et al. (2004), N-SCAN: New Vibro-Modulation System for Crack Detection, Monitoring and Characterization, *AIP Conference Proceedings*, Vol. 700, Issue 1, pp. 1414-1421.

Résumé étendu en français

Dans les domaines industrielles de pointe (nucléaire, aéronautique, etc ...), évaluer les dégâts des matériaux est la clé pour contrôler la durabilité et la fiabilité des matériaux en service. Dans cette perspective, il est nécessaire non seulement de quantifier le préjudice, mais également d'identifier les différents mécanismes responsables. Il est donc essentiel de caractériser la matière et d'identifier les indicateurs les plus sensibles de la présence de dommages pour éviter leur ruine et de les utiliser de façon optimale. Afin de résoudre ce problème, les méthodes acoustiques semblent être intéressantes en raison de leur aspect non-destructive et leur sensibilité aux dommages. Ainsi, les méthodes acoustiques ultrasoniques linéaires ont souvent montré leur capacité à caractériser l'endommagement par des changements de vitesse et l'atténuation des ondes ultrasonores. Cependant, plusieurs expériences ont montré que les méthodes acoustiques linéaires ne sont pas suffisamment sensibles pour détecter et localiser les dommages. Souvent, les premiers mécanismes d'endommagement sont les précurseurs de fracture finale, ainsi ils sont donc très importants d'être identifiés. Face à cette difficulté, les méthodes acoustiques non linéaires offrent une alternative importante qui permet de détecter et de caractériser les faibles endommagements, même localisés ou potentiellement diffusés. Ainsi, ces dernières années, l'acoustique non linéaire est de plus en plus comme nouvelle façon très prometteuse en matière d'évaluation et de contrôle des matériaux de structure non-destructive. En effet, même si les non-linéarités peuvent être pertinents dans les matériaux hétérogènes tels que des rochers et des matériaux à base de ciment, ils augmentent de manière significative, en présence de dommages. De nombreuses applications potentielles existent en acoustique non linéaires pour la caractérisation des deux macroscopique fissures localisées et diffuse l'évaluation de la fissuration en raison de la présence de micro-fissures. Dans ce dernier cas, grâce à leur sensibilité élevée, des méthodes acoustiques non linéaires sont particulièrement efficaces en particulier dans la détection et la caractérisation de l'endommagement précoce. Les techniques les plus connues en acoustique non linéaire sont les techniques de résonance. Ces techniques de résonance sont puissantes et présentent de nouveaux outils dans les interrogatoires de fissuration dans les matériaux. En raison de la non-linéarité matériau, une onde peut déformer, ce qui crée des harmoniques annexés multiplication des ondes de différentes fréquences.

En revanche, de nombreuses structures en béton dans le cours de leur vie, l'évaluation de la durabilité est un paramètre clé et nécessaire afin de savoir si la sécurité est bien assurée ou non. La présence de fissures, en raison de contraintes mécaniques ou effets dépendant du temps (retrait,

fluage ...) est l'un des principaux facteurs qui peuvent influencer sur la durabilité et la fonctionnalité des structures en béton en termes de résistance, perméabilité et de transfert des propriétés.

L'autocicatrisation de fissures est un phénomène agissant positivement dans les problèmes de durabilité des matériaux à base de ciment. Ce processus peut avoir lieu qu'en présence de l'eau (CO₂ dissous est pas toujours nécessaire), et se compose de réactions chimiques des composés exposés sur les surfaces fissurées. Ces réactions produisent des cristaux, et l'accumulation de ceux-ci à partir des surfaces opposées d'une fissure peuvent rétablir la continuité du matériau fini. L'exigence essentielle, à l'eau, est la présence de composés capables d'une réaction ultérieure. Ainsi, le ciment, hydraté ou non, est l'élément réactif essentielle. Il y a deux principales hypothèses concernant les réactions de guérison: l'hydratation du clinker non hydraté disponible dans la microstructure du béton durci (important pour le béton à faible / ciment de l'eau), ou la précipitation du carbonate de calcium CaCO₃. Certaines études effectuées jusqu'à présent mettre en évidence le phénomène d'auto-guérison au moyen de tests de perméabilité à l'eau. Une diminution du débit à travers le béton fissuré est la principale technique utilisée pour caractériser l'auto-cicatrisation des fissures.

L'objectif de ce travail est la caractérisation de l'endommagement thermique et mécanique dans le mortier par les ondes acoustiques non linéaires. La corrélation entre les paramètres acoustiques linéaires et non-linéaires étudiée est basée sur les essais expérimentaux et la modélisation.

Des mesures expérimentales des paramètres acoustiques non linéaires en fonction de la taille de la fissure et la température ont été effectuées sur mortier.

Les vitesses ont montré une diminution et les paramètres non-linéaires ont montré une augmentation en augmentant le degré de fissuration.

Pour l'endommagement thermique, des éprouvettes cylindriques ont été préparées et ont été caractérisées par l'étude de la porosité et la saturation. Ensuite, la température contrôle la dégradation. En effet, l'acoustique linéaire (UPV) et l'acoustique non linéaire (génération d'harmoniques) ont été appliqués afin de quantifier l'endommagement. Les essais acoustiques linéaires ont prouvé que les vitesses transversales, longitudinales et le module d'Young du mortier diminue en fonction de la température. Les essais acoustiques non linéaires ont montré l'augmentation du bêta fonction de la température.

Pour l'endommagement mécaniques et l'autocicatrisation, des anneaux de mortier ont été préparés et fissurés en contrôlant la taille de chaque fissure. Ensuite, le phénomène

d'autocicatrisation est suivi par la perméabilité et les essais acoustiques. Les essais de perméabilité ont montré que le débit d'air et la taille de la fissure diminue rapidement au cours du premier mois, puis lentement durant le reste du processus d'autocicatrisation. D'autre part, les tests acoustiques non linéaires ont montré que « alpha » et « bêta » diminuent durant le processus de l'autocicatrisation qui signifie que les paramètres non linéaires sont un bon indicateur pour caractériser ce phénomène.

En outre, l'analyse des résultats expérimentaux indique que la technique de résonance de fréquence est plus efficace pour caractériser les défauts dans le mortier de la génération d'harmoniques plus élevés.

A partir des essais expérimentaux et dans le but d'obtenir un résultat plus général indépendant de notre cas d'étude, les paramètres non linéaires ont été liés à un index d'endommagement. Une corrélation polynomiale de 2^{ème} degré a été établie entre les paramètres non linéaires et l'index d'endommagement.

Un modèle numérique basé sur la méthode des volumes finis a été proposé afin d'établir une corrélation entre la taille de la fissure et le flux d'air. Les résultats numériques ont été comparés avec les résultats des tests de perméabilité et montré un bon accord.

Les résultats de ce travail représentent un bon départ pour étudier le phénomène de l'autocicatrisation par les ondes acoustiques non linéaires.

Caractérisation de l'endommagement thermique et mécanique dans le mortier par les ondes acoustiques non linéaires

L'objectif de ce travail est la caractérisation de l'endommagement thermique et mécanique dans le mortier par les ondes acoustiques non linéaires. La corrélation entre les paramètres acoustiques linéaires et non-linéaires étudiée est basée sur les essais expérimentaux et la modélisation. Pour l'endommagement thermique, des éprouvettes cylindriques ont été préparées et ont été caractérisées par l'étude de la porosité et la saturation. En effet, l'acoustique linéaire et l'acoustique non linéaire (génération d'harmoniques) ont été appliqués afin de quantifier l'endommagement. Les essais acoustiques linéaires ont prouvé que les vitesses transversales, longitudinales et le module d'Young du mortier diminue en fonction de la température. Les essais acoustiques non linéaires ont montré l'augmentation du bêta fonction de la température.

Pour l'endommagement mécaniques et l'autocicatrisation, des anneaux de mortier ont été préparés et fissurés en contrôlant la taille de chaque fissure. Ensuite, le phénomène d'autocicatrisation est suivi par la perméabilité et les essais acoustiques. Les essais de perméabilité ont montré que le débit d'air et la taille de la fissure diminue rapidement au cours du premier mois, puis lentement durant le reste du processus d'autocicatrisation. D'autre part, les tests acoustiques non linéaires ont montré que « alpha » et « bêta » diminuent durant le processus de l'autocicatrisation qui signifie que les paramètres non linéaires sont un bon indicateur pour caractériser ce phénomène. A partir des essais expérimentaux et dans le but d'obtenir un résultat plus général indépendant de notre cas d'étude, les paramètres non linéaires ont été liés à un index d'endommagement. Une corrélation polynomiale de 2ème degré a été établie entre les paramètres non linéaires et l'index d'endommagement. Les résultats de ce travail représentent un bon départ pour étudier le phénomène de l'autocicatrisation par les ondes acoustiques non linéaires.

Mots clés: acoustique non linéaire, autocicatrisation, mortier, endommagement thermique , endommagement mécanique, acoustique linéaire, porosité, fréquence de résonance , génération d'harmoniques.

Characterization of heat and mechanical damage in mortar by nonlinear acoustic waves

The objective of this work is the characterization of heat and mechanical damage in the mortar by the nonlinear acoustic waves. The correlation between non-linear/linear acoustic parameters and damage in mortar is studied based on experiments and modelling. For the heat damage, cylindrical specimens were prepared and were characterized by studying the porosity and saturation. Indeed, the linear acoustic (UPV) and non-linear acoustic (Higher harmonic generation) were applied to characterize the damage. The linear acoustic tests have shown that the longitudinal, transverse velocities and modulus of Young of the mortar decreases in function of the temperature. The non-linear acoustic tests have shown that beta increases in function of the temperature.

For the mechanical damage and the self-healing, an annular specimens were prepared and cracked by controlling the size of each crack. Then the self-healing phenomenon was characterized by the permeability and the acoustic tests. Indeed, the permeability tests have shown that the airflow and the crack size decreases quickly in the first month then slowly for the rest of the self-healing process. On the other hand, the non-linear acoustic tests shown that the alpha and beta decreases according to the self healing process which means that the nonlinear parameters are a good indicators to characterize the self-healing. Moreover, the analysis of the experimental results indicates that the frequency resonant technique is more efficient to characterize the defects in the mortar than the higher harmonic generation. From the experimental tests and to get a general result independent for our case study, the nonlinear parameters were related to a damage index. A polynomial correlations of a 2nd degree was established between the nonlinear parameters and the index damage. The findings of this work should be most appropriate as a foundation for the study of the self healing by the nonlinear acoustic waves.

Keys words: Keywords: nonlinear acoustic, self-healing, mortar, heat damage, mechanical damage, linear acoustic, porosity, resonant frequency, higher harmonic generation.